MINERAL SURFACE CATALYZED POLYMERIZATION OF ESTROGEN AND MICROBIAL DEACTIVATION BY Fe^{3+}-SATURATED MONTMORILLONITE: A POTENTIALLY LOW COST MATERIAL FOR WATER DECONTAMINATION

A Dissertation Presented

by

Chao Qin

to

The Department of Crop and Soil Environmental Sciences

in partial fulfillment of the requirements

for the degree of

Doctor of Philosophy

in the field of

Crop and Soil Environmental Sciences

Kang Xia, Chair

Matthew J. Eick

Diego Troya

Chao Shang

Virginia Polytechnic Institute and State University

Blacksburg, Virginia

December 2016

Keywords: Fe^{3+}-saturated montmorillonite, 17β-estradiol, wastewater, polymerization, microbial deactivation, paper impregnation

MINERAL SURFACE CATALYZED POLYMERIZATION OF ESTROGEN AND MICROBIAL DEACTIVATION BY FE^{3+}-SATURATED MONTMORILLONITE: A POTENTIALLY LOW COST MATERIAL FOR WATER DECONTAMINATION

Chao Qin

Abstract

With advantages of high cation exchange capacity, swelling-shrinking property and large specific surface area, monmtorillonite is chosen as a carrier and modified with Fe^{3+} saturation for estrogen decontamination. 17β-Estradiol (βE2) has highest estrogenic activity among estrogens and is selected as representative compound. Rapid βE2 transformation in the presence of Fe^{3+}-saturated montmorillonite in aqueous system was observed and βE2 oligomers were the major βE2 transformation products. About 98% of βE2 were transformed into oligomers which are $>10^7$ times less water-soluble than βE2 and therefore are much less bioavailable and mobile.

Fe^{3+}-saturated montmorillonite catalysis achieved highest βE2 removal efficiency at neutral solution pH and higher temperature. Common cations did not have impact on the reaction efficiency. Dissolved organic matter slightly reduced βE2 removal efficiency. Regardless of wastewater source, ~40% βE2 removal efficiency was achieved for wastewater effluents when they were exposed to same dosage of Fe^{3+}-saturated montmorillonite as that for simple water systems which achieved ~83% removal efficiency. For real wastewater that contained higher organic matter, higher dosage of Fe^{3+}-saturated montmorillonite would be needed to create available reaction sites for βE2.

This thesis also reports that Fe^{3+}-saturated montmorillonite effectively deactivate wastewater microorganisms. Microbial deactivation rate was 92±0.6% when secondary wastewater effluent was mixed with Fe^{3+}-saturated montmorillonite at 35 mg/mL for 30 min, and further increased to 97±0.6% after 4-h exposure. Freeze-drying Fe^{3+}-saturated montmorillonite

after each usage resulted in 82±0.5% microbial deactivation efficiency even after fourth consecutive use.

For convenient application, Fe^{3+}-saturated montmorillonite was further impregnated into filter paper through wet-end addition and formed uniformly impregnated paper. Scanning electron microscopy (SEM) imaging showed Fe^{3+}-saturated montmorillonite was evenly dispersed over cellulose fiber surface. When filtering 50 mL and 200 mL water spiked with live *Escherichia coli* (*E. coli*) cells at 3.67×10^{8} CFU/mL, Fe^{3+}-saturated montmorillonite impregnated paper with 50% mineral weight loading deactivated *E. coli* with 99% and 77%, respectively. Dielectrophoresis and impedance analysis of filtrate confirmed that the deactivated *E. coli* passing through Fe^{3+}-saturated montmorillonite paper did not have trapping response due to higher membrane permeability and conductivity. The results demonstrate feasibility of using Fe^{3+}-saturated montmorillonite impregnated paper for convenient point-of-use drinking water disinfection.

MINERAL SURFACE CATALYZED POLYMERIZATION OF ESTROGEN AND MICROBIAL DEACTIVATION BY Fe^{3+}-SATURATED MONTMORILLONITE: A POTENTIALLY LOW COST MATERIAL FOR WATER DECONTAMINATION

Chao Qin

General Audience Abstract

In this thesis, Fe^{3+}-saturated montmorillonite was produced in an eco-friendly way to serve as cost-effective material for both efficient estrogen removal and microbial deactivation from wastewater. 17β-Estradiol (βE2), a common estrogen compound, was quickly removed by Fe^{3+}-saturated montmorillonite and the transformation products could be easily settled down from wastewater and became less bioavailable. Fe^{3+}-saturated montmorillonite also demonstrated durability over different environmental conditions in wastewater and still achieved satisfied βE2 removal efficiency. Moreover, Fe^{3+}-saturated montmorillonite could rapidly deactivate the microbes in wastewater effluent and can be promising wastewater disinfection method in the future. Fe^{3+}-saturated montmorillonite immobilized filer paper was also produced and has great potential to be used as a cost-effective filtration purifier for safe drinking water.

Acknowledgements

First, I express greatest gratitude to my advisor Dr. Kang Xia, who always offered me valuable ideas and guidance during my PhD study. I will always remember her strict scientific attitude and passionate spirit towards research in the future career.

I would also thank all my committee members for their directions: Dr. Matthew J. Eick provided many helpful instructions on soil chemistry background; Dr. Diego Troya offered generous help on computational modeling part; Dr. Chao Shang gave me directions and assistance on instrumental analysis.

I thank all current and former colleagues: Hubert Walker, Li Ma, Theresa Sosienski, Shan Sun, Chaoqi Chen, Junxue Wu, Hanh Le, Julia Cushman, William Vesely, Fatmaalzhraa Awad, Bee Khim Chim and Huiqin Guo for all the joyful time we spent together in CSES Department.

I dedicate this thesis to my family for their unconditional love and support. Thanks my husband Mingjie, I am truly grateful for your endless love, understanding, encouragement and patience. I love you all dearly.

My work was financially supported by USDA-NIFA award (No.2013-67019-21355), Virginia Agricultural Experiment Station and the Hatch Program of the National Institute of Food and Agriculture, U.S. Department of Agriculture.

Table of Contents

List of Tables

List of Figures

Chapter 1. Introduction

1.1 Background

Over the past decades, there has been growing public concern on endocrine-disrupting chemicals (EDCs) that can produce adverse effects on human and wildlife by interacting with the endocrine system. Among EDCs, steroidal estrogens are of particular environmental concern because they are the most potent species with the lowest observed adverse effect levels (LOAEL, down to 10 ng/L) for aquatic organisms, which is orders of magnitude lower than other anthropogenic EDCs.[1, 2] There are two important anthropogenic sources releasing estrogens into environment: concentrated animal feeding operations (CAFOs) and municipal wastewater treatment facilities. Estrogen loads from CAFOs have been considered as the major contributor, which is estimated to account for greater than 90% of the total estrogen hormones loading to the environment.[3] When animal manure is applied on agricultural fields as nutrient source, the associated estrogen compounds can be transported to surface water and groundwater by runoff and leaching processes, especially for the areas with frequent and heavy rainfall events.[4-7] Another important path for estrogens entering into the environment is the effluent discharge from wastewater treatment plants. Traditional methods of wastewater treatment, such as activated sludge treatment, cannot be used to effectively remove these estrogens compounds and they remain in effluent to be discharged into receiving aquatic environment,[8, 9] contributing to feminization effect on the aquatic wildlife in the downstream of discharge point.[10] Moreover, the detection of estrogens in source water and even finished water samples from drinking water utilities indicated potential public health risk of long-time exposure on estrogen contamination.[11, 12] Estrone (E1), 17β-estradiol (βE2), 17α-ethynylestradiol (EE2) and estriol (E3) are the main natural estrogens

which are commonly found in sewage treatment. These estrogens are all 18-C steroids with a phenol moiety which is responsible for their estrogenic activity.[13] The βE2 shows the highest biological activity followed by EE2, E1 and E3. Currently, there are very limited resources evaluating processes for estrogen removal from the environment, hence effective treatments are needed for estrogens remediation.[14]

Montmorillonite is the most prominent dioctahedral smectite group mineral found in soils. An ideal 1/2 unit cell formula for the mineral montmorillonite is $Na_{0.4}(Al_{1.6}Mg_{0.4})Si_4O_{10}(OH)_2$.[15] A representative structure of montmorillonite is illustrated in Figure 1.1. It is 2:1 type silicate clay that is characterized by one octahedral sheet sandwiched between two tetrahedral sheets. Due to isomorphous substitution, it generally has high permanent negative charge in the lattice layer. The negative permanent charges mainly derived from substitution of Al^{3+} with Mg^{2+} ions in the octahedral sheet.[16] These permanent negative charges therefore account for the high cation exchange capacity and shrinking-swelling property of montmorillonite. The 2:1 layers are loosely held to adjacent layers by electrostatic interactions between negatively charged layers and interlayer cations (Figure 1.1). With relative low layer charge between 0.2 and 0.6 per 1/2-unit cell,[15] montmorillonite interlayer surfaces are easily accessible to water molecules and significantly expands. When it re-dries, the swelling interlayer space collapses and shrinks upon dehydration, making its unique swelling and shrinking property responsive to environment moisture.[17] The overall internal surface area (~550-650 m^2/g) exposed between the layers far exceeds the external surface area (~80-150 m^2/g) and contributes to over 80% of high total specific surface area of montmorillonite.

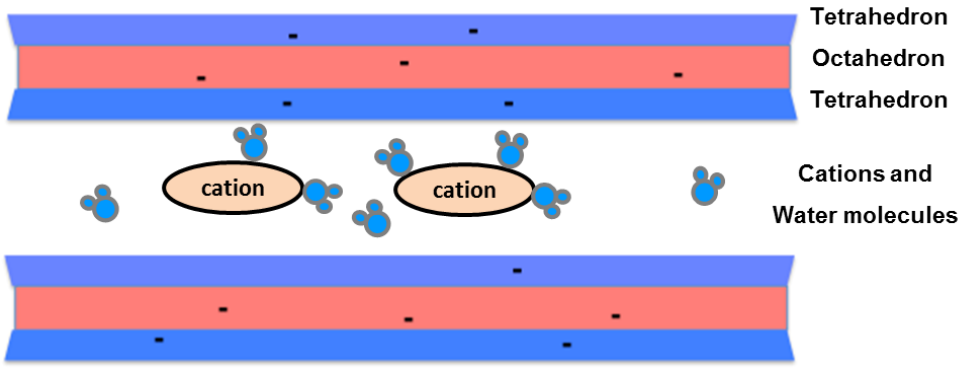

Figure 1.1 Model of two crystal layers and an interlayer characteristic of montmorillonite.

With high cation exchange capacity (70-120 $cmol_c$ kg^{-1}) and large specific surface area (~700-800 m^2/g), montmorillonite has been increasingly explored as the sorbent for heavy metal removal from aqueous systems. With its wide distribution in natural soil environment, the cost of montmorillonite sorbent is only around $0.04-0.12/kg, which is more inexpensive than other common sorbents such as activated carbon (price: $20-22/kg).[18] Extensive studies have confirmed the technical feasibility of using montmorillonite sorbent to achieve excellent removal of toxic heavy metals from contaminated water.[19, 20] Moreover, certain surfactants have been used to modify montmorillonite through cation exchange and replacement of interlayer cations with organic cationic compounds.[21, 22] Studies shown that surfactant modified montmorillonite exhibits higher sorption capacity for organic contaminants.[23] Surfactants intercalated into montmorillonite interlayer change surface properties from hydrophilic to hydrophobic, therefore greatly enhance hydrophobic organic compounds adsorption by dominant role of partition mechanism.[24, 25]

Besides its excellent sorption capacity, montmorillonite can also provide active sites that allow various surface-catalyzed reactions for organic molecules to take place. The d-spacing of air-dry montmorillonite obtained by X-ray diffraction is 12.1 Å for Na-montmorillonite and 15.2 Å for Ca-montmorillonite,[26] after subtracting montmorillonite mineral thickness of 9.5 Å, the

interlayer spacing is approximate to 2.6-5.7 Å. Depending on the ionic strength of an aqueous solution and the type of interlayer cations, the interlayer spacing of montmorillonite can expand up to approximately 10 Å or even complete layer dispersion. The expanded montmorillonite interlayer provides accessible reaction sites that allow surface-catalyzed reactions for organic molecules.[27-29]

Numerous studies have reported a variety of aromatic molecules transformation mediated by montmorillonite saturated with transition metal cations. With unfilled *d* orbitals of exchanging cations, Cu^{2+}-montmorillonite or Fe^{3+}-montmorillonite surface can rapidly transform triclosan, pentachlorophenol, and dioxin under mild reaction conditions at room temperature.[30-34] During the reaction, the organic molecule donates an electron to the sorbed metal cations on montmorillonite surfaces and turn into an organic cation. This is followed by oxidative transformation and dimerization of the radicalized aromatic molecules. Moreover, successive polymerization in addition to dimerization of aromatic molecules through formed radical cations has also been observed.[30, 31] After reduction of metal cations, the Cu^{+} and Fe^{2+} produced can be quickly oxidized back to Cu^{2+} and Fe^{3+} in aerobic conditions for further catalytic reactions. The radical coupling reaction between the metal cations and organic molecules has been extended to include phenol, chlorophenols, pentachlorophenol, chloroanisole, dioxin and chlorodioxins.[35] For these reasons, Fe^{3+}-saturated montmorillonite has been proposed as a promising catalyst for the polymerization of aromatic contaminants.[30, 31, 33, 36] Rapid organic compound polymerization catalyzed by Fe^{3+}-saturated montmorillonite has also been reported in recent studies for pentachlorophenol, phenolic acids, and triclosan.[30, 31, 33] Furthermore, strong complexation between aromatic molecules and the exchanged Fe^{3+} on montmorillonite surface could help contribute to enhanced electron transfer, oxidation, transformation, and polymerization of aromatics on the surface of Fe^{3+}-saturated

montmorillonite.[33] The large polymeric products during oxidative coupling reaction are generally biologically inactive with low aqueous solubility, and therefore can be easily settled from water or immobilized in soil.[37, 38] Polymerization of organic contaminants is a potentially cost-effective means for their removal from wastewater. Overall, such montmorillonite-based system might be useful for decontaminating aromatic pollutants present in wastewater or superfund sites under mild reaction conditions.

Some natural smectite clays have also been reported to possess antibacterial properties and used to treat bacterial infections in medicinal applications.[39] These smectite clays show the beneficial effect on gastrointestinal illnesses and promoting rapid healing of wounds. The illness and wound healing property of smectite clays is attributed to its large surface area that allows sorption of toxins, metals, and oils from the skin or digestive tract.[39, 40] Mineralogy and chemical composition analysis showed that the natural clays with antibacterial property are dominantly Fe-smectites.[41] Analysis of antibacterial natural clay leachates showed that relatively abundant exchangeable ions such as Fe^{3+}, Co^{2+}, Ni^{2+}, Cu^{2+} and Zn^{2+} are present compared to non-antibacterial clay leachate, linking these exchangeable cations to the antibacterial properties of those minerals.[42] However, mechanism of how natural smectites sterilize bacteria has not yet been clearly identified. [43]

Recently, antibacterial transition metal ions have been proposed to intercalate into montmorillonite interlayer to further enhance its antibacterial properties. The synthesized Cu^{2+}, Zn^{2+} and Ag^{+} exchanged montmorillonite have demonstrated effective antibacterial effects towards *Escherichia coli* and *Staphylococcus aureus* strain.[44-47] Studies also showed that the released Cu^{2+} cations from montmorillonite surface is very low and the antibacterial properties mainly can be ascribed to the exchanged Cu^{2+} cations on the mineral surfaces. Also the close

association of bacteria with the modified montmorillonite surface is required to exert antibacterial activity.[47] Modified antibacterial montmorillonite has the following advantages: [44] 1) It is difficult for the free metal cations to contact with bacteria in water. Therefore, high cation concentrations in water must be used during application;[45] 2) The added metal cations could not be recycled after use and they are also often toxic to human health; 3) The large specific surface area and high cation exchange capacity of montmorillonite guarantee high sorption capacity of the desired cations onto interlayers that allow efficient and direct contact between bacteria and antibacterial cations when dispersed into water; 4) Montmorillonite is widely distributed in the natural environment, and the cation exchanged montmorillonite is easy to synthesize eco-friendly at low cost. Although Cu^{2+}, Zn^{2+} and Ag^{+} exchanged montmorillonite have shown satisfactory antibacterial activity, the possible leaching of these toxic metal ions in water could possess potential threat to public health. Iron is an essential trace element for human and iron leaching would not affect the quality of drinking water. In this study, we therefore proposed to develop Fe^{3+}-saturated montmorillonite as an alternative to disinfect water. To the best of our knowledge, this is the first study on antibacterial activity of Fe^{3+}-saturated montmorillonite.

Furthermore, when treating water, it is not practical and convenient for the end users to frequently centrifuge and separate metal cation exchanged montmorillonite from treated water after each use. Numerous researches have been conducted on developing immobilization method to efficiently attach antibacterial materials onto various supporting materials.[48] Common supporting materials include polymer membranes, natural biopolymer fibers (cotton, wool and cellulose) and inorganic materials.[49-52] Commonly used methods to incorporate the antibacterial materials with the supporting materials are surface deposition and incorporation within the matrix.[48]

Previous research has shown that cellulose paper has great advantages over other supporting materials. [53, 54] An ideal support should allow constant contact and interaction between the antimicrobial materials and bacteria and enable even distribution antimicrobial materials on the supporting materials.[48] The porous structure and hydrophilic cellulose fiber allow paper to sorb nanoparticle suspension by capillary forces and produce high nanoparticle loading onto paper upon drying.[54] With the advantages of high porosity, mechanical strength, high water absorbency and natural abundance, cellulose paper material has been used as support matrix.[53-56] There are two main approaches to attach target nanomaterial onto a paper matrix: wet-end addition and surface treatment. While surface treatment merely coats the target nanomaterial over dry paper sheet surface, wet-end impregnation is made to permeate the paper fiber structure, which allows better contact and complete deposit of target particles onto individual fibers in three dimensions before paper sheet formation.[57] There have been recent reports of successful incorporation of bactericidal agents (silver, copper nanoparticle, graphene) into paper matrix for effective point-of-use water disinfection treatment.[55, 56, 58-60]

Hence, the overall goal of this thesis was to investigate the effectiveness and mechanisms of removal of estrogens and microorganisms from aqueous media representing wastewater or contaminated water using Fe^{3+}-saturated montmorillonite. Detailed objectives and the associated hypothesis are:

1.2 Objectives and Hypothesis.

Objective 1. To characterize Fe^{3+}-saturated montmorillonite catalyzed 17β-estradiol oligomerization reaction effectiveness, kinetics, mechanism, and pathway (**Chapter 2**).

Hypothesis. Fe^{3+}-saturated montmorillonite can catalyze oxidative oligomerization of estrogens, resulting in transformation products that are less water soluble and bioavailable.

Objective 2. To test the effectiveness of Fe^{3+}-saturated montmorillonite in catalysis of βE2 polymerization under different environmental relevant conditions and in secondary wastewater effluents (**Chapter 3**).

Hypothesis. Fe^{3+}-saturated montmorillonite can have stable performance over βE2 removal efficiency in simple water systems; However, the complicated wastewater matrices might have negative impact on the removal efficiency.

Objective 3. To test the effectiveness of Fe^{3+}-saturated montmorillonite for microbial deactivation in wastewater (**Chapter 4**).

Hypothesis. Fe^{3+}-saturated montmorillonite can achieve rapid and satisfactory microbial deactivation efficiency for wastewater sample and it can show durability after consecutive use.

Objective 4. To construct Fe^{3+}-saturated montmorillonite impregnated filter paper for effective deactivation of *Escherichia coli* (*E. coli*) in water (**Chapter 5**).

Hypothesis. Fe^{3+}-saturated montmorillonite can be uniformly immobilized over cellulose fiber matrix and *E. coli* bacteria in water can be quickly deactivated after it is filtered through the Fe^{3+}-saturated montmorillonite impregnated filter paper.

1.3 References

1. Routledge, E.; Sheahan, D.; Desbrow, C.; Brighty, G.; Waldock, M.; Sumpter, J., Identification of estrogenic chemicals in STW effluent. 2. In vivo responses in trout and roach. *Environmental Science & Technology* **1998,** *32*, (11), 1559-1565.
2. Daston, G. P.; Gooch, J. W.; Breslin, W. J.; Shuey, D. L.; Nikiforov, A. I.; Fico, T. A.; Gorsuch, J. W., Environmental estrogens and reproductive health: a discussion of the human and environmental data. *Reproductive Toxicology* **1997,** *11*, (4), 465-481.
3. Khanal, S. K.; Xie, B.; Thompson, M. L.; Sung, S.; Ong, S.-K.; Van Leeuwen, J., Fate, transport, and biodegradation of natural estrogens in the environment and engineered systems. *Environmental science & technology* **2006,** *40*, (21), 6537-6546.
4. Kjær, J.; Olsen, P.; Bach, K.; Barlebo, H. C.; Ingerslev, F.; Hansen, M.; Sørensen, B. H., Leaching of estrogenic hormones from manure-treated structured soils. *Environmental science & technology* **2007,** *41*, (11), 3911-3917.
5. Shrestha, S. L.; Casey, F. X. M.; Hakk, H.; Smith, D. J.; Padmanabhan, G., Fate and transformation of an estrogen conjugate and its metabolites in agricultural soils. *Environmental science & technology* **2012,** *46*, (20), 11047-11053.
6. Mansell, D. S.; Bryson, R. J.; Harter, T.; Webster, J. P.; Kolodziej, E. P.; Sedlak, D. L., Fate of endogenous steroid hormones in steer feedlots under simulated rainfall-induced runoff. *Environmental science & technology* **2011,** *45*, (20), 8811-8818.
7. Yang, Y.-Y.; Gray, J. L.; Furlong, E. T.; Davis, J. G.; ReVello, R. C.; Borch, T., Steroid Hormone Runoff from Agricultural Test Plots Applied with Municipal Biosolids. *Environmental Science & Technology* **2012,** *46*, (5), 2746-2754.
8. Hashimoto, T.; Murakami, T., Removal and degradation characteristics of natural and synthetic estrogens by activated sludge in batch experiments. *Water research* **2009,** *43*, (3), 573-582.
9. Baynes, A.; Green, C.; Nicol, E.; Beresford, N.; Kanda, R.; Henshaw, A.; Churchley, J.; Jobling, S., Additional Treatment of Wastewater Reduces Endocrine Disruption in Wild Fish□ A Comparative Study of Tertiary and Advanced Treatments. *Environmental science & technology* **2012,** *46*, (10), 5565-5573.
10. Gibson, R.; Smith, M. D.; Spary, C. J.; Tyler, C. R.; Hill, E. M., Mixtures of estrogenic contaminants in bile of fish exposed to wastewater treatment works effluents. *Environmental science & technology* **2005,** *39*, (8), 2461-2471.
11. Benotti, M. J.; Trenholm, R. A.; Vanderford, B. J.; Holady, J. C.; Stanford, B. D.; Snyder, S. A., Pharmaceuticals and endocrine disrupting compounds in US drinking water. *Environmental Science & Technology* **2008,** *43*, (3), 597-603.
12. Fan, Z.; Hu, J.; An, W.; Yang, M., Detection and Occurrence of Chlorinated Byproducts of Bisphenol A, Nonylphenol, and Estrogens in Drinking Water of China: Comparison to the Parent Compounds. *Environmental science & technology* **2013,** *47*, (19), 10841-10850.
13. Khanal, S. K.; Xie, B.; Thompson, M. L.; Sung, S.; Ong, S.-K.; Leeuwen, J. v., Fate, transport, and biodegradation of natural estrogens in the environment and engineered systems. *Environmental Science & Technology* **2006,** *40*, (21), 6537-6546.
14. Puma, G. L.; Puddu, V.; Tsang, H. K.; Gora, A.; Toepfer, B., Photocatalytic oxidation of multicomponent mixtures of estrogens (estrone (E1), 17β-estradiol (E2), 17α-ethynylestradiol (EE2) and estriol (E3)) under UVA and UVC radiation: photon absorption, quantum yields and

rate constants independent of photon absorption. *Applied Catalysis B: Environmental* **2010,** *99*, (3), 388-397.
15. Essington, M. E., *Soil and water chemistry: An integrative approach*. CRC press: 2015.
16. Weil, R. R.; Brady, N. C., *The Nature and Properties of Soils, Global Edition*. Pearson Education Limited: 2016.
17. McBride, M. B., *Environmental chemistry of soils*. Oxford university press: 1994.
18. Bhattacharyya, K. G.; Gupta, S. S., Adsorption of a few heavy metals on natural and modified kaolinite and montmorillonite: a review. *Adv. Colloid Interface Sci.* **2008,** *140*, (2), 114-131.
19. Abollino, O.; Aceto, M.; Malandrino, M.; Sarzanini, C.; Mentasti, E., Adsorption of heavy metals on Na-montmorillonite. Effect of pH and organic substances. *Water Res.* **2003,** *37*, (7), 1619-1627.
20. Ismadji, S.; Soetaredjo, F. E.; Ayucitra, A., *Clay materials for environmental remediation*. Springer: 2015; Vol. 25.
21. de Paiva, L. B.; Morales, A. R.; Díaz, F. R. V., Organoclays: properties, preparation and applications. *Applied Clay Science* **2008,** *42*, (1), 8-24.
22. Sanchez-Martin, M.; Rodriguez-Cruz, M.; Andrades, M.; Sanchez-Camazano, M., Efficiency of different clay minerals modified with a cationic surfactant in the adsorption of pesticides: influence of clay type and pesticide hydrophobicity. *Applied Clay Science* **2006,** *31*, (3), 216-228.
23. Yan, L.-G.; Wang, J.; Yu, H.-Q.; Wei, Q.; Du, B.; Shan, X.-Q., Adsorption of benzoic acid by CTAB exchanged montmorillonite. *Applied Clay Science* **2007,** *37*, (3), 226-230.
24. Wang, L.; Wang, A., Adsorption properties of Congo Red from aqueous solution onto surfactant-modified montmorillonite. *J. Hazard. Mater.* **2008,** *160*, (1), 173-180.
25. Xi, Y.; Frost, R. L.; He, H.; Kloprogge, T.; Bostrom, T., Modification of Wyoming montmorillonite surfaces using a cationic surfactant. *Langmuir* **2005,** *21*, (19), 8675-8680.
26. McBride, M. B., Adsorption and oxidation of phenolic compounds by iron and manganese oxides. *Soil Science Society of America Journal* **1987,** *51*, (6), 1466-1472.
27. Adams, J. M.; Davies, S. E.; Graham, S. H.; Thomas, J. M., Catalyzed reactions of organic molecules at clay surfaces: Ester breakdown, dimerizations, and lactonizations. *J. Catal.* **1982,** *78*, (1), 197-208.
28. Kaneda, K., Cation-exchanged montmorillonites as solid acid catalysts for organic synthesis. *Synlett* **2007,** *2007*, (07), 0999-1015.
29. Zavaglia, R.; Guigo, N.; Sbirrazzuoli, N.; Mija, A.; Vincent, L., Complex kinetic pathway of furfuryl alcohol polymerization catalyzed by green montmorillonite clays. *The Journal of Physical Chemistry B* **2012,** *116*, (28), 8259-8268.
30. Liyanapatirana, C.; Gwaltney, S. R.; Xia, K., Transformation of triclosan by Fe (III)-saturated montmorillonite. *Environmental science & technology* **2009,** *44*, (2), 668-674.
31. Gu, C.; Li, H.; Teppen, B. J.; Boyd, S. A., Octachlorodibenzodioxin formation on Fe (III)-montmorillonite clay. *Environmental Science & Technology* **2008,** *42*, (13), 4758-4763.
32. Boyd, S. A.; Mortland, M. M., Dioxin radical formation and polymerization on Cu (II)-smectite. *Nature* **1985,** *316*, (6028), 532-535.
33. Polubesova, T.; Eldad, S.; Chefetz, B., Adsorption and oxidative transformation of phenolic acids by Fe (III)-montmorillonite. *Environ. Sci. Technol.* **2010,** *44*, (11), 4203-4209.

34. Pinnavaia, T. J.; Hall, P. L.; Cady, S. S.; Mortland, M., Aromatic radical cation formation on the intracrystal surfaces of transition metal layer lattice silicates. *The Journal of Physical Chemistry* **1974,** *78*, (10), 994-999.
35. Mortland, M. M.; Boyd, S. A., Polymerization and dechlorination of chloroethenes on copper (II)-smectite via radical-cation intermediates. *Environ. Sci. Technol.* **1989,** *23*, (2), 223-227.
36. Gu, C.; Liu, C.; Ding, Y.; Li, H.; Teppen, B. J.; Johnston, C. T.; Boyd, S. A., Clay Mediated Route to Natural Formation of Polychlorodibenzo-p-dioxins. *Environmental science & technology* **2011,** *45*, (8), 3445-3451.
37. Huang, Q.; Weber, W. J., Transformation and removal of bisphenol A from aqueous phase via peroxidase-mediated oxidative coupling reactions: efficacy, products, and pathways. *Environmental science & technology* **2005,** *39*, (16), 6029-6036.
38. Lu, J.; Huang, Q.; Mao, L., Removal of acetaminophen using enzyme-mediated oxidative coupling processes: I. Reaction rates and pathways. *Environmental science & technology* **2009,** *43*, (18), 7062-7067.
39. Carretero, M. I., Clay minerals and their beneficial effects upon human health. A review. *Applied Clay Science* **2002,** *21*, (3), 155-163.
40. Velde, B., Composition and mineralogy of clay minerals. In *Origin and mineralogy of clays*, Springer: 1995; pp 8-42.
41. B Williams, L.; E Haydel, S.; Giese Jr, F.; D Eberl, D., Chemical and mineralogical characteristics of French green clays used for healing. *Clays Clay Miner.* **2008,** *56*, (4), 437-452.
42. Otto, C. C.; Haydel, S. E., Exchangeable ions are responsible for the in vitro antibacterial properties of natural clay mixtures. *PLoS One* **2013,** *8*, (5), e64068.
43. Williams, L.; Holland, M.; Eberl, D.; Brunet, T.; De Courrsou, L. B., Killer clays! Natural antibacterial clay minerals. *Mineralogical Society Bulletin* **2004**, (139), 3-8.
44. Tong, G.; Yulong, M.; Peng, G.; Zirong, X., Antibacterial effects of the Cu (II)-exchanged montmorillonite on Escherichia coli K88 and Salmonella choleraesuis. *Veterinary microbiology* **2005,** *105*, (2), 113-122.
45. Hu, C. H.; Xu, Z. R.; Xia, M. S., Antibacterial effect of Cu 2+-exchanged montmorillonite on Aeromonas hydrophila and discussion on its mechanism. *Veterinary microbiology* **2005,** *109*, (1), 83-88.
46. Magana, S. M.; Quintana, P.; Aguilar, D. H.; Toledo, J. A.; Angeles-Chavez, C.; Cortes, M. A.; Leon, L.; Freile-Pelegrín, Y.; López, T.; Sánchez, R. M. T., Antibacterial activity of montmorillonites modified with silver. *J. Mol. Catal. A: Chem.* **2008,** *281*, (1), 192-199.
47. Özdemir, G.; Limoncu, M. H.; Yapar, S., The antibacterial effect of heavy metal and cetylpridinium-exchanged montmorillonites. *Applied Clay Science* **2010,** *48*, (3), 319-323.
48. Moritz, M.; Geszke-Moritz, M., The newest achievements in synthesis, immobilization and practical applications of antibacterial nanoparticles. *Chem. Eng. J.* **2013,** *228*, 596-613.
49. Barani, H.; Montazer, M.; Samadi, N.; Toliyat, T., In situ synthesis of nano silver/lecithin on wool: enhancing nanoparticles diffusion. *Colloids and Surfaces B: Biointerfaces* **2012,** *92*, 9-15.
50. Teli, M.; Sheikh, J., Antibacterial and acid and cationic dyeable bamboo cellulose (rayon) fabric on grafting. *Carbohydr. Polym.* **2012,** *88*, (4), 1281-1287.
51. Xue, C.-H.; Chen, J.; Yin, W.; Jia, S.-T.; Ma, J.-Z., Superhydrophobic conductive textiles with antibacterial property by coating fibers with silver nanoparticles. *Appl. Surf. Sci.* **2012,** *258*, (7), 2468-2472.

52. Cao, X.; Tang, M.; Liu, F.; Nie, Y.; Zhao, C., Immobilization of silver nanoparticles onto sulfonated polyethersulfone membranes as antibacterial materials. *Colloids and surfaces B: Biointerfaces* **2010,** *81*, (2), 555-562.
53. Dankovich, T. A., Microwave-assisted incorporation of silver nanoparticles in paper for point-of-use water purification. *Environmental Science: Nano* **2014,** *1*, (4), 367-378.
54. Ngo, Y. H.; Li, D.; Simon, G. P.; Garnier, G., Paper surfaces functionalized by nanoparticles. *Adv. Colloid Interface Sci.* **2011,** *163*, (1), 23-38.
55. Dankovich, T. A.; Levine, J. S.; Potgieter, N.; Dillingham, R.; Smith, J. A., Inactivation of bacteria from contaminated streams in Limpopo, South Africa by silver-or copper-nanoparticle paper filters. *Environmental science: water research & technology* **2016,** *2*, (1), 85-96.
56. Hu, W.; Peng, C.; Luo, W.; Lv, M.; Li, X.; Li, D.; Huang, Q.; Fan, C., Graphene-based antibacterial paper. *Acs Nano* **2010,** *4*, (7), 4317-4323.
57. Shen, J.; Song, Z.; Qian, X.; Ni, Y., A review on use of fillers in cellulosic paper for functional applications. *Industrial & Engineering Chemistry Research* **2010,** *50*, (2), 661-666.
58. Dankovich, T. A.; Gray, D. G., Bactericidal paper impregnated with silver nanoparticles for point-of-use water treatment. *Environmental science & technology* **2011,** *45*, (5), 1992-1998.
59. Dankovich, T. A.; Smith, J. A., Incorporation of copper nanoparticles into paper for point-of-use water purification. *Water Res.* **2014,** *63*, 245-251.
60. Jaisai, M.; Baruah, S.; Dutta, J., Paper modified with ZnO nanorods–antimicrobial studies. *Beilstein journal of nanotechnology* **2012,** *3*, (1), 684-691.

Chapter 2. Surface Catalyzed Oxidative Oligomerization of 17β-estradiol by Fe^{3+}-Saturated Montmorillonite

(Published in Environmental Science & Technology)[1]

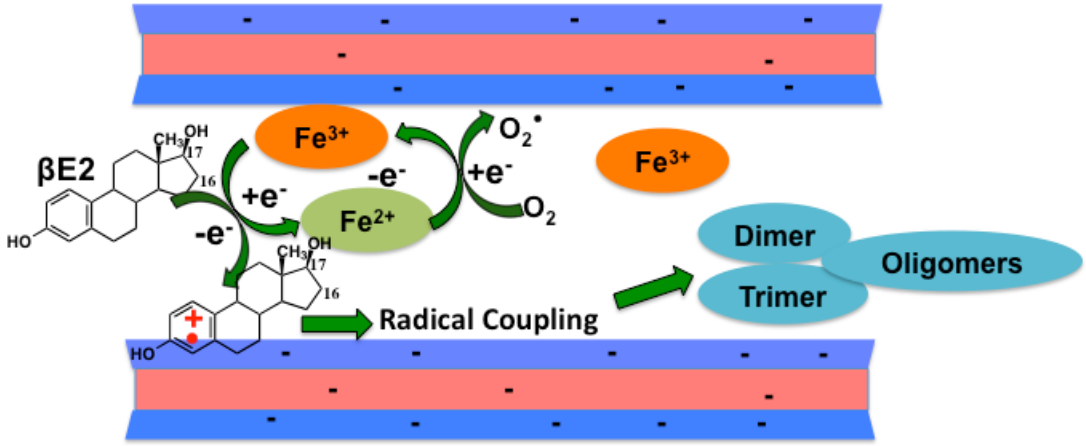

Notes: The abstract figure is only for simple demonstration of possible reaction mechanism. Sizes of different components do not reflect their actual size levels for comparison.

Abstract

With wide spread detection of endocrine disrupting compounds including hormones in wastewater, there is a need to develop cost-effective remediation technologies for their removal from wastewater. Previous research has shown that Fe^{3+}-saturated montmorillonite is effective in quickly transforming phenolic organic compounds such as pentachlorophenol, phenolic acids, and triclosan via surface-catalyzed oligomerization. However, little is known about its effectiveness and reaction mechanisms when reacting with hormones. In this study, the reaction kinetics of Fe^{3+}-saturated montmorillonite catalyzed 17β-estradiol (βE2) transformation was investigated. The transformation products were identified using liquid chromatography coupled with mass spectrometry and

their structures were further confirmed using computational approach. Rapid βE2 transformation in the presence of Fe^{3+}-saturated montmorillonite in an aqueous system was detected. The disappearance of βE2 follows first-order kinetic while the overall catalytic reaction follows the second order kinetic with an estimated reaction rate constant of 200±24 $(\text{mmol βE2/g mineral})^{-1}h^{-1}$. The half life of βE2 in this system was estimated to be 0.50±0.06 h. βE2 oligomers were found to be the major products of βE2 transformation when exposed to Fe^{3+}-saturated montmorillonite. About 98% of βE2 were transformed into βE2 oligomers which are $>10^7$ times less water soluble than βE2 and, therefore, are much less bioavailable and mobile then βE2. The formed oligomers quickly settled from the aqueous phase and were not accumulated on the reaction sites of the interlayer surfaces of Fe^{3+}-saturated montmorillonite, the major reason for the observed >84% βE2 removal efficiency even after five consecutive usages of the same of Fe^{3+}-saturated montmorillonite. The results from this study clearly demonstrated that Fe^{3+}-saturated montmorillonite has a great potential to be used as a cost-effective material for effective removal of phenolic organic compounds from wastewater.

2.1 Introduction

The prevalent worldwide detection of endocrine disrupting compounds (EDCs) in the aquatic environment[2-5] as well as in drinking water[6, 7] have caused increasing concerns about their adverse environmental impact. Natural estrogens including 17β-estradiol (βE2) are of particular environmental concern among EDCs because they can negatively affect certain aquatic organisms at a level as low as 10 ng/L, which is orders of magnitude lower than the lowest observed adverse effect levels (LOAEL) for other anthropogenic EDCs.[8] The adverse impact of estrogens on aquatic organisms includes fish egg production inhibition and sex reversal of males, which ultimately could result in the collapse of local fish populations.[9-11]

Municipal wastewater treatment plants (WWTP) are one of the major sources contributing to elevated natural estrogens in the environment.[12, 13] Research has demonstrated that existing wastewater treatment technologies are not effective at removing estrogens to levels below biological significance.[14, 15] Significant effort has been made to develop wastewater treatment technologies capable of reducing levels of estrogens and other EDCs in treated wastewater to environmental insignificant levels before wastewater effluent is released into the environment.[16-18] While treatment technologies utilizing granular activated carbon (GAC), ozonation, and chlorine dioxide have provided promising results for effective removal of estrogens from WWTP effluents,[19] the application of those treatment technologies has been restricted by high cost of installation and maintenance.[14]

Recent research has shown that Fe^{3+}-saturated montmorillonite can rapidly transform phenolic organic compounds such as pentachlorophenol, phenolic acids, and triclosan via surface-catalyzed oligomerization.[20-22] Compared to parent compounds, the

oligomerized compounds are much less water soluble and, therefore, less bioavailable or biologically active.[23] Montmorillonite, a 2:1 layered aluminosilicate mineral that is widely distributed worldwide,[24] has enormous potential as a platform for nano-scale surface catalyzed chemical reactions.[25, 26] In aqueous environment, the interlayer cations of montmorillonite attract water, resulting in an expansion of the interlayer spacing to approximately 4-10 Å depending on the type of interlayer cations.[27-29] This interlayer space is wide enough for small size organic molecules such as βE2 (12 Å × 6 Å × 4 Å, Table 2.1) to move into the interlayer space, and it also provides a large interlayer surface area that allows surface-catalyzed reactions for organic molecules. The mechanisms of montmorillonite surface catalyzed chemical reactions involve reduction of mineral interlayer cations such as Cu^{2+} and Fe^{3+} and oxidation of organic compounds resulting in organic compound radicals that are highly susceptible to further oligomerization and/or degradation reactions.[30,31] The objective of this study was to investigate, using experimental and computational approaches, the transformation kinetics and pathways of βE2 transformation catalyzed by Fe^{3+}-saturated montmorillonite. Because it has the highest estrogenic activity among estrogens, βE2 was selected as representative compound for this investigation.

Table 2.0.1 Estimated average dimension of E2 and its dimers and trimers *

Compound	Average dimension (Å)		
	L	**W**	**H**
E2	12.2	5.6	3.8
dimers	17.4	10.0	7.2
trimers	19.6	14.6	8.8

*Estimated using free software Jmol (http://jmol.sourceforge.net/download/).

2.2 Materials and Methods

2.2.1 Chemicals and Materials

Estrone (E1) (≥99%) and 17β-estradiol (βE2) (≥98%) were purchased from Sigma-Aldrich (St. Louis, MO). Ferric Chloride (hexahydrate, ≥97%), HPLC grade acetonitrile, ethyl acetate and acetone were purchased from Fisher Scientific (Fair Lawn, NJ). Na^+-montmorillonite (SWy-2, Crook County, Wyoming) was obtained from the Source Clays Repository of the Clay Minerals Society (Purdue University, West Lafayette, IN). The cation exchange capacity and theoretical external surface area of SWy-2 provided by the Clay Minerals Society were 76.4 $cmol_c/kg$ and 31.82 ± 0.22 m^2/g, respectively. The ultrapure water used in this study was produced by Millipore Milli-Q water purification system (Milford, MA).

2.2.2 Fe^{3+}-saturated montmorillonite preparation

Na^+-montmorillonite (SWy-2) was fractionated to <2 μm clay-sized particles before Fe^{3+} saturation following the procedure in Arroyo et al.[32] 10 grams of <2 μm Na^+-montmorillonite was then mixed with 400 mL 0.1 M $FeCl_3$ on a magnetic stir plate for 8 h before centrifugation at 4500 rpm for 20 min. The sediment was re-suspended in another

400 mL 0.1 M $FeCl_3$. The above procedure was repeated six times in order to saturate the montmorillonite interlayer with Fe^{3+}. The Fe^{3+}-saturated montmorillonite was then repeatedly washed with 100 mL HPLC grade water followed by centrifugation at 4500 rpm for 20 min until no Cl^- was detected in the supernatant with an $AgNO_3$ test. Removal of Cl^- from the system indicates the removal of other cations such as Na^+ and Ca^{2+}, which can compete with Fe^{3+} for the interlayer surface sites. The washed Fe^{3+}-saturated montmorillonite was finally freeze-dried for future experiment use. More details for preparation of Fe^{3+}-saturated montmorillonite can be found elsewhere.[22]

2.2.3 Reaction of βE2 with Fe^{3+}-saturated montmorillonite

One hundred μL βE2 stock solution (βE2 dissolved in acetone at 1.36 mg/mL) was mixed with 50 mg Fe^{3+}-saturated montmorillonite in 20 mL glass vials to produce an initial concentration of 0.01 mmol βE2/g of mineral. After complete evaporation of acetone, a carrier solvent, from glass vial under a fume hood, 1.5 ml ultrapure water was added into each glass vial and shaken in darkness at 25°C on an incubator shaker at 120 rpm for up to 10 days. The pH of Milli-Q water is measured as 6.3, which is close to the typical domestic wastewater before treatment (pH ranges from 6.5 to 8.5). Similar experimental procedure was conducted using Na^+-montmorillonite. The same amount of βE2 was added to a 1.5 mL $FeCl_3$ solution which contained the same amount of Fe^{3+} as that in the Fe^{3+}-saturated montmorillonite system (determined as 0.997 mmol Fe^{3+}/g montmorillonite). There were triplicates per treatment. At given intervals, triplicate vials from each treatment were collected and the content of each vial was immediately analyzed for βE2 and its transformation products using the methods described below.

2.2.4 Extraction Method

Upon termination of the reaction, each collected sample was centrifuged at 4000 rpm for 30 min. The supernatant of each centrifuged sample was collected and filtered through a 0.2 μm Thermo PVDF filter before HPLC analysis for βE2 and E1. The remaining sediment of each sample was then freeze-dried for 15 min., mixed with 3 mL ethyl acetate, sonicated for 30 min., and then centrifuged at 4000 rpm for 30 min. One mL ethyl acetate extract of each sample was collected and then evaporated to dryness using a Vacuum Evaporator (RapidVap, Labconco) at 35°C. The dried residue was re-dissolved in 1 mL acetonitrile and water (v/v, 40:60), filtered through a 0.2 μm Thermo PTFE filter before HPLC analysis for βE2 and LC/MS/MS analysis for E1. The amount of βE2 transformed at the termination of the experiment was calculated by:

βE2 added - (βE2 remained in the aqueous phase + βE2 remained in the sediment phase)

2.2.5 HPLC analysis of βE2

The βE2 in the aqueous phase and sediment extracts was quantified using a HPLC system coupled with a fluorescence detector (Agilent 1260 Infinity, Agilent Co., CA, USA). The analytical column was EC-C18 column (3.0 × 50 mm, 2.7 μm, Agilent Poroshell 120). The mobile phase consisted of acetonitrile/water (v/v, 60:40). The mobile phase flow rate was 0.5 mL/min. The column temperature was maintained at 30°C and the injection volume was 20 μL. βE2 was detected by the fluorescence detector at an excitation wavelength of 280 nm and an emission wavelength of 310 nm. The limit of detection (LOD) and the limit of quantification (LOQ) were determined as 10 ppb and 25 ppb, respectively.

2.2.6 Identification of βE2 transformation products

Transformation products were not detected in the aqueous phase at the termination of experiment. The βE2 transformation products in the ethyl acetate extracts of the sediment phase were identified using a liquid chromatography-triple quadrupole mass spectrometer (6490 LC/QQQ, Agilent Co., CA, USA). Electron spray negative ionization mode was used. Total ionization chromatography was collected in the m/z range of 50-1400. The analytical column was Eclipse C18 column (3.0 × 50 mm, Agilent). The mobile phase gradient was programmed as: 0-6 min, 30% acetonitrile and 70% water; 6-22 min, 60% acetonitrile and 40% water; 22-22.5 min, 80% acetonitrile and 20% water; 22.5-24.5 min, 90% acetonitrile and 10% water; 24.5-25 min, 30% acetonitrile and 70% water. The mobile phase flow rate was 0.4 mL /min. The injection volume was 10 μL. The column temperature was maintained at 40°C. The MS parameters were: probe capillary voltage at 3.5 kV, sheath gas flow at 8 L/min, nebulizer pressure at 45 psi.

2.2.7 Determination of Accurate Masses for βE2 Oligomer Products Using UPLC-ESI-Q-TOF

The accurate masses of transformation products were further confirmed using ultra performance liquid chromatography-quadrupole-time-of-flight mass spectrometry (UPLC-Q-TOF, Waters Acquity I-class UPLC coupled with a Synapt G2-S High Definition Mass Spectrometer, Waters Corp., Milford, MA) in electron negative ionization mode. Sample separation was performed on a Waters Acquity I-class UPLC system (Waters, Corp., Milford, MA) equipped with a Acquity UPLC BEH column (C18, 1.7 μm, 2.1 x 50 mm, Waters, Corp., Milford, MA) maintained at 35.0° C. A binary solvent comprised of water (Spectrum Chemicals, New Brunswick, NJ) with 0.1% formic acid (Sigma, St. Louis, MO)

(A) and acetonitrile (Spectrum Chemicals, New Brunswick, NJ) (B). The mobile phase gradient was programmed as following: 0 -1 min 40% B, 1-8 min ramped to 95% B and hold at 95% B for 0.5 min, 8.5-10 min ramped down to 40% B and hold at 40% B for additional 0.5 min. The mobile phase flow rate was 0.2 ml/min. The injection volume was 1 μL.

The analytes were eluted to a Synapt G2-S mass spectrometer (Waters, Corp., Milford, MA) equipped with an electron spray ionization (ESI) probe with high resolution mode. The ions were collected in negative ionization mode. The source conditions were as follows: capillary voltage 2.5 kV, cone voltage 40V, source temperature 80°C, source offset 80.0, nebulizer gas 6.0 bar, desolvation temperature 150°C and cone and desolvation gas flows were 50 and 500 L/h, respectively. Data was collected in MS^E mode which provided simultaneous collection of MS and MS/MS spectra. The mass scan range was set from 50 to 1800 and the scan time was set to 0.2 seconds for both low (2) and high (10-45) collision energy scans. For accurate mass calibration of mass spectrometer, leucine-enkephlan (Waters Corp., Milford, MA) at a concentration of 200 ng/ml was continually infused through the reference sprayer at 5 μL/min with a scan time of 0.1 seconds and a scan frequency of 20 sec.

2.2.8 Computational Study

All geometry optimizations for the βE2 monomer and all possible dimer and trimer species resulting from the catalyzed coupling reactions in Fe^{3+}-saturated montmorillonite were carried out with the B3LYP density functional theory (DFT) method and the 6-31G* basis set as implemented in the Gaussian09 suite of programs. The relative energies of all

dimer and trimer isomers were used to evaluate the thermodynamic stability of all the possible βE2 transformation products.

2.3 Results and Discussion

2.3.1 Kinetics of Fe^{3+}-saturated montmorillonite catalyzed βE2 transformation

As shown in Figure 2.1, in the presence of Fe^{3+}-saturated montmorillonite, βE2 rapidly disappeared within the first two hours following first-order kinetic with an estimated overall second-order reaction rate constant of 200±24 (mmol βE2/g mineral)$^{-1}h^{-1}$. The half life of βE2 in this system was estimated to be 0.50±0.06 h. Within the first two hours only 20% of initially added βE2 remained. Close to 100% of the initially added βE2 was transformed on the 5th day. However, transformation of βE2 was much slower in the presence of Na^{+}-montmorillonite comparing to the system containing Fe^{3+}-saturated montmorillonite. Even after 10 days, about 82% of initially added βE2 still remained in the Na^{+}-montmorillonite system. When βE2 was incubated with $FeCl_3$ solution that contained the same amount of Fe^{3+} that was saturated in the montmorillonite system, close to 94% of initially added βE2 remained in the system after 10 days, indicating limited βE2 transformation.

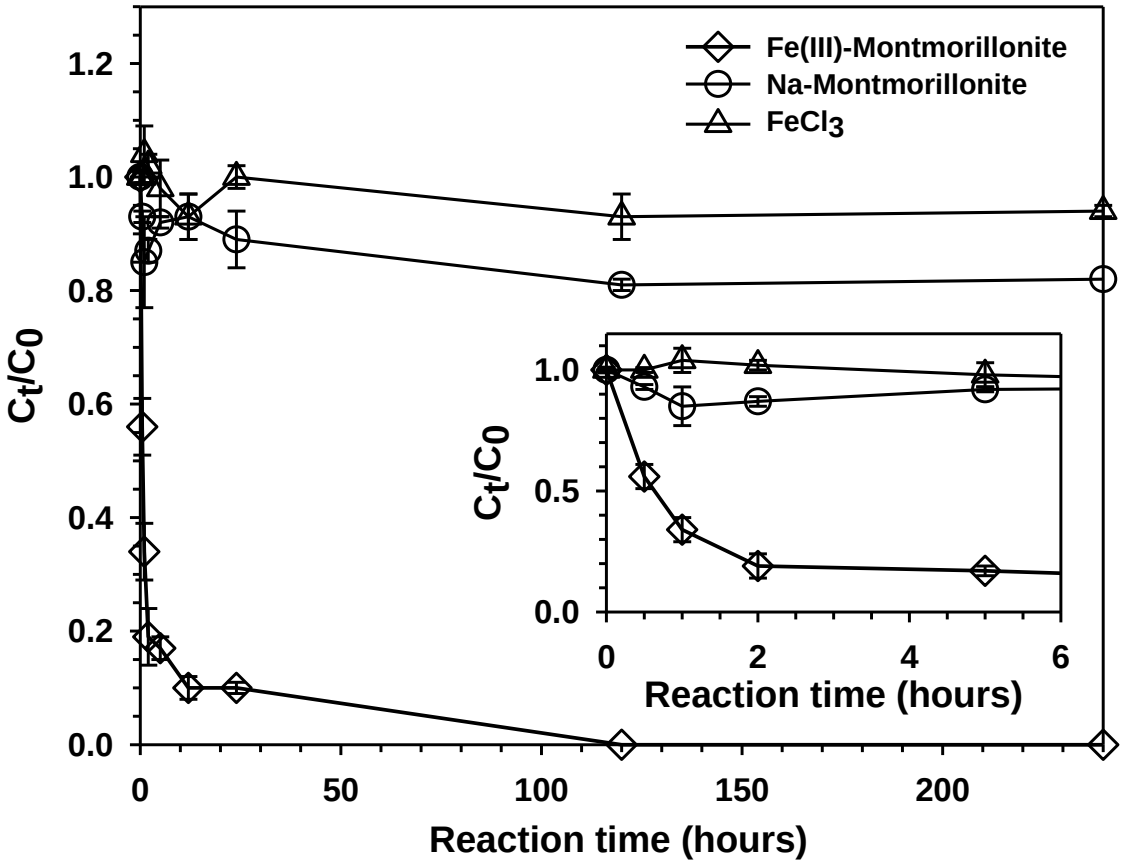

Figure 2.1 βE2 transformation kinetics in aqueous systems containing Fe^{3+}-saturated montmorillonite, Na^{+}-montmorillonite, and 33.2 mM $FeCl_3$ treatment. The initial βE2 concentration was 0.01 mmol βE2 /g of mineral. The amount of Fe^{3+} in the $FeCl_3$ system was equivalent to amount of Fe^{3+} saturated on the montmorillonite.

Previous studies had investigated reaction of aromatic compounds with transition metal cations (e.g., Fe^{3+}, Cu^{2+}) saturated montmorillonite.[20, 21, 33-36] The results lead to the proposal that during the reaction, electrons were donated by the unsaturated organic compounds to the metal cations sorbed on the negatively charged interlayer surfaces of montmorillonite, resulting in formation of radical cations of aromatic molecules and reduced metal cations such as Fe^{2+}, Cu^{+}, which can be oxidized back to Fe^{3+}, Cu^{2+} in aerobic conditions.[33, 35, 37] The formed organic radicals are not stable and can be further degraded[33] or oligomerized.[34, 38]

The observed rapid βE2 transformation in the Fe^{3+}-saturated montmorillonite system (Figure 2.1) suggests redox reactions between βE2 and Fe^{3+}, similar to the mechanism proposed by previous studies.[21, 22] Because the lone pair electrons on the phenolic functional group and the benzene ring π cloud of βE2 structure are conjugated, the phenolic functional group is prone to undergo an electron-transfer reaction with Fe^{3+} to form a free βE2 radical. The unpaired electron of the resulting βE2 radical may delocalize through resonance to the respective conjugated positions of the neighboring benzene ring. The data shown in Figure 2.1 further demonstrated that the redox reaction is mainly facilitated and enhanced by mineral surface chemistry based on the fact that less than 6% of βE2 was removed in the Na^+-montmorillonite aqueous system as well as in the $FeCl_3$ solution, where Fe^{3+} was not sorbed to montmorillonite surfaces in both systems.

Although Na^+-montmorillonite naturally contains structural Fe(III) evenly distributed in the octahedral layers of the mineral at a concentration of approximately 0.61 mmol Fe(III)/g mineral,[39] the inaccessibility of the Fe(III) trapped in the octahedral layer and lack of surface reaction sites with Fe^{3+} contributed to the limited and slow βE2 transformation in the Na^+-montmorillonite system (Figure 2.1). Microbial contribution to the βE2 transformation in the Na^+-montmorillonite system, although expected to be low, cannot be excluded without additional microbial activity characterization. In the $FeCl_3$ solution, the phenolic group of βE2 interact with Fe^{3+} via outer sphere complexation,[20] resulting in limited electron transfer from βE2 to Fe^{3+} because of the aqueous layer around Fe^{3+}. In the Fe^{3+}-saturated montmorillonite system, the planar negatively charged montmorillonite interlayer surfaces catalyze the oxidative transformation of βE2 by surface sorbed Fe^{3+}, most likely via enhancement of precursor inner sphere complexation of the

organic reductant and the metal oxidant and the associated electron transfer within a precursor complex,[40] resulting in the formation of βE2 radicals and their further transformation.

2.3.2 βE2 transformation products-experimental observation

The products formed during Fe^{3+}-saturated montmorillonite mediated βE2 transformation were characterized using LC/MS. The LC/triple quadruple MS extracted ion chromatograms of a sample collected 5 days after βE2 was incubated with Fe^{3+}-saturated montmorillonite are shown in Figure 2.2. In addition to parent compound βE2 ($[M-H]^-$, m/z = 271), peaks with m/z = 269, 541, 811, and 1081 were observed (Figure 2.2). The appearance of peak with m/z = 269 indicates the formation of deprotonated E1 ($[M-H]^-$) during βE2 transformation. The five peaks (D_1-D_5) with retention time of 4.12, 4.87, 5.36, 5.60, and 7.06 min each has m/z = 541, suggesting formation of βE2 dimers with molecular weight of 542 (βE2×2-2H=542). The three peaks (T_1-T_3) clustered between 6.50 and 7.50 min in Figure 2.2 each has m/z = 811, indicating formation of βE2 trimers with molecular weight of 812 (βE2×3-4H=812). The broad peak appears at retention time of 11.50 min has m/z = 1081, suggesting molecular mass of 1082, which corresponds to βE2 tetramer (272×4-6H=1082). Table 2.2 shows a close match between the theoretical molecular mass of the proposed βE2 transformation products and those detected using a UPLC-ESI-Q-TOF.

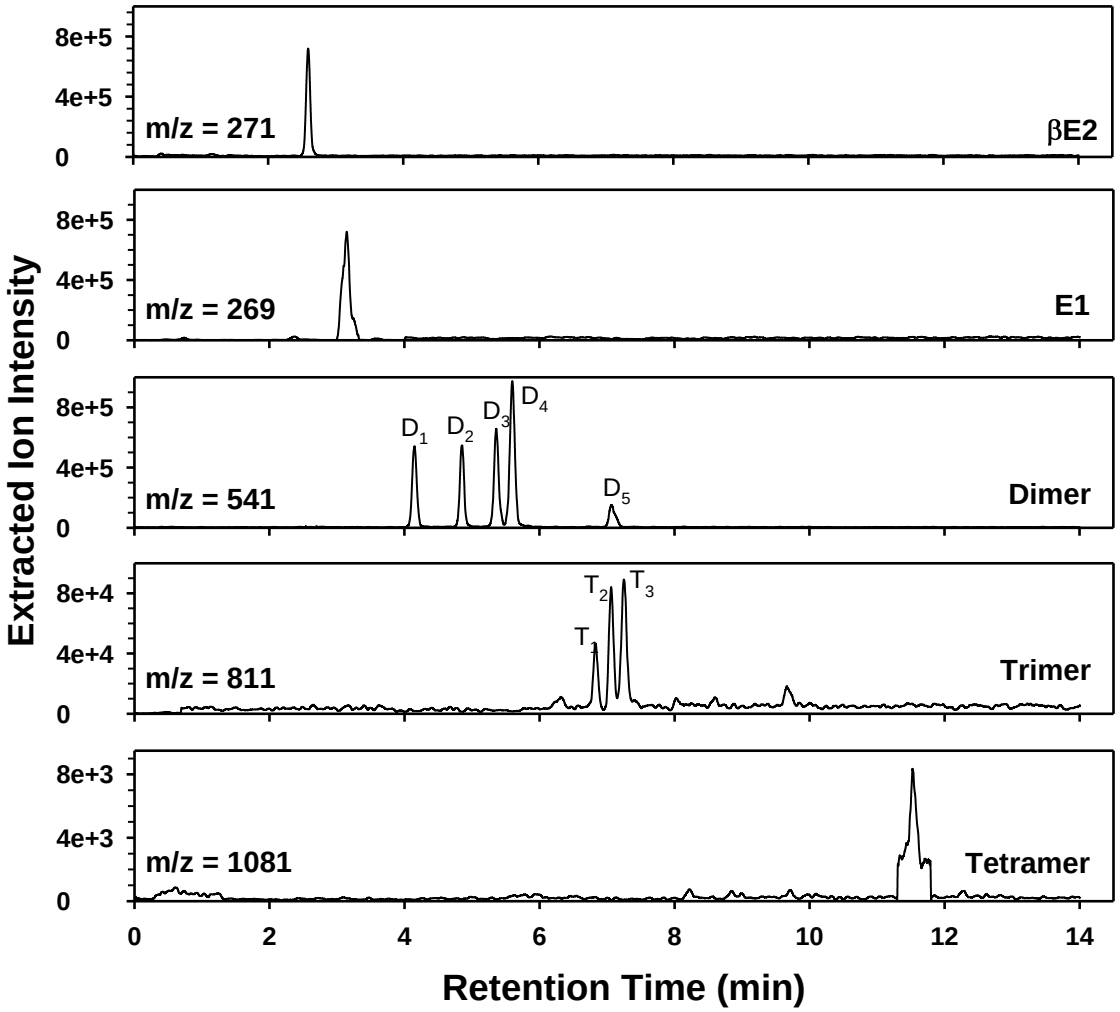

Figure 2.2 LC/MS extracted ion chromatograms of compounds in a sample collected 5 days after βE2 was incubated with Fe^{3+}-saturated montmorillonite.

Table 2.2 Accurate mass measurement of βE2 transformation products in Fe^{3+}-saturated montmorillonite system.

Products*		Retention Time (min)	Formula	Molecular Mass (u)	
				Experimental[#]	Theoretical
βE2		2.597	$C_{18}H_{24}O_2$	272.21	272.38
E1		3.238	$C_{18}H_{22}O_2$	270.21	270.16
βE2 Dimers	D_1	4.119	$C_{36}H_{46}O_4$	542.3386	542.3396
	D_2	4.873			
	D_3	5.358			
	D_4	5.604			
	D_5	7.059			
βE2 Trimers	T_1	6.828	$C_{54}H_{68}O_6$	812.5013	812.5016
	T_2	7.067			
	T_3	7.261			
Tetramer		11.544	$C_{72}H_{90}O_8$	1082.6660	1082.6636

*peaks are shown in Figure 2.2.
#mass spectra are shown in Figures 2.3, S2.4, and S2.5.

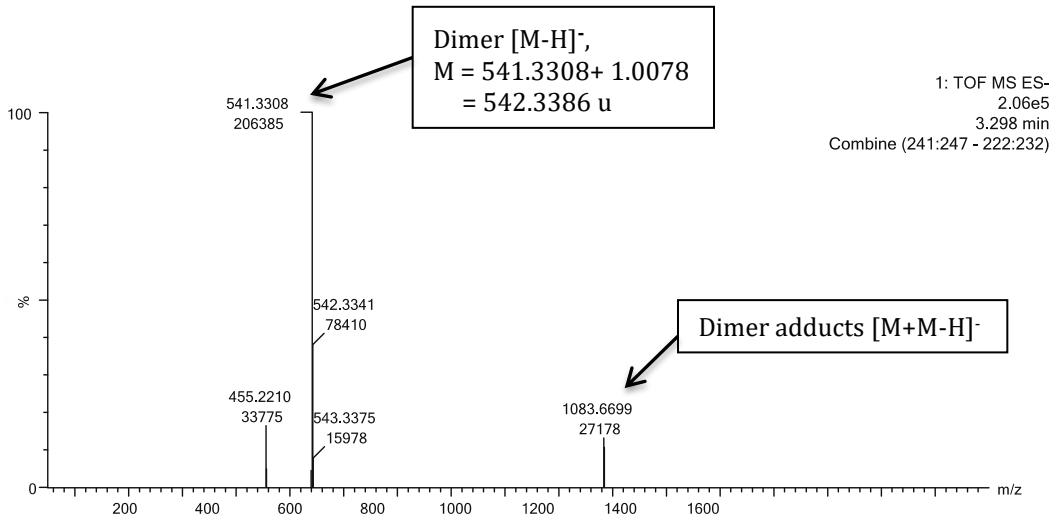

Figure 2.3 UPLC-ESI-Q-TOF extracted negative ion mass spectrum for βE2 dimer (D1, Figure 2.2). The mass spectra for all the other dimers are similar to this one.

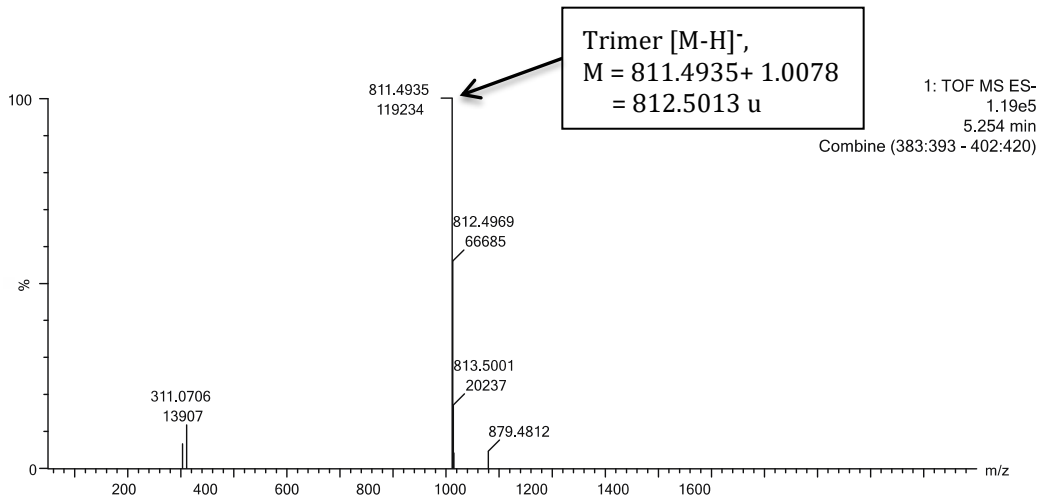

Figure 2.4 UPLC-ESI-Q-TOF extracted negative ion mass spectrum for βE2 trimer (T1, Figure 2.2). The mass spectra for all the other timers are similar to this one.

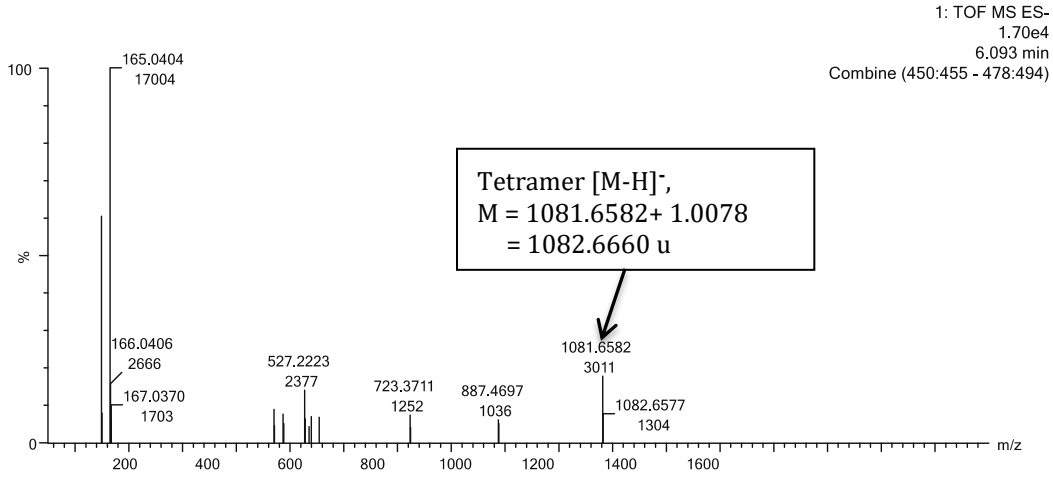

Figure 2.5 UPLC-ESI-Q-TOF extracted negative ion mass spectrum for βE2 tetramer (Figure 2.2)

As shown in Figure 2.6, in the Fe^{3+}-saturated montmorillonite system the production of E1 rapidly increased initially, reached to peak level after 0.5 h, and then disappeared from the system at day 5. Compared to the amount of βE2 initially added to the system, only a small fraction of E1 was produced, with a maximum mole ratio of E1/E2 at 0.99±0.20% after 0.5 hours of reaction when the E1 level reached to its maximum.

Previous researches have shown that E1 produced by oxidation of βE2 can be quickly converted back to βE2 via reduction.[41, 42] It is possible that oxidation of the Fe^{2+} produced from Fe^{3+}-E2 redox reaction quickly reduced E1 back to βE2.

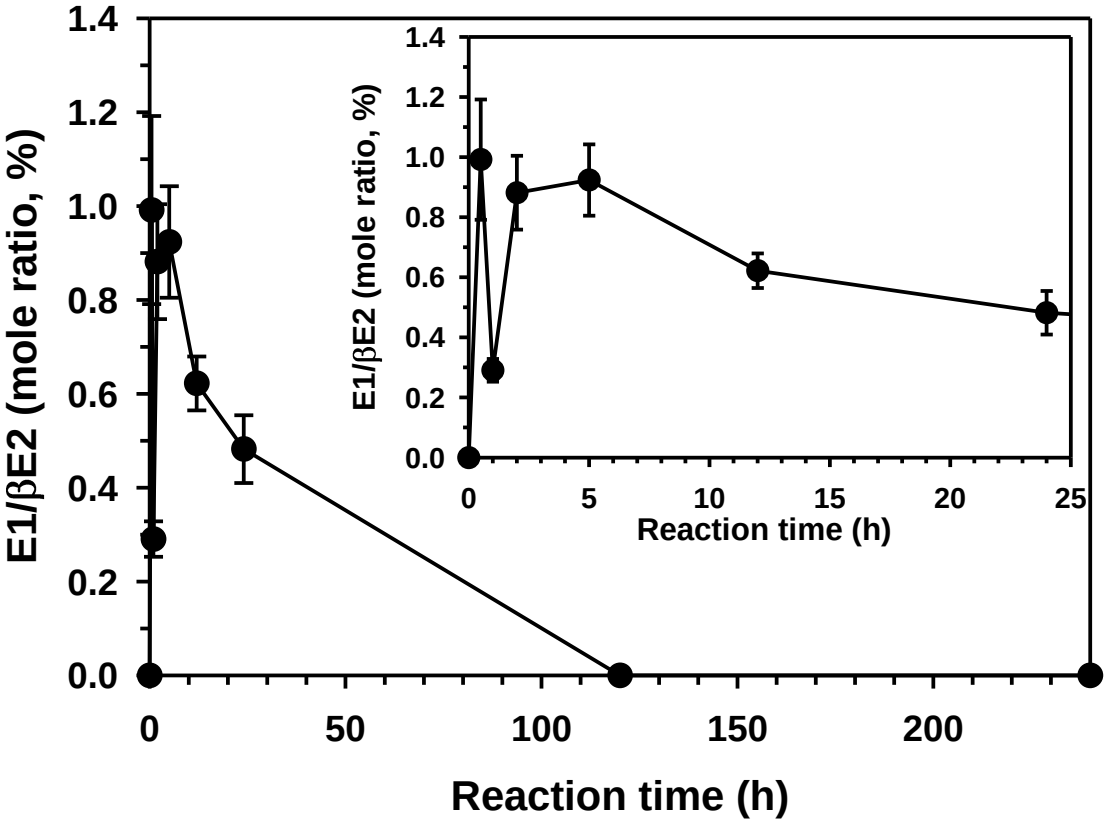

Figure 2.6 Formation kinetics of E1 during βE2 reaction with Fe^{3+}-saturated montmorillonite. The initial βE2 concentration was 0.01 mmol βE2 /g of mineral.

Due to lack of analytical standards, βE2 dimer, trimer, and tetramer levels were not quantified. As shown in Figure 2.7, the sum of five dimer peak areas, an indicator of detected level of all five dimers in the ethyl acetate extract of sediment phase, increased rapidly and reached the maximum within the first hour of reaction. The total peak area of all five dimers decreased after 2 hours and remained unchanged up to 5 hours. Its level

went back up slightly at 12 hour followed by a steady decrease thereafter, but remained detectable at 10 days. Similar trend was observed for the peak area sum of the three trimers for the first 12 hours of reaction, however, its level remained constant between 12 hours and 5 days of reaction. After 10 days of reaction, the peak sum of trimers decreased slightly but also remained detectable (Figure 2.7). The peak area ratio of ethyl acetate extractable dimers and trimers decreased sharply from around 65 at 0.5 h to 24 at 1 h, and slowly decreased thereafter to around 11 after 5 days of reaction, and remained unchanged until day 10 (Figure 2.7). This observation suggests that after βE2 dimers were formed initially some of them were further transformed to trimers, while some of the trimers were further transformed into other products, resulting in relatively steady dimer/trimer peak area ratio at longer reaction time. The observation of tetramer production (Figure 2.2, Table 2.2) confirms that some trimers were further transformed into tetramers. It is suspected that the low detectable level of ethyl acetate extractable tetramers, as reflected in the small peak area of the broad tetramer peak shown in Figure 2.2, was mostly due to decreased solvent solubility/extractability with increased chain length of oligomers.

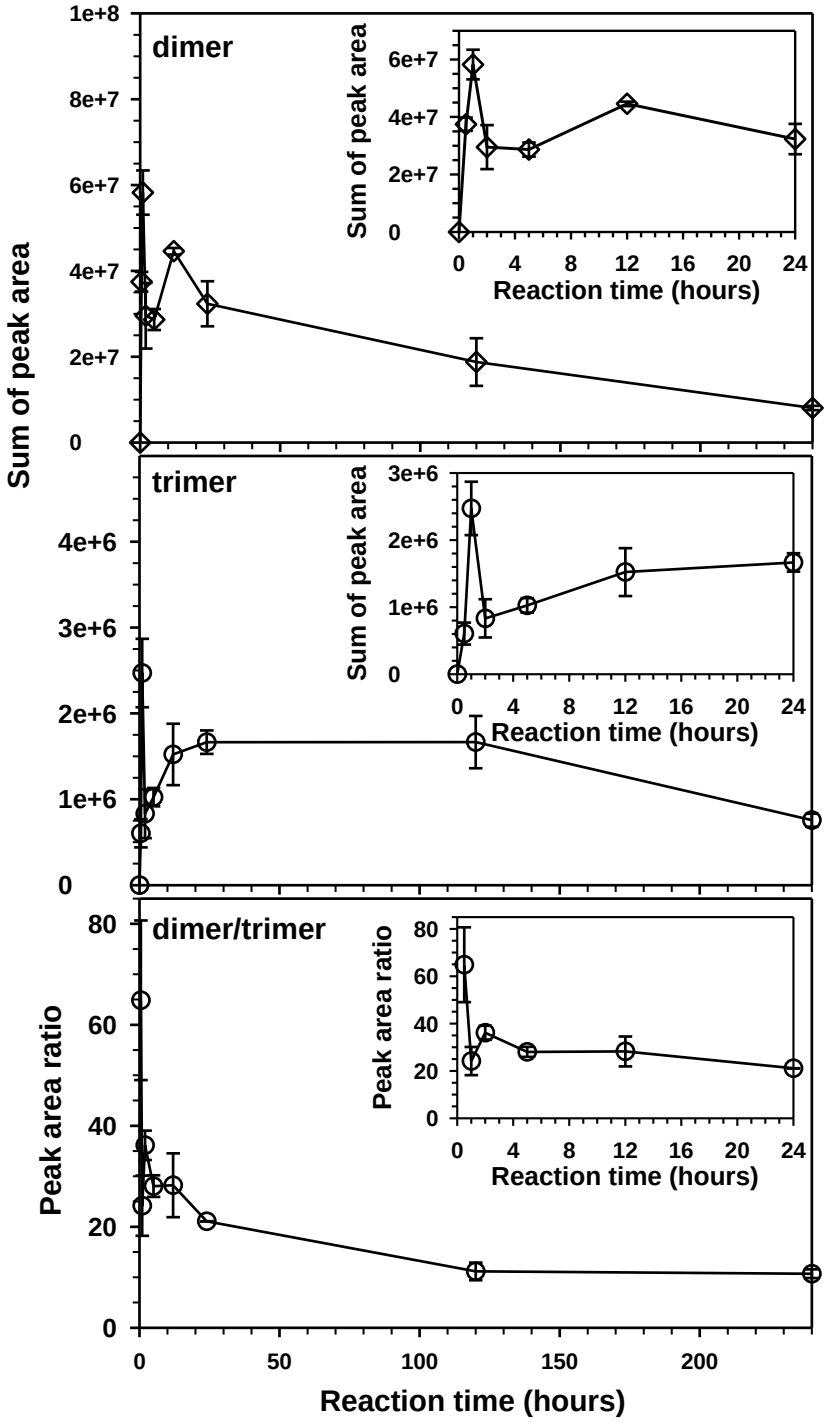

Figure 2.7 Formation kinetics of dimers and trimers during βE2 reaction with Fe^{3+}-saturated montmorillonite. The initial βE2 concentration was 0.01 mmol βE2 /g of mineral.

As shown in Table 2.4, the calculated water solubility of βE2 dimers, trimers, and tetramers are about 1.6×10^2, 1.7×10^5, and 2.3×10^7 times, respectively, lower than that for βE2 (23.7 mg/L). It is most likely that the oligomers were settled with the mineral phase once formed during the reaction and were too insoluble to be extracted by any solvents, resulting in their no-detection on LC/MS. To test this hypothesis, the organic C content in the sediment after 5 days of reaction between βE2 and Fe^{3+}-saturated montmorillonite was determined. The amount of organic C detected in the 5-day sediment samples was on average about 98.1% of that in the βE2 initially added to the system. As shown in Figure 2.1, about 99.7% of initially added βE2 was transformed at day 5, suggesting most of the βE2 transformation products were settled with the mineral phase, most like as highly insoluble βE2 oligomers. The X-ray diffraction (XRD) data in Table 2.3 shows that the difference between the interlayer spacing of freeze-dried sediment collected from βE2 + Fe^{3+}-saturated montmorillonite system after 5-day reaction was only 0.3 Å larger than that of freeze dried sediment from the Fe^{3+}-saturated montmorillonite only system. Considering that the average dimensions of dimers and trimers are 17 Å × 10 Å × 7 Å and 20 Å × 15 Å × 9 Å, respectively (Table 2.1) and even larger dimensions for higher oligomers, it is unlikely that the formed oligomers are trapped in between the interlayer spacing of Fe^{3+}-saturated montmorillonite. Instead, the XRD data suggests the possibility that the βE2 oligomers formed at the interlayer spacing of Fe^{3+}-saturated montmorillonite can be easily separated from the mineral surfaces during extraction and settled on their own with the mineral sediment.

Table 2.3 X-Ray Diffraction (XRD) analysis of freeze-dried sediment phase of samples after 5 days of reaction.

Sample	d_{001}(Å)
Fe^{3+}-saturated montmorillonite	13.43±0.13
βE2 + Fe^{3+}-saturated montmorillonite	13.73± 0.19
Na^{+}-montmorillonite	12.44±0.04

Table 2.4 Calculated water solubility of βE2 and its oligomers.

Compound	Average water solubility (mg/L)*
βE2	23.7
Dimer	0.15
Trimer	1.38×10^{-4}
Tetramer	1.03×10^{-6}

* Calculated using online software: ALOGPS 2.1 (http://www.vcclab.org/lab/alogps/)

2.3.3 βE2 transformation products-computational characterization

The LC/MS results demonstrated that the molecular mass of detected βE2 oligomer products followed the pattern of nM - 2(n - 1) (Table 2.2), where n is the number of coupling βE2 monomer and M is the molecular mass of βE2. Such pattern often indicates radical coupling reactions, where a dimer is formed by covalent bonding of two parent monomers with elimination of two hydrogen atoms.[23] The dimers could further undergo coupling reactions and yield larger oligomers.[23, 43, 44] To further identify possible structures of βE2 dimers and trimers, relative thermodynamic stability of βE2 dimer and trimer products were computed using electronic structure calculations (Table 2.5). Because the number of possible isomers for the association of four or more βE2 radicals grows intractably large, computational exploration of oligomers other than dimers and trimers was not approached. Based on the spin and charge density computational results published

by Mao et al.,[45] possible coupling products were predicted and the relative energy of each coupling products was calculated. The computational results suggested that βE2 dimers were most likely formed by the bond coupling of unsubstituted O1, C3, and C7 on the phenolic ring of a βE2 radical with those on the second βE2 to form eight dimer conformers as listed in Table 2.5. The computer-optimized relative energy for the eight dimer conformers listed in Table 2.5 shows that 7-3', 3-7', and 3-3' dimer coupling species have similar relative energies and the highest thermodynamic stability, indicating their highest possibility of formation compared to other species during the reaction. Compared to the relative energies of the three most likely formed dimer species, the relative energy of 1-3', 7-7', and 1-7' dimer coupling species increased by 1.5, 3.3, and 4.9 kcal/mol, respectively. The relative energies for the 3-1' and 7-1' dimer coupling species are similar and both are slightly higher than that for the 1-7' dimer. The ranking of the calculated relative energy of the dimer species (Table 2.5) suggests the formation possibility of dimer coupling species as: 7-3' ≈ 3-7' ≈ 3-3' > 1-3' > 7-7' > 1-7' > 3-1' ≈ 7-1'. Dimer conformers with 7-3', 3-7', 3-3', 1-3', and 7-7' bond couplings were also observed by NMR for oxidative coupling reactions of βE2 in laccase or peroxidase/H_2O_2 systems.[46, 47]

Table 2.5 Relative molecular energy for βE2 dimers and trimers

	Example of molecular structure of parent compounds	Bonding positions	Relative energy* (kcal/mol)
Dimers	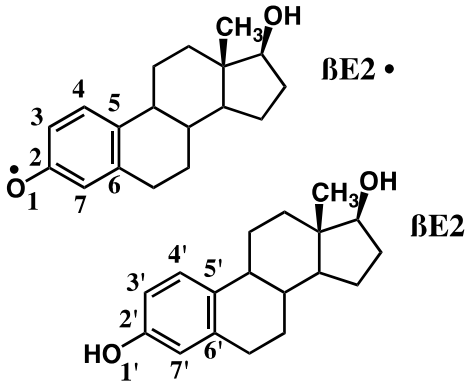	7-3’	0.0
		3-7’	0.2
		3-3’	0.6
		1-3’	2.1
		7-7’	3.9
		1-7’	5.5
		3-1’	5.9
		7-1’	6.0
Trimers		7-3’, 3-3’’	0.0
		3-3’, 7-7’’	1.0
		7-3’, 3-7’’	3.1
		7-7’, 3-3’’	3.2

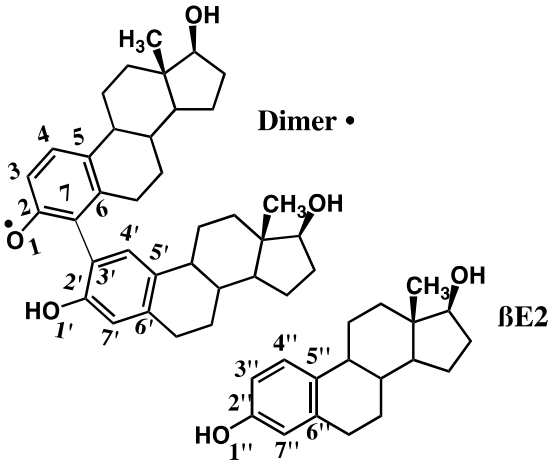	Dimer • ßE2	3-3', 7-3''	3.6

*Relative energy referred to the lowest energy of a compound within the same oligomer series.

Computational results showed that a βE2 trimer was slightly more likely formed by coupling reaction of a βE2 dimer radical to a neutral βE2 molecule rather than coupling reaction between an βE2 radical and a neutral βE2 dimer because the relative energy of former reaction is on average 1.8 kcal/mol lower than that of the later reaction scenario. Table 2.5 lists five trimer conformers with the lowest relative energies among all possible trimer products. The formation possibility of trimer coupling species are: (7-3', 3-3'') > (3-3', 7-7'') > (7-3', 3-7'') ≈ (7-7', 3-3'') ≈ (3-3', 7-3''). Figure 2.8 and 2.9 illustrate the optimized molecular structures of dimers and trimers listed in Table 2.5.

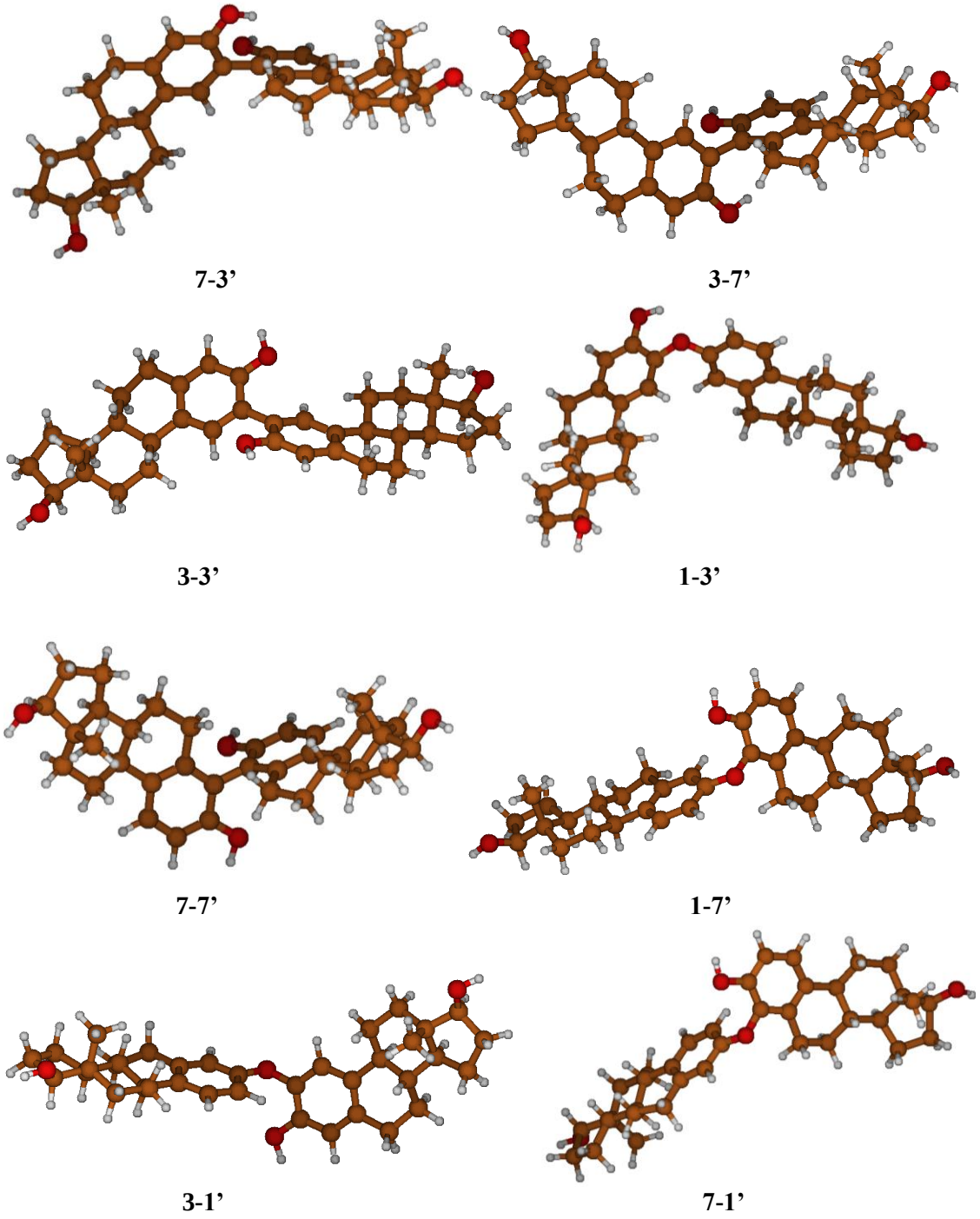

Figure 2.8 Molecular structure of E2 dimer conformers. (C atom: brown; H atom: white; and O atom: red). The 3-D structures were displayed using free software Jmol (http://jmol.sourceforge.net/download/). The coordinates of each structure is provided in Appendix Table S1.

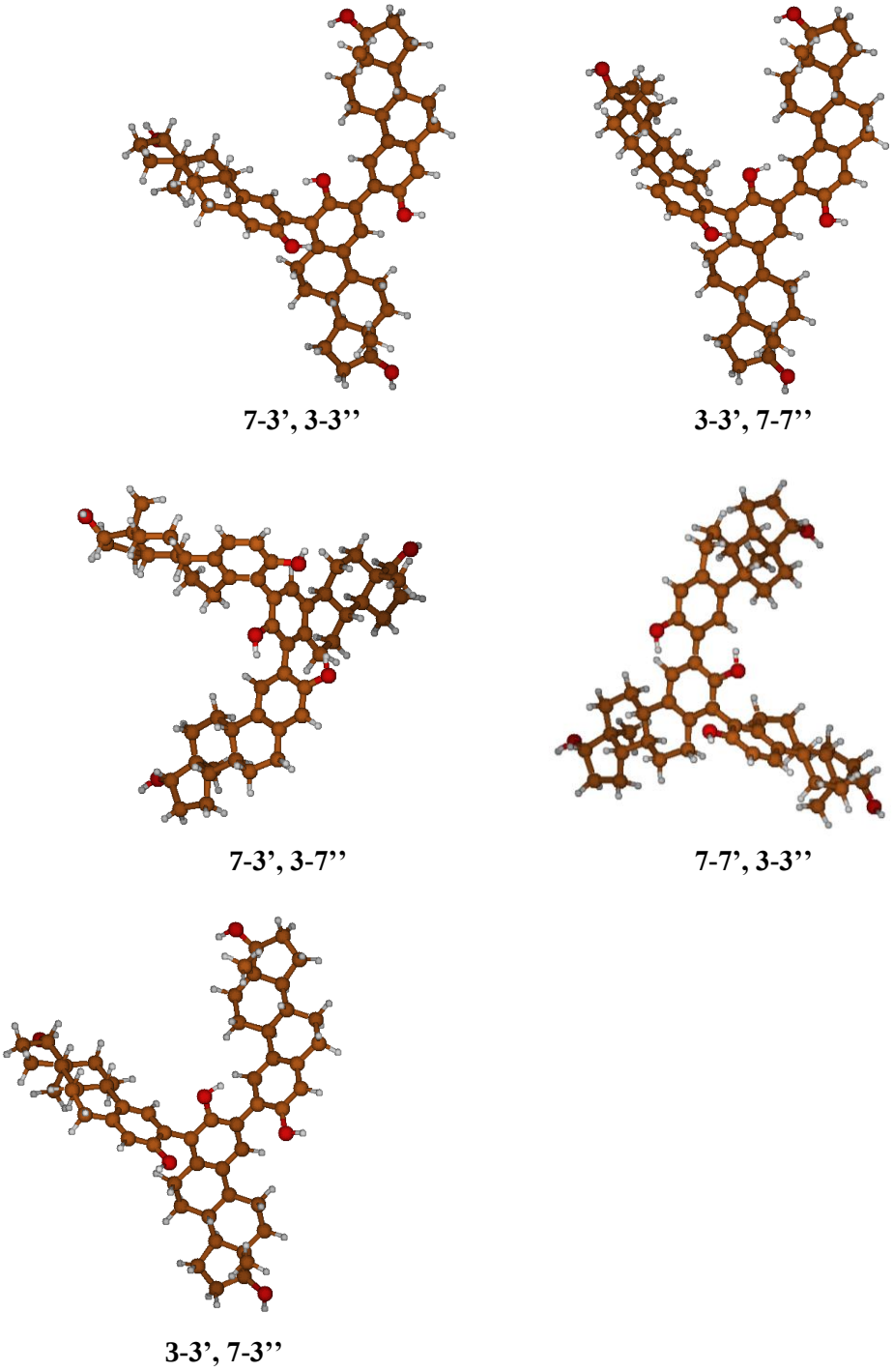

Figure 2.9 Molecular structure of βE2 trimer conformers. (C atom: brown; H atom: white; and O atom: red). The 3-D structures were displayed using free software Jmol (http://jmol.sourceforge.net/download/). The coordinates of each structure is provided in Appendix Table S1.

The experimental data of this paper suggest that βE2 oligomers are the major products of reaction between βE2 and Fe^{3+}-saturated montmorillonite in an aqueous system. The βE2 oligomerization is catalyzed by the Fe^{3+} sorbed on montmorillonite interlayer surfaces, producing highly insoluble βE2 oligomers. Using the relative thermodynamic stability predicted by electronic structure calculations, a schematic of the plausible reaction pathways is shown in Figure 2.10.

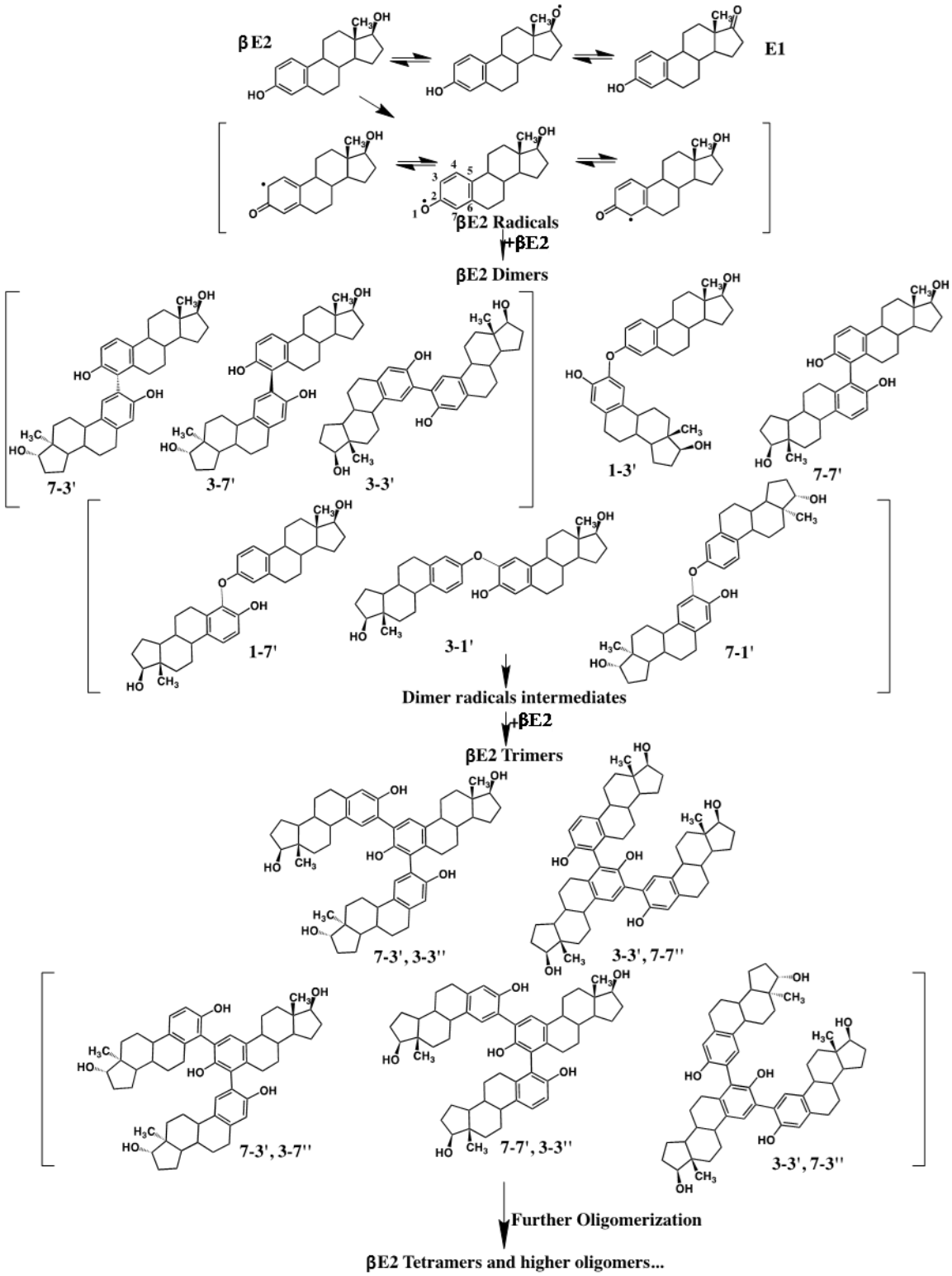

Figure 2.10 Proposed reaction pathways for Fe^{3+}-saturated montmorillonite catalyzed βE2 oligomerization.

2.4 Environmental Implication

This study provided, for the first time, experimental evidence that ~98% of βE2 was transformed into highly water insoluble oligomers in an aqueous system containing Fe^{3+}-saturated montmorillonite and at pH level that is similar to the pH range (6.5 to 8.5) of typical domestic wastewater. With an estimated reaction rate constant of ~200 (mmol E2/g mineral)$^{-1}h^{-1}$ and a half-life of ~0.50 h, Fe^{3+}-saturated montmorillonite can potentially be used for removal of βE2 and other hormones during wastewater treatment processes. The βE2 oligomers, which are $>10^7$ times less water soluble than βE2 (Table 2.4), can be settled out of the aqueous phase during wastewater treatment processes and become much less bioavailable and mobile than the parent compound. Previous research has shown that triclosan dimers and trimers formed in the presence of Fe^{3+}-saturated montmorillonite exhibited high chemical stability in highly oxidative and reductive conditions,[48] implying that other oligomers formed in similar reactions could potentially be stable under natural environment conditions.

In addition, because oligomers are not accumulated over the reaction sites on the interlayer surfaces of Fe^{3+}-saturated montmorillonite, it is possible for the oligomerization reaction at the reaction sites to occur repeatedly, resulting in extended effectiveness of Fe^{3+}-saturated montmorillonite for removal of contaminants from wastewater. As shown in Figure 2.11, even after five consecutive 5-day reaction cycles using the same Fe^{3+}-saturated montmorillonite and the same initial level of βE2 at each cycle, the βE2 removal efficiency remained at >84%.

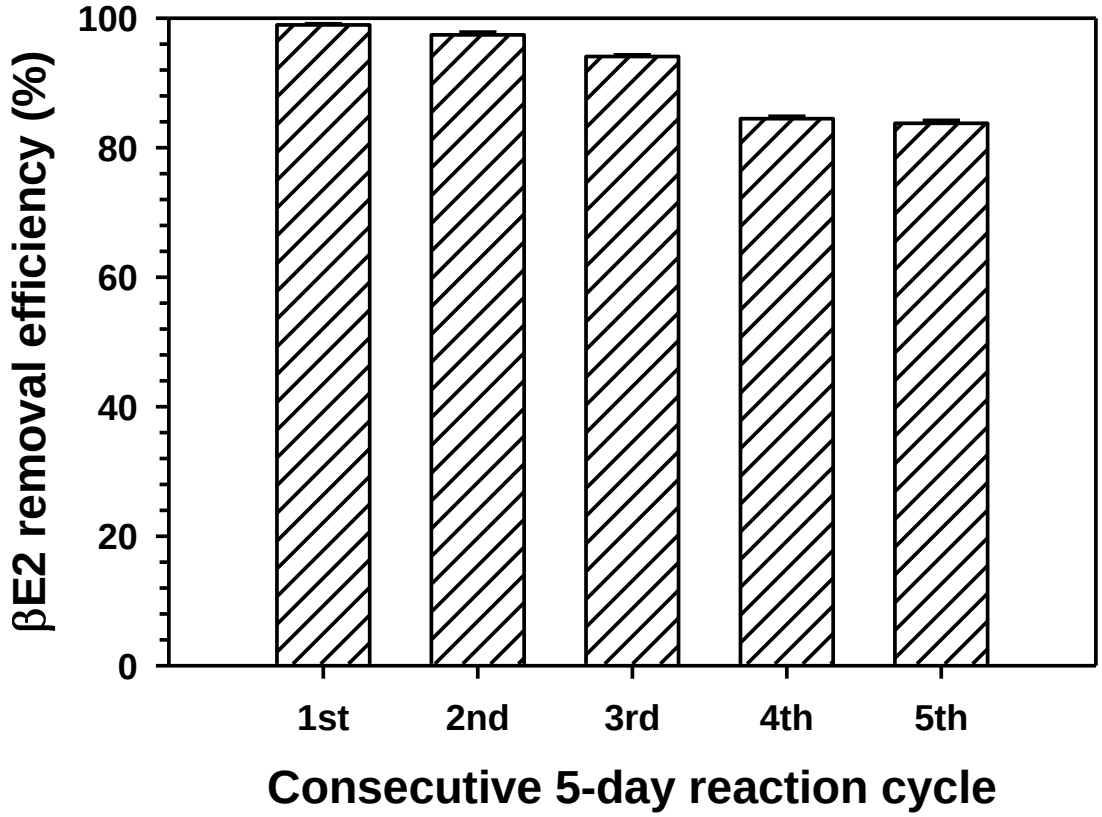

Figure 2.11 βE2 removal efficiency of consecutive 5-day reaction cycles using the same Fe^{3+}-saturated montmorillonite. The concentration of βE2 at the beginning of each reaction cycle was 0.01 mmol βE2 /g of mineral.

It is important to point out that βE2 concentration much higher than that detected in typical WWTP effluents was used for this study because the focus of this study was to assess the capacity of the Fe^{3+}-saturated montmorillonite to polymerize βE2 and to understand the reaction pathways. Investigation on the concentration dependence of this reaction is important and would warrant a separate study. Our previous investigation on Fe^{3+}-saturated montmorillonite catalyzed polymerization of triclosan (TCS) demonstrated inverse correlation between TCS half-life and initial TCS concentration.[22] Reduction of 30 times in initial TCS concentration resulted in 400% reduction in TCS half life. Similar inverse correlation between reaction rate and initial concentration is, therefore, expected

for Fe^{3+}-saturated montmorillonite catalyzed polymerization of βE2. The half life of E2 in the current study using high initial E2 concentration was about 0.5 hours. Its half life is expected to be much shorter than 0.5 hours at lower initial E2 concentrations based on the result from our previous investigation.[22] However, even 0.5 hour is well within the 1-5 day hydraulic retention time in typical secondary wastewater treatment plants.[49]

In summary, because montmorillonite is a widely distributed mineral worldwide, the preparation of Fe^{3+}-saturated montmorillonite is straightforward and low cost, and Fe^{3+}-saturated montmorillonite has fast removal rate, high removal efficiency, and repeated usage, it has a great potential as a cost effective material for effective removal of phenolic organic compounds from domestic wastewater as well as animal lagoon effluent.

ACKNOWLEDGEMENTS

We would like to acknowledge the financial support from USDA-AFRI award (No.2009-65102-05923). Funding for this work was provided in part, by the Virginia Agricultural Experiment Station and the Hatch Program of the National Institute of Food and Agriculture, U.S. Department of Agriculture.

2.5 References

1. Qin, C.; Troya, D.; Shang, C.; Hildreth, S.; Helm, R.; Xia, K., Surface catalyzed oxidative oligomerization of 17β-estradiol by Fe3+-saturated montmorillonite. *Environmental science & technology* **2014,** *49*, (2), 956-964.
2. Kolpin, D. W.; Furlong, E. T.; Meyer, M. T.; Thurman, E. M.; Zaugg, S. D.; Barber, L. B.; Buxton, H. T., Pharmaceuticals, hormones, and other organic wastewater contaminants in US streams, 1999-2000: A national reconnaissance. *Environmental science & technology* **2002,** *36*, (6), 1202-1211.
3. Yamamoto, A.; Kakutani, N.; Yamamoto, K.; Kamiura, T.; Miyakoda, H., Steroid hormone profiles of urban and tidal rivers using LC/MS/MS equipped with electrospray ionization and atmospheric pressure photoionization sources. *Environmental science & technology* **2006,** *40*, (13), 4132-4137.
4. Chang, H.; Wan, Y.; Hu, J., Determination and source apportionment of five classes of steroid hormones in urban rivers. *Environmental science & technology* **2009,** *43*, (20), 7691-7698.
5. Stasinakis, A. S.; Gatidou, G.; Mamais, D.; Thomaidis, N. S.; Lekkas, T. D., Occurrence and fate of endocrine disrupters in Greek sewage treatment plants. *Water Research* **2008,** *42*, (6), 1796-1804.
6. Benotti, M. J.; Trenholm, R. A.; Vanderford, B. J.; Holady, J. C.; Stanford, B. D.; Snyder, S. A., Pharmaceuticals and endocrine disrupting compounds in US drinking water. *Environmental Science & Technology* **2008,** *43*, (3), 597-603.
7. Fan, Z.; Hu, J.; An, W.; Yang, M., Detection and Occurrence of Chlorinated Byproducts of Bisphenol A, Nonylphenol, and Estrogens in Drinking Water of China: Comparison to the Parent Compounds. *Environmental science & technology* **2013,** *47*, (19), 10841-10850.
8. Routledge, E. J.; Sheahan, D.; Desbrow, C.; Brighty, G. C.; Waldock, M.; Sumpter, J. P., Identification of estrogenic chemicals in STW effluent. 2. In vivo responses in trout and roach. *Environmental Science & Technology* **1998,** *32*, (11), 1559-1565.
9. Thorpe, K. L.; Maack, G.; Benstead, R.; Tyler, C. R., Estrogenic wastewater treatment works effluents reduce egg production in fish. *Environmental science & technology* **2009,** *43*, (8), 2976-2982.
10. Lange, A.; Paull, G. C.; Hamilton, P. B.; Iguchi, T.; Tyler, C. R., Implications of persistent exposure to treated wastewater effluent for breeding in wild roach (Rutilus rutilus) populations. *Environmental science & technology* **2011,** *45*, (4), 1673-1679.
11. Kidd, K. A.; Blanchfield, P. J.; Mills, K. H.; Palace, V. P.; Evans, R. E.; Lazorchak, J. M.; Flick, R. W., Collapse of a fish population after exposure to a synthetic estrogen. *Proceedings of the National Academy of Sciences* **2007,** *104*, (21), 8897-8901.
12. Griffith, D. R.; Kido Soule, M. C.; Matsufuji, H.; Eglinton, T. I.; Kujawinski, E. B.; Gschwend, P. M., Measuring Free, Conjugated, and Halogenated Estrogens in Secondary Treated Wastewater Effluent. *Environmental science & technology* **2014,** *48*, (5), 2569-2578.

13. Combalbert, S.; Hernandez-Raquet, G., Occurrence, fate, and biodegradation of estrogens in sewage and manure. *Applied Microbiology and Biotechnology* **2010,** *86*, (6), 1671-1692.
14. Baynes, A.; Green, C.; Nicol, E.; Beresford, N.; Kanda, R.; Henshaw, A.; Churchley, J.; Jobling, S., Additional Treatment of Wastewater Reduces Endocrine Disruption in Wild Fish A Comparative Study of Tertiary and Advanced Treatments. *Environmental science & technology* **2012,** *46*, (10), 5565-5573.
15. Ings, J. S.; Servos, M. R.; Vijayan, M. M., Hepatic transcriptomics and protein expression in rainbow trout exposed to municipal wastewater effluent. *Environmental science & technology* **2011,** *45*, (6), 2368-2376.
16. Eggen, R. I. L.; Hollender, J.; Joss, A.; Schärer, M.; Stamm, C., Reducing the Discharge of Micropollutants in the Aquatic Environment: The Benefits of Upgrading Wastewater Treatment Plants. *Environmental science & technology* **2014,** *48*, (14), 7683-7689.
17. Suri, R. P. S.; Singh, T. S.; Abburi, S., Influence of alkalinity and salinity on the sonochemical degradation of estrogen hormones in aqueous solution. *Environmental science & technology* **2010,** *44*, (4), 1373-1379.
18. Frontistis, Z.; Drosou, C.; Tyrovola, K.; Mantzavinos, D.; Fatta-Kassinos, D.; Venieri, D.; Xekoukoulotakis, N. P., Experimental and modeling studies of the degradation of estrogen hormones in aqueous TiO2 suspensions under simulated solar radiation. *Industrial & Engineering Chemistry Research* **2012,** *51*, (51), 16552-16563.
19. Filby, A. L.; Shears, J. A.; Drage, B. E.; Churchley, J. H.; Tyler, C. R., Effects of advanced treatments of wastewater effluents on estrogenic and reproductive health impacts in fish. *Environmental science & technology* **2010,** *44*, (11), 4348-4354.
20. Polubesova, T.; Eldad, S.; Chefetz, B., Adsorption and oxidative transformation of phenolic acids by Fe (III)-montmorillonite. *Environmental science & technology* **2010,** *44*, (11), 4203-4209.
21. Gu, C.; Li, H.; Teppen, B. J.; Boyd, S. A., Octachlorodibenzodioxin formation on Fe (III)-montmorillonite clay. *Environmental science & technology* **2008,** *42*, (13), 4758-4763.
22. Liyanapatirana, C.; Gwaltney, S. R.; Xia, K., Transformation of triclosan by Fe (III)-saturated montmorillonite. *Environmental science & technology* **2009,** *44*, (2), 668-674.
23. Lu, J.; Huang, Q.; Mao, L., Removal of acetaminophen using enzyme-mediated oxidative coupling processes: I. Reaction rates and pathways. *Environmental science & technology* **2009,** *43*, (18), 7062-7067.
24. Allen, B. L., and B. F. Hajek, Mineral Occurrence in Soil Environments. In *Minerals in Soil Environments*, Second ed.; Dixon, J. B., and S. B. Weed, Ed. Soil Science Society of America: Madison, 1989; pp 199-278.
25. Seger, M. R.; Maciel, G. E., NMR investigation of the behavior of an organothiophosphate pesticide, chlorpyrifos, sorbed on montmorillonite clays. *Environmental science & technology* **2006,** *40*, (3), 797-802.
26. Wei, J.; Furrer, G.; Kaufmann, S.; Schulin, R., Influence of clay minerals on the hydrolysis of carbamate pesticides. *Environmental science & technology* **2001,** *35*, (11), 2226-2232.

27. Tambach, T. J.; Bolhuis, P. G.; Hensen, E. J. M.; Smit, B., Hysteresis in Clay Swelling Induced by Hydrogen Bonding: Accurate Prediction of Swelling States. *Langmuir* **2005,** *22*, (3), 1223-1234.
28. Grygar, T., D. Hradil, P.Bezdicka, B. Dousova, L. Capek, and O. Schneeweiss., Fe(III)-modified Montmorillonite and Bentonite: Synthesis, Chemical and UV-Vis spectral Characterization, Arsenic Sorption, and Catalysis of Oxidative Dehydrogenation of Propane. *Clays and Clay Minerals* **2007,** *55*, 165-176.
29. Wallis, P. J.; Chaffee, A. L.; Gates, W. P.; Patti, A. F.; Scott, J. L., Partial Exchange of Fe(III) Montmorillonite with Hexadecyltrimethylammonium Cation Increases Catalytic Activity for Hydrophobic Substrates. *Langmuir* **2009,** *26*, (6), 4258-4265.
30. Boyd, S. A.; Mortland, M. M., Radical formation and polymerization of chlorophenols and chloroanisole on copper(II)-smectite. *Environmental Science & Technology* **1986,** *20*, (10), 1056-1058.
31. Gu, C.; Li, H.; Teppen, B. J.; Boyd, S. A., Octachlorodibenzodioxin Formation on Fe(III)-Montmorillonite Clay. *Environmental Science & Technology* **2008,** *42*, (13), 4758-4763.
32. Arroyo, L. J.; Li, H.; Teppen, B. J.; Boyd, S. A., A simple method for partial purification of reference clays. *Clays and clay minerals* **2005,** *53*, (5), 511-519.
33. Govindaraj, N.; Mortland, M. M.; Boyd, S. A., Single electron transfer mechanism of oxidative dechlorination of 4-chloroanisole on copper (II)-smectite. *Environmental science & technology* **1987,** *21*, (11), 1119-1123.
34. Boyd, S. A.; Mortland, M. M., Dioxin radical formation and polymerization on Cu (II)-smectite. *Nature* **1985,** *316*, (6028), 532-535.
35. Boyd, S. A.; Mortland, M. M., Radical formation and polymerization of chlorophenols and chloroanisole on copper (II)-smectite. *Environmental science & technology* **1986,** *20*, (10), 1056-1058.
36. Mortland, M. M.; Boyd, S. A., Polymerization and dechlorination of chloroethenes on copper (II)-smectite via radical-cation intermediates. *Environmental science & technology* **1989,** *23*, (2), 223-227.
37. Pal, S.; Bollag, J.-M.; Huang, P. M., Role of abiotic and biotic catalysts in the transformation of phenolic compounds through oxidative coupling reactions. *Soil Biology and Biochemistry* **1994,** *26*, (7), 813-820.
38. Gu, C.; Liu, C.; Ding, Y.; Li, H.; Teppen, B. J.; Johnston, C. T.; Boyd, S. A., Clay Mediated Route to Natural Formation of Polychlorodibenzo-p-dioxins. *Environmental science & technology* **2011,** *45*, (8), 3445-3451.
39. Vantelon, D.; Montarges-Pelletier, E.; Michot, L. J.; Pelletier, M.; Thomas, F.; Briois, V., Iron distribution in the octahedral sheet of dioctahedral smectites. An Fe K-edge X-ray absorption spectroscopy study. *Physics and Chemistry of Minerals* **2003,** *30*, (1), 44-53.
40. Gu, C.; Liu, C.; Johnston, C. T.; Teppen, B. J.; Li, H.; Boyd, S. A., Pentachlorophenol radical cations generated on Fe (III)-montmorillonite initiate octachlorodibenzo-p-dioxin formation in clays: Density functional theory and fourier transform infrared studies. *Environmental science & technology* **2011,** *45*, (4), 1399-1406.

41. Zheng, W.; Li, X.; Yates, S. R.; Bradford, S. A., Anaerobic Transformation Kinetics and Mechanism of Steroid Estrogenic Hormones in Dairy Lagoon Water. *Environmental Science & Technology* **2012,** *46*, (10), 5471-5478.
42. Mashtare, M. L.; Lee, L. S.; Nies, L. F.; Turco, R. F., Transformation of 17α-estradiol, 17β-estradiol, and estrone in sediments under nitrate-and sulfate-reducing conditions. *Environmental science & technology* **2013,** *47*, (13), 7178-7185.
43. Mao, L.; Lu, J.; Habteselassie, M.; Luo, Q.; Gao, S.; Cabrera, M.; Huang, Q., Ligninase-mediated removal of natural and synthetic estrogens from water: II. Reactions of 17β-estradiol. *Environmental science & technology* **2010,** *44*, (7), 2599-2604.
44. Lloret, L.; Eibes, G.; Moreira, M. T.; Feijoo, G.; Lema, J. M., Removal of Estrogenic Compounds from Filtered Secondary Wastewater Effluent in a Continuous Enzymatic Membrane Reactor. Identification of Biotransformation Products. *Environmental science & technology* **2013,** *47*, (9), 4536-4543.
45. Mao, L.; Huang, Q.; Luo, Q.; Lu, J.; Yang, X.; Gao, S., Ligninase-mediated removal of 17β-estradiol from water in the presence of natural organic matter: Efficiency and pathways. *Chemosphere* **2010,** *80*, (4), 469-473.
46. Pezzella, A.; Lista, L.; Napolitano, A.; d'Ischia, M., Oxidative coupling of 17β-estradiol: inventory of oligomer products and configuration assignment of atropoisomeric C4-linked biphenyl-type dimers and trimers. *The Journal of Organic Chemistry* **2004,** *69*, (17), 5652-5659.
47. Nicotra, S.; Intra, A.; Ottolina, G.; Riva, S.; Danieli, B., Laccase-mediated oxidation of the steroid hormone 17β-estradiol in organic solvents. *Tetrahedron: Asymmetry* **2004,** *15*, (18), 2927-2931.
48. Liyanapatirana, C. Oxidative transformation of antimicrobial compounds by ferric-modified montmorillonite. http://library.msstate.edu/etd/show.asp?etd=etd-04252011-101445
49. Hammer, M. J., and M.J. Hammer, Jr., *Water and wastewater Biodegradability of some antibiotics, elimination of the genotoxtechnology*. 4th ed.; Prentice Hall: Upper Saddle River, NJ., 2001.

Chapter 3. Removal of 17β-estradiol from Wastewater Using Fe^{3+}-Saturated Montmorillonite

(To be submitted to Science of the Total Environment)

Abstract

Among endocrine-disrupting chemicals, steroidal estrogens are of particular environmental concern due to their disruptive effect on biological functions of humans and animals even at extremely low concentrations. Effluent discharge from wastewater treatment plants is a significant source for estrogens entering into the environment, resulting in their frequent detection in surface water. Estrogens cannot be completely removed by conventional wastewater treatment processes and remain in effluent discharged into receiving aquatic environment, contributing to feminization effect on the aquatic wildlife in the downstream of discharge point. Our previous study has shown that 17β-estradiol (βE2) can be rapidly removed from pure water due to its polymerization catalyzed by Fe^{3+}-saturated montmorillonite. It is unknown if Fe^{3+}-saturated montmorillonite can also effectively polymerize βE2 in water with other matrices or real world wastewater effluents with complex matrices. Therefore, the effects of dissolved organic matter, pH, temperature, and common cations on Fe^{3+}-saturated montmorillonite catalyzed βE2 polymerization were investigated in this study. Results showed that Fe^{3+}-saturated montmorillonite catalysis achieved highest βE2 removal efficiency at neutral solution pH and higher temperature. Common cations did not have impact on the reaction efficiency. The presence of dissolved organic matter in model water system slightly reduced βE2 removal efficiency. The βE2 removal efficiency was also tested

for wastewater secondary effluents from three wastewater treatment plants. Regardless of the source of wastewater, ~40% βE2 removal efficiency was achieved for the wastewater effluents, when they were exposed to the same dosage of Fe^{3+}-saturated montmorillonite as that for the simple pure water systems, which achieved ~83% removal efficiency. Because of matrix interferences, especially from dissolved organic matter (DOM) in real world wastewater effluents, higher dosage of Fe^{3+}-saturated montmorillonite would be needed to create more available reaction sites for βE2. The finding from this study demonstrated that Fe^{3+}-saturated montmorillonite is a promising low cost material for effective removal of phenolic estrogen compounds from domestic wastewater effluents.

3.1. Introduction

Endocrine-disrupting chemicals (EDCs) have been frequently detected in the natural environment, wastewater effluents, and even drinking water systems [1-3]. This results in an increasing public concern due to their negative impacts on endocrine systems of humans and other organisms [4, 5]. Natural estrogens are EDCs that can cause adverse physiological and development effects even at levels as low as 10 ng/L (parts per trillion, ppt) [6]. Concentrated animal feeding facilities, animal manure land application, and municipal wastewater treatment plants (WWTPs) are major sources contributing to elevated estrogens occurrence in the environment [2, 7, 8]. Conventional WWTP treatment processes are not designed for removal of estrogens below its biological significance levels [9, 10]. The residual estrogens in discharged WWTP effluents have already been found to cause physiological changes in certain aquatic organisms, resulting in potential adverse impact on the ecological heath of receiving surface water [11-13]. Current effort in developing new wastewater treatment approaches for further enhancing estrogen removal

efficiency has largely relied on activated carbon, chlorination, ozonation, ultraviolet irradiation and membrane separation [2, 14]. Although some of the recently developed treatment technologies have exhibited significantly enhanced EDC removal efficiencies [15], the cost for installation, operation, and maintenance could be a key factor that prevents some communities from adopting the new technologies [9].

Recently, utilization of the oxidative coupling processes catalyzed by minerals [16-19] or enzymes [20-22] has been proposed as an alternative effective removal approach for many EDCs that have aromatic structure or contain phenolic functional groups. However, one major disadvantage of enzymatic approach for EDC removal is that enzymes are easily subjected to inactivation in wastewater matrix [23], making the approaches of using minerals for wastewater treatment more practical. Among the minerals that have been tested for EDC removal from water [24-26], Fe^{3+}-saturated montmorillonite has exhibited potential for fast removal rates and high removal efficiencies for EDCs such as triclosan and βE2 without any extra energy consumption [27, 28]. It was also shown to be stable in aqueous systems and can be reusable.

Because of its high specific surface area, high cation exchange capacity, and shrinking-swelling properties, montmorillonite (a 2:1 layer aluminosilicate mineral) can be used as a platform for many nanoscale surface catalyzed organic chemical reactions [27-30]. The montmorillonite surface catalyzed organic chemical reactions involve reduction of the interlayer transitional metal ions such as Cu^{2+} and Fe^{3+} coupled with oxidation of organic compounds, resulting in organic compound radicals that are highly susceptible to further oligomerization and/or degradation reactions [17, 27, 28, 31]. The formed oligomers have water solubility of 10^2 - 10^7 times lower than that of the parent compound, and thus significantly lowered bioavailability favoring their separation and removal from the aqueous phase [27, 28].

It is important to point out that, studies up to date on mineral-catalyzed EDC removal have largely been conducted in simple model systems using pure water as aqueous medium with a major focus on the proof of concept feasibility test and understanding the reaction mechanisms and pathways. It is unknown if the mineral-catalyzed EDC removal is also applicable to more complexed real world wastewater. It is therefore important to learn the impact of different environmental conditions such as temperature, pH, common cations, and dissolved organic matter on the mineral-catalyzed EDC removal reactions. For this study, the effects of above listed environmental factors on the effectiveness of Fe^{3+}-saturated montmorillonite-catalyzed removal of βE2 from water were investigated. The Fe^{3+}-saturated montmorillonite was also used to treat a local WWTP effluent water that contain βE2.

3.2 Materials and methods

3.2.1 Chemicals and Materials

17β-estradiol (βE2) (≥98%) and humic acid sodium salt (technical grade) were purchased from Sigma-Aldrich (St. Louis, MO). Ferric chloride (hexahydrate, ≥97%), sodium chloride (≥99%), calcium chloride (≥99%), HPLC grade acetonitrile, methanol, and ethyl acetate were purchased from Fisher Scientific (Fair Lawn, NJ). Na^{+}-montmorillonite (SWy-2, Crook County, Wyoming) was obtained from the Source Clays Repository of the Clay Minerals Society (Purdue University, West Lafayette, IN). The ultrapure water used in this study was produced by a Millipore Milli-Q water purification system (Milford, MA). The Fe^{3+}-saturated montmorillonite was prepared by cation exchange with $FeCl_3$ using a procedure described in detail in our previous work [28].

3.2.2 Experimental setup

In a 20 mL glass vial, 25 μL of βE2 stock solution (600 μg/mL in methanol) was mixed with 1.5 mL ultrapure water to reach 10 μg/mL before 15 mg of Fe^{3+}-saturated montmorillonite or Na^{+}-montmorillonite was added. The Na^{+}-montmorillonite was used as control treatment. Immediately after the mixtures of βE2 and Fe^{3+}-saturated montmorillonite or Na^{+}-montmorillonite were prepared, the following listed additional treatments were conducted to test the impact of pH, dissolved organic matter, common cations, and temperature on the effectiveness of Fe^{3+}-saturated montmorillonite-catalyzed removal of βE2 from water. For the treatments that examined the pH effect, 0.1 M NaOH or 0.1 M HCl were used to adjust the initial pH of the aqueous solution to pH 3, 6, and 9 before adding Fe^{3+}-saturated montmorillonite to start the reaction. Those covered typical pH levels for most domestic and industrial wastewater [32, 33]. No buffer was used for pH adjustment to avoid potential reactions between buffer chemicals and Fe^{3+}-saturated montmorillonite. Humic acid was added to an above prepared 20 mL glass vial containing βE2 and Fe^{3+}-saturated montmorillonite or Na^{+}-montmorillonite to achieve a final organic carbon content at 15 mg/L, a level within the concentration ranges of dissolved organic carbon in wastewater secondary effluents [34]. Similarly appropriate amount of $CaCl_2$ or NaCl was added to the above prepared 20 mL glass vial to reach final Ca^{2+} or Na^{+} concentration at 10 mM, a representative level in wastewater secondary effluents [35]. This was to test the effect of cations commonly detected in wastewater effluents on the βE2 removal in the presence of Fe^{3+}-saturated montmorillonite. For the treatments testing the impact of environmental temperature on the βE2 removal efficiency, the prepared mixtures of βE2 and Fe^{3+}-saturated montmorillonite or Na^{+}-montmorillonite were subject to 10°C, 25°C, and 40°C, which covered common ambient temperatures for WWTPs [36, 37].

The sample vials with different pH, dissolved organic matter, and common cation treatments were then shaken at 25 °C, while the vials designated for the temperature effect tests were shaken at the targeted temperatures. All samples were shaken in darkness on an incubator shaker for 30 min at 150 rpm before centrifugation at 4000 rpm for 1 min to separate the aqueous phase and the mineral phase. The amounts of βE2 remaining in the aqueous phase and the mineral phase were immediately processed and analyzed using the methods described in section 3.2.3. There were triplicates for each treatment.

Secondary wastewater effluents collected from three different municipal WWTPs were used to test the effectiveness of Fe^{3+}-saturated montmorillonite-catalyzed removal of βE2 from real wastewater samples with much more complex matrices than that of simple DI water systems. Activated sludge process is used as secondary treatment process in all three WWTPs. Secondary effluent samples from those WWTPs were collected, immediately stored in coolers packed with ice, and transported within a couple of hours back to the lab. Once in the lab, the collected water samples were immediately filtered through glass fiber membrane filters (1.6 μm pore size, Fisher Scientific, Fair Lawn, NJ) to remove particulates and suspended solids and then stored at -20°C prior to use.

In a 20 mL glass vial, 1.5 mL of the above prepared wastewater effluent sample spiked with appropriate amount of βE2 to achieve a final concentration of 0.1 mg/L was mixed with 15 mg Fe^{3+}-saturated montmorillonite and shaken in darkness at 25ºC on an incubator shaker for 5 min, 10 min, 15 min, 30 min, 2 h, and 4 h at 150 rpm before separation of the aqueous phase and the mineral phase by centrifugation at 4000 rpm for 1 min. The remaining βE2 in the aqueous and mineral phases was immediately processed and analyzed using the methods described in section 3.2.3. There were triplicates for each treatment.

The βE2 removal efficiency at the termination of a treatment was calculated by:

$$\frac{\text{initial } \beta\text{E2} - (\beta\text{E2 remained in the aqueous phase} + \beta\text{E2 remained in the sediment phase})}{\text{initial } \beta\text{E2}} \text{ x } 100\%$$

3.2.3 Sample extraction, cleanup, and analysis

For the experiment using simple deionized (DI) water, each aqueous phase sample collected at the termination of a treatment was filtered through a 0.2 μm PVDF syringe filter (Thermo Fisher, Rockwood, TN) followed by analysis for βE2 using high performance liquid chromatography (HPLC, Agilent 1260 Infinity, Agilent Co., CA, USA) apparatus with fluorescent detector. For the experiment using secondary wastewater effluents, each aqueous phase sample collected at the termination of a treatment was diluted to 100 mL using ultrapure water, acidified to pH ~2 using 5 M HCl, and then cleaned up and extracted using solid phase extraction (SPE) on Oasis HLB cartridges (60mg/3cc, Waters, Massachusetts). After pre-conditioning a SPE cartridge with 3 mL methanol and then 3 mL water, a diluted and acidified aqueous phase sample was loaded onto the SPE cartridge at a flow rate of 5 mL/min and followed by rinsing the loaded cartridge with 10 mL water to remove sample matrices. The cartridges were then allowed to dry under vacuum (20 inHg) for 20 min before βE2 was finally eluted off the SPE cartridge with 3 mL methanol and then analyzed by HPLC.

The mineral sediment collected at the termination of each treatment was freeze-dried for 10 min to remove the trapped residual water. To extract the βE2 that remained in the mineral phase, the freeze-dried mineral phase was mixed with 3 mL ethyl acetate, sonicated for 30 min, and then centrifuged at 4000 rpm for 5 min to separate the ethyl acetate phase from the mineral phase. The ethyl acetate phase was collected and then evaporated to dryness on a Vacuum Evaporator (RapidVap, Labconco, Kansas City, MO) at 20% speed, 35°C, and 100 mbar vacuum. The dried residue was re-constituted in 1 mL acetonitrile and water (v/v, 40:60) and filtered through a 0.2

μm PTFE syringe filter (Thermo Fisher, Rockwood, TN) before the HPLC analysis for βE2.

The βE2 in the final extracts of the aqueous phase and mineral phase from each treatment were quantified using a HPLC system coupled with a fluorescence detector (Agilent 1260 Infinity, Agilent, Santa Clara, CA). The analytical column was EC-C18 column (3.0×50 mm, 2.7 μm, Poroshell 120, Agilent, Santa Clara, CA). Mobile phase A and B were 5 mM ammonium acetate and acetonitrile, respectively. The mobile phase gradient was programmed as: 0 min, 80% A and 20% B; 7 min, 15% A and 75% B, 7-7.5 min, 15% A and 75% B, 9 min, 80% A and 20% B, and 9-11 min, 80% A and 20% B. The mobile phase flow rate was 0.4 mL/min. The column temperature was maintained at 30°C. The injection volume was 40 μL. The βE2 was detected by the fluorescence detector at excitation and emission wavelengths of 280 and 310 nm, respectively. The limit of detection (LOD) and the limit of quantification (LOQ) were determined as 2 and 5 ng/mL, respectively. The recoveries for the aqueous phase and the mineral phase were 96.1 ± 0.9% and 83.8 ± 0.6%, respectively.

3.2.4 Statistical analysis

The Student's *t*-test was performed using the Microsoft Excel® software to evaluate the data collected from different treatments. Differences were considered statistically significant if the resultant p value was < 0.05. Data points in all figures are presented by the mean, with the standard deviation indicated by the error bars.

3.3 Results and discussion

3.3.1 Impact of pH, temperature, organic C, and common cations on the effectiveness of Fe^{3+}-saturated montmorillonite-catalyzed removal of βE2 spiked into DI water

Comparing to exposure to Fe^{3+}-saturated montmorillonite, the βE2 removal efficiencies were much lower and in the range of only 11 to 19% when it was exposed to Na^{+}-montmorillonite at different experimental conditions (data not shown). When 10 μg βE2 was exposed for 30 min at 25°C to 15 mg of Fe^{3+}-saturated montmorillonite in 1.5 mL DI water, the βE2 removal efficiency was the highest at pH = 6, reaching 82±1.9%, while its removal efficiencies were lower at pH = 3 and 9 with similar levels of 75±1.5% and 73±3.2%, respectively (Figure 3.1). A previous study has shown that βE2 removal in a system containing Fe^{3+}-saturated montmorillonite requires their sorption onto the montmorillonite surfaces, followed by surface-catalyzed redox reaction that result in the formation of βE2 radicals that are highly susceptible to their further oligomerization [28]. Because its pKa = 10.7, βE2 molecules are in the neutral form within the wastewater relevant pH range (3-9) tested for this study. In addition, the permanent charges on montmorillonite are pH independent [38]. At the investigated pH range for this study, the βE2 sorption to montmorillonite surfaces is therefore not significantly affected by the pH change in the water system [39]. It is reasonable to assume that comparing with acidic and basic conditions, near neutral pH might have enhanced the redox reactions on the montmorillonite surfaces, formation of free radicals, or oligomerization, resulting in the observed higher βE2 removal efficiency at pH 6. Moreover, Fe^{3+} is more prone to be hydrolyzed at higher pH, and therefore has less vacant coordination sites enabling stronger interaction with reactant compound in the montmorillonite [18]. While at low pH levels, Fe^{3+}-saturated montmorillonite surface is more protonated and this might suppress the electron transfer between mineral and βE2. Further research is needed to pinpoint the exactly

mechanism(s) affected by the pH change.

The relatively high and stable βE2 removal efficiency in the Fe^{3+}-saturated montmorillonite containing aqueous system over the tested pH range for this study is contrary to the findings for systems containing enzyme or MnO_2 systems [40, 41]. It was shown that enzymes were susceptible to rapid inactivation below the pH range of 4-8, resulting in < 10% removal rates for phenolic compounds [40]. Also, βE2 removal catalyzed by MnO_2 was substantially inhibited (over 75%) when solution pH increased from 4 to 8 [41]. Because MnO_2 surface has negative charge at pH 4 [42] and this charge will increase in magnitude with increasing pH, which could make MnO_2 surface more hydrophilic and therefore reduce estrogen accessibility to reactive surface sites.

Figure 3.1 shows the βE2 removal efficiency when 15 μg βE2 was exposed for 30 min, at pH=6 and 10°C, 25°C, and 40°C, to 15 mg of Fe^{3+}-saturated montmorillonite in 1.5 mL DI water. The βE2 removal efficiency increased linearly (R^2 = 0.99) with increasing temperature within the tested temperature range. The average βE2 removal efficiency at 40°C was 17% higher than that at 10°C. Previous work has proven that Fe^{3+}-saturated montmorillonite catalyzed oxidation and polymerization reaction are endothermic [43].

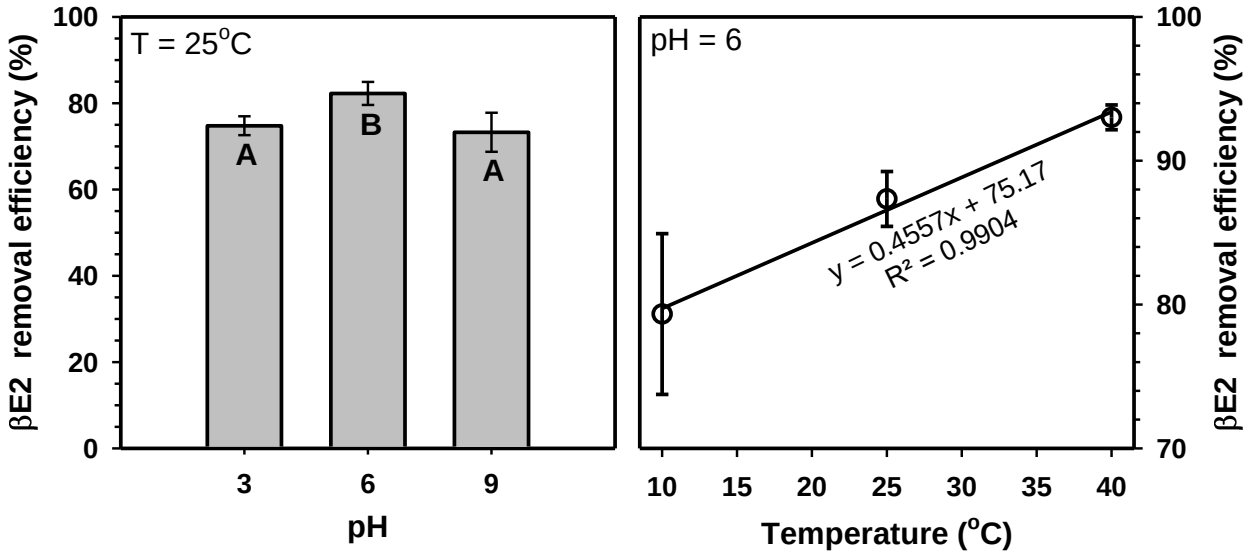

Figure 3.1 Effect of pH and temperature on βE2 removal from simple water systems. Reaction time: 30 min. Initial βE2 concentration: 10 µg/mL. Fe^{3+}-saturated montmorillonite content: 10 mg/mL. Different letters indicate statistical difference ($p < 0.05$).

Dissolved organic matter is ubiquitous in natural aquatic environment as well as in wastewater [44]. Dissolved organic matter possesses various reactive functional groups with resulting high tendency to interfere with many environmental reactions [45, 46]. It is therefore important to evaluate the impact of dissolved organic matter on the catalytic efficiency of Fe^{3+}-saturated montmorillonite in βE2 transformation. Although commercial humic acid is not ideal candidate to completely represent true dissolved organic matter in wastewater, it could still be used as simplified organic matter surrogate to evaluate the impact of dissolved organic matter on βE2 removal reaction. Figure 3.2 shows that when 15 µg βE2 was exposed for 30 min at pH = 6 and 25°C to 15 mg of Fe^{3+}-saturated montmorillonite in 1.5 mL DI water containing dissolved organic matter (15 mg C/L), the βE2 removal efficiency was 74±1.9%, a rate significantly lower than the 82±2.7% removal efficiency achieved in the pure water system without the presence of dissolved organic matter. Generally, dissolved organic matter could have potentially dual impacts on βE2

reaction. Firstly, dissolved organic matter contains electron rich moieties such as phenolic and anilinic functional groups, which are susceptible to react with Fe^{3+}-saturated montmorillonite and become self-coupled, which therefore compete with βE2 for redox reaction sites [47], resulting in a reduced efficiency in βE2 removal. Secondly, dissolved organic matter can also have cross-coupling with βE2 molecules in the presence of Fe^{3+}-saturated montmorillonite and promote βE2 removal, in which similar cross-coupling reactions have been reported between natural organic matter and acetaminophen [48]. In this study, βE2 removal efficiency was suppressed in the presence of natural organic matter, indicating the competition process impact mainly dominates the reaction. Comparing to the observed adverse impacts of dissolved organic matter on enzyme catalyzed EDCs removal [47, 49, 50], its impact on Fe^{3+}-saturated montmorillonite-catalyzed βE2 removal is significantly lower. The presence of 5 mg C/L natural organic matter decreased the efficiency of laccase catalyzed removal of tetrabromobisphenol A by ~40% after 1 h reaction as compared with the same system without natural organic matter presence [50]. An increase in the relative amount of Fe^{3+}-saturated montmorillonite in the system might provide more redox reaction sites that are available to both dissolved organic matter and βE2 and therefore, further increase βE2 removal efficiency.

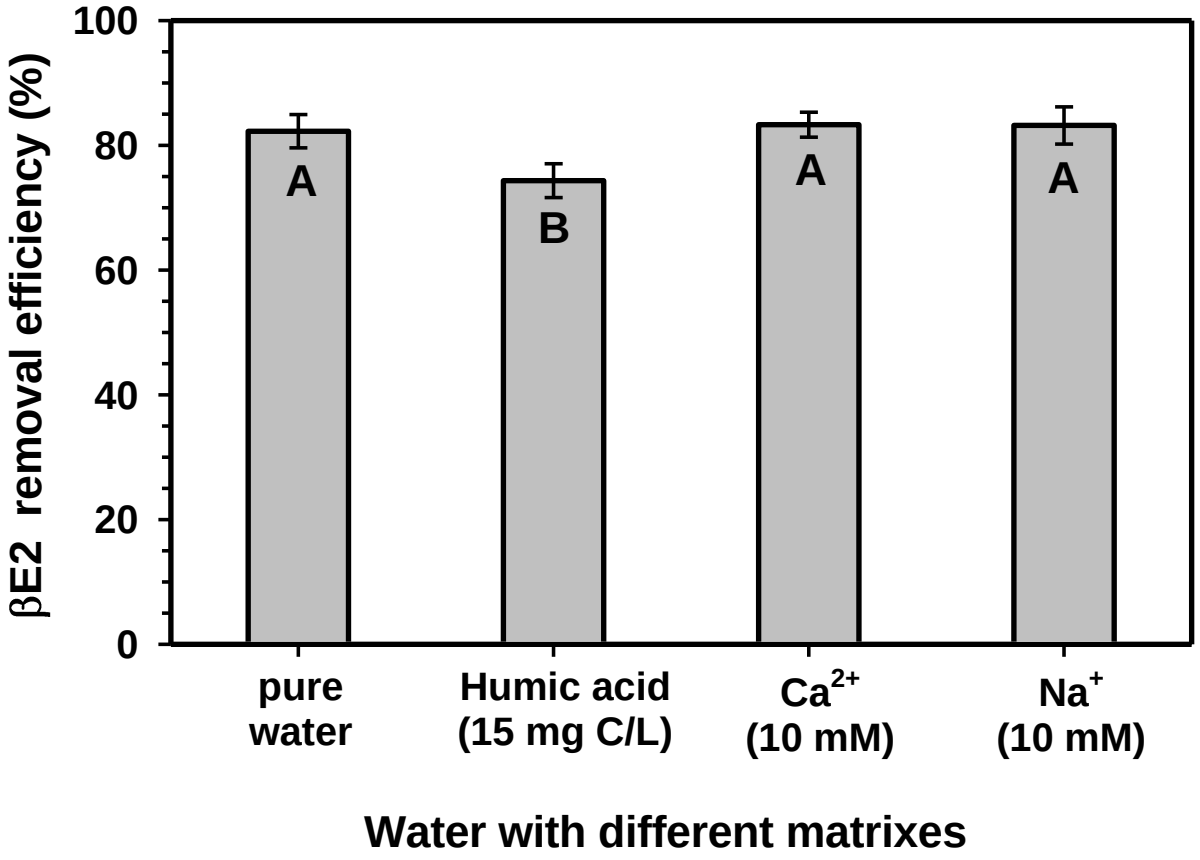

Figure 3.2 Effect of dissolved organic matter and mono- and divalent cations on βE2 removal from simple water systems. Reaction time: 30 min. Initial βE2 concentration: 10 μg/mL. Fe^{3+}-saturated montmorillonite content: 10 mg/mL. Dissolved organic matter concentration: 15 mg C/L. Different letters indicate statistical difference ($p<0.05$).

As shown in Fig. 3.2, the presence of cations that are common in wastewater effluents did not significantly affect βE2 removal efficiency at 25°C and pH=6. The βE2 removal efficiencies remained around 83% for both Ca^{2+}- and Na^{+}-containing systems. This result suggests strong inner-sphere complexation of βE2 with Fe^{3+}-saturated montmorillonite clay surface [18] that is not affected by the presence of other mono- and divalent cations due to their weaker sorption affinities on Fe^{3+}-saturated montmorillonite surface [51]. Metal ions are often reported to suppress the oxidative power of manganese dioxide mineral to organic compounds by complexing with reactants or occupying reactive surface sites, which result in much slower reaction rates [16].

However, as shown in this study, in an aqueous system containing Fe^{3+}-saturated montmorillonite the inhibition effect from coexisting mono- and divalent cations on βE2 oxidation and oligomerization is not significant.

3.3.2 Effectiveness of Fe^{3+}-saturated montmorillonite-catalyzed βE2 removal from wastewater secondary effluents

The feasibility of using Fe^{3+}-saturated montmorillonite for βE2 removal in real-world wastewater matrix was tested in this study by adding Fe^{3+}-saturated montmorillonite to wastewater secondary effluents collected from three different conventional wastewater treatment plants. In these experiments, appropriate amount of βE2 was spiked to each wastewater effluent sample to reach a final concentration of 0.1 μg/mL, which is the upper concentration limit of environmentally-relevant levels for common wastewater samples.

As shown in Figure 3.3, the source of wastewater effluent did significantly affect βE2 removal kinetics in the presence of Fe^{3+}-saturated montmorillonite. The βE2 removal efficiency rapidly reached to ~ 30% during the first 15 min reaction with Fe^{3+}-saturated montmorillonite at 15 mg/L and slowly increased to ~40% after 240 min. This βE2 removal efficiency is much lower than the ~ 80% removal efficiency achieved for the simple water systems (Figure 3.1 & 3.2), which is most likely due to the interferences from the complex matrices, in particular dissolved organic matter, in the wastewater samples. The molar ratios of dissolve organic C to βE2 in the wastewater effluents were around 2269:1, 65 times higher than that in the above studied simple water system containing dissolved humic acid. This suggested that the excess dissolved organic matter could out compete the βE2 molecules for the reactive sites on Fe^{3+}-saturated montmorillonite. Therefore, to achieve higher βE2 removal efficiency in real-world wastewater, more Fe^{3+}-saturated montmorillonite is needed than simple systems with less dissolved organic matter. Figure 3.4

further confirms that the mass ratio of Fe^{3+}-saturated montmorillonite/βE2 does affect the βE2 removal efficiency. In a simple DI water system, this ratio needs to be higher than 1000 in order to provide sufficient reaction sites to reach > 80% βE2 removal efficiency. In the presence of dissolved organic matter, this mass ratio would therefore need to be higher. Similarly, it was reported that horseradish peroxidase dose of 8-10 U/mL was required to achieve the same removal efficiency for estrogens in municipal wastewater while only 0.032 U/mL horseradish peroxidase was needed to treat synthetic water [52, 53].

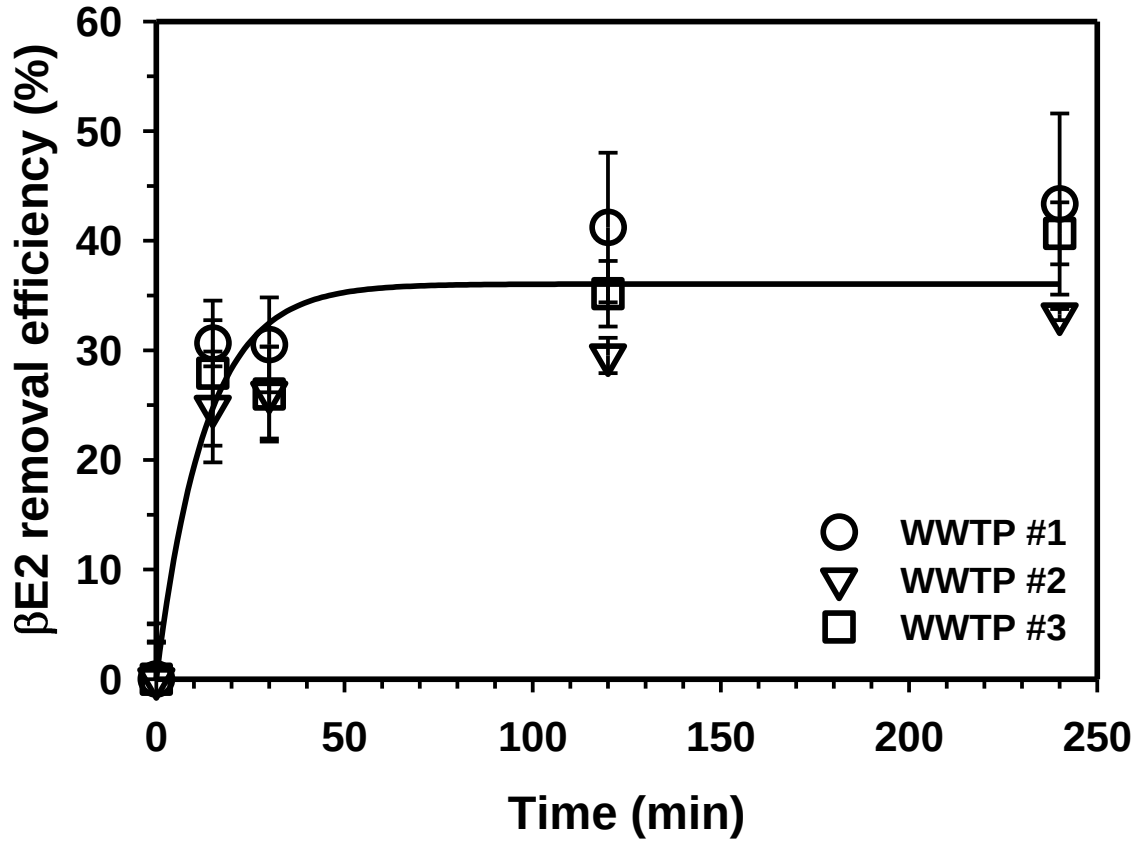

Figure 3.3 βE2 removal kinetics in wastewater secondary effluents collected from three wastewater treatment plants. Initial βE2 concentration: 0.1 μg/mL. Fe^{3+}-saturated montmorillonite content: 10 mg/mL.

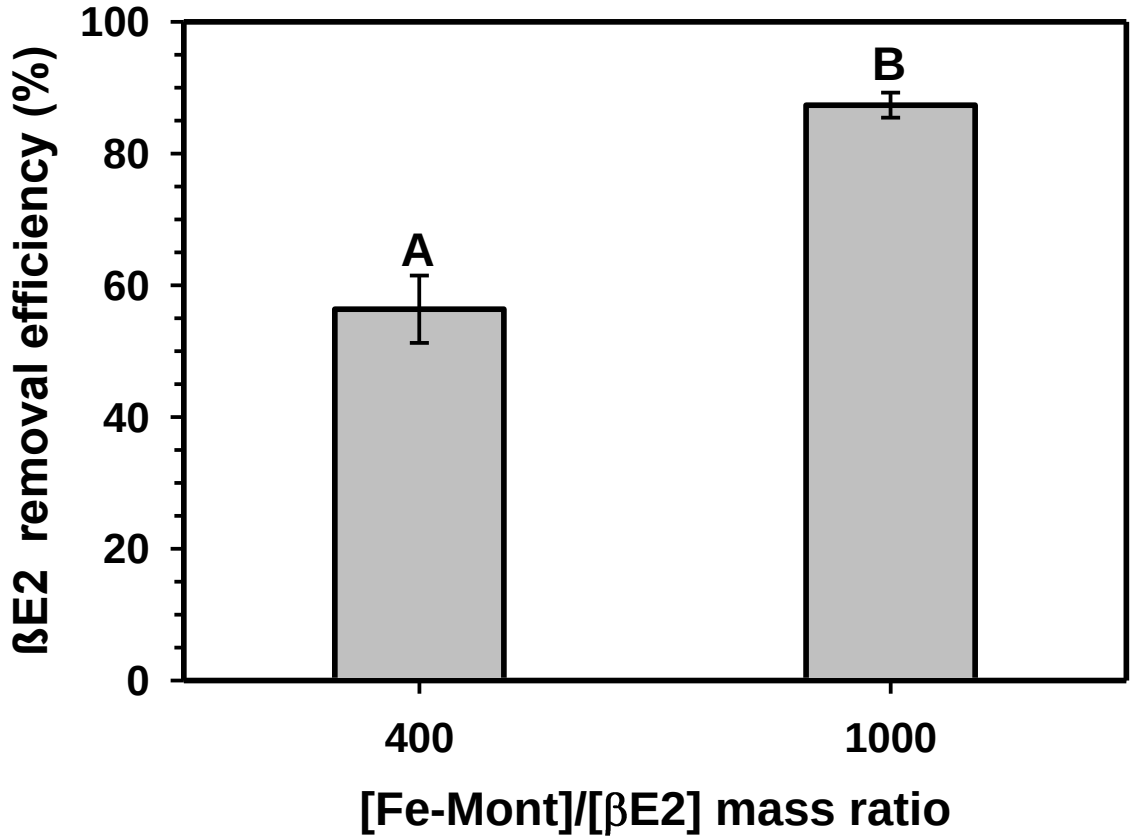

Figure 3.4 βE2 removal efficiencies in simple water systems with two different mass ratios of Fe^{3+}-saturated montmorillonite/βE2. Reaction time: 30 min. Different letters indicate statistical difference ($p< 0.05$).

Moreover, our previous study indicated that βE2 oligomers including dimers, trimers and tetramers are the main catalyzed products from Fe^{3+}-saturated montmorillonite mediated radical coupling reaction [28]. In a ligninase-enzyme mediated study, the formed βE2 coupling oligomer products did not exhibit any potent estrogenic activity, showing that the estrogenicity of treated solution was completely eliminated without secondary risk by oxidative coupling processes [21]. These results indicated that Fe^{3+}-saturated montmorillonite treatment has the great efficiency in both βE2 and estrogenicity removal, therefore it could be utilized in practical application for effective estrogens removal in wastewater matrix.

3.4 Conclusions

In summary, our study elucidated that Fe^{3+}-saturated montmorillonite catalysis achieved highest βE2 removal efficiency at neutral solution pH and higher temperature. Common cations did not have impact on the reaction efficiency. The presence of dissolved organic matter in simple DI water system slightly reduced βE2 removal efficiency under the designed experimental conditions. The βE2 removal efficiencies were significantly reduced when wastewater secondary effluents were used to replace DI water due to high levels of dissolved organic matter, but adverse effects of dissolved organic matter in effluents can be offset by increasing dosage of Fe^{3+}-saturated montmorillonite to increase the available reaction sites. The laboratory of batch experimental results in this study provide evidence that Fe^{3+}-saturated montmorillonite can be utilized with high stability in practical applications for elimination of estrogen and other phenolic pollutants in wastewater. Removal of estrogen and other EDCs from municipal wastewater discharged effluent will help reduce the health threat to the receiving aquatic ecosystems. Further research should also focus on developing technologies for immobilization of Fe^{3+}-saturated montmorillonite onto fixed supporting materials that enable continuous-flow large scale efficient treatment of wastewater.

Acknowledgements

We acknowledge the financial support from USDA-AFRI award (No. 2013-67019-21355). Funding for this work was provided, in part, by the Virginia Agricultural Experiment Station and the Hatch Program of the National Institute of Food and Agriculture, U.S. Department of Agriculture. We would like to sincerely thank: Blacksburg-VPI Sanitation Authority Treatment Plant; Christiansburg Wastewater Treatment Facility; and Roanoke Regional Waste Pollution

Control Plant for assistance with wastewater sample collection.

3.5 References

1. Kolpin, D. W.; Furlong, E. T.; Meyer, M. T.; Thurman, E. M.; Zaugg, S. D.; Barber, L. B.; Buxton, H. T., Pharmaceuticals, hormones, and other organic wastewater contaminants in US streams, 1999-2000: A national reconnaissance. *Environmental science & technology* **2002,** *36*, (6), 1202-1211.
2. Kim, S. D.; Cho, J.; Kim, I. S.; Vanderford, B. J.; Snyder, S. A., Occurrence and removal of pharmaceuticals and endocrine disruptors in South Korean surface, drinking, and waste waters. *Water Res.* **2007,** *41*, (5), 1013-1021.
3. Fan, Z.; Hu, J.; An, W.; Yang, M., Detection and Occurrence of Chlorinated Byproducts of Bisphenol A, Nonylphenol, and Estrogens in Drinking Water of China: Comparison to the Parent Compounds. *Environmental science & technology* **2013,** *47*, (19), 10841-10850.
4. Soto, A. M.; Sonnenschein, C., Environmental causes of cancer: endocrine disruptors as carcinogens. *Nature Reviews Endocrinology* **2010,** *6*, (7), 363-370.
5. Yang, M.; Park, M. S.; Lee, H. S., Endocrine disrupting chemicals: human exposure and health risks. *Journal of Environmental Science and Health Part C* **2006,** *24*, (2), 183-224.
6. Routledge, E. J.; Sheahan, D.; Desbrow, C.; Brighty, G. C.; Waldock, M.; Sumpter, J. P., Identification of estrogenic chemicals in STW effluent. 2. In vivo responses in trout and roach. *Environmental Science & Technology* **1998,** *32*, (11), 1559-1565.
7. Griffith, D. R.; Kido Soule, M. C.; Matsufuji, H.; Eglinton, T. I.; Kujawinski, E. B.; Gschwend, P. M., Measuring free, conjugated, and halogenated estrogens in secondary treated wastewater effluent. *Environmental science & technology* **2014,** *48*, (5), 2569-2578.
8. Combalbert, S.; Hernandez-Raquet, G., Occurrence, fate, and biodegradation of estrogens in sewage and manure. *Appl. Microbiol. Biotechnol.* **2010,** *86*, (6), 1671-1692.
9. Baynes, A.; Green, C.; Nicol, E.; Beresford, N.; Kanda, R.; Henshaw, A.; Churchley, J.; Jobling, S., Additional Treatment of Wastewater Reduces Endocrine Disruption in Wild Fish□ A Comparative Study of Tertiary and Advanced Treatments. *Environmental science & technology* **2012,** *46*, (10), 5565-5573.
10. Ings, J. S.; Servos, M. R.; Vijayan, M. M., Hepatic transcriptomics and protein expression in rainbow trout exposed to municipal wastewater effluent. *Environmental science & technology* **2011,** *45*, (6), 2368-2376.
11. Thorpe, K. L.; Maack, G.; Benstead, R.; Tyler, C. R., Estrogenic wastewater treatment works effluents reduce egg production in fish. *Environmental science & technology* **2009,** *43*, (8), 2976-2982.
12. Lange, A.; Paull, G. C.; Hamilton, P. B.; Iguchi, T.; Tyler, C. R., Implications of persistent exposure to treated wastewater effluent for breeding in wild roach (Rutilus rutilus) populations. *Environmental science & technology* **2011,** *45*, (4), 1673-1679.
13. Kidd, K. A.; Blanchfield, P. J.; Mills, K. H.; Palace, V. P.; Evans, R. E.; Lazorchak, J. M.; Flick, R. W., Collapse of a fish population after exposure to a synthetic estrogen. *Proceedings of the National Academy of Sciences* **2007,** *104*, (21), 8897-8901.
14. Esplugas, S.; Bila, D. M.; Krause, L. G. T.; Dezotti, M., Ozonation and advanced oxidation technologies to remove endocrine disrupting chemicals (EDCs) and pharmaceuticals

and personal care products (PPCPs) in water effluents. *J. Hazard. Mater.* **2007,** *149*, (3), 631-642.
15. Filby, A. L.; Shears, J. A.; Drage, B. E.; Churchley, J. H.; Tyler, C. R., Effects of advanced treatments of wastewater effluents on estrogenic and reproductive health impacts in fish. *Environmental science & technology* **2010,** *44*, (11), 4348-4354.
16. Lin, K.; Liu, W.; Gan, J., Oxidative removal of bisphenol A by manganese dioxide: efficacy, products, and pathways. *Environmental science & technology* **2009,** *43*, (10), 3860-3864.
17. Gu, C.; Li, H.; Teppen, B. J.; Boyd, S. A., Octachlorodibenzodioxin formation on Fe (III)-montmorillonite clay. *Environmental science & technology* **2008,** *42*, (13), 4758-4763.
18. Polubesova, T.; Eldad, S.; Chefetz, B., Adsorption and oxidative transformation of phenolic acids by Fe (III)-montmorillonite. *Environmental science & technology* **2010,** *44*, (11), 4203-4209.
19. Jia, H.; Zhao, J.; Li, L.; Li, X.; Wang, C., Transformation of polycyclic aromatic hydrocarbons (PAHs) on Fe (III)-modified clay minerals: Role of molecular chemistry and clay surface properties. *Applied Catalysis B: Environmental* **2014,** *154*, 238-245.
20. Lu, J.; Huang, Q.; Mao, L., Removal of acetaminophen using enzyme-mediated oxidative coupling processes: I. Reaction rates and pathways. *Environmental science & technology* **2009,** *43*, (18), 7062-7067.
21. Mao, L.; Lu, J.; Habteselassie, M.; Luo, Q.; Gao, S.; Cabrera, M.; Huang, Q., Ligninase-mediated removal of natural and synthetic estrogens from water: II. Reactions of 17β-estradiol. *Environmental science & technology* **2010,** *44*, (7), 2599-2604.
22. Lloret, L.; Eibes, G.; Moreira, M. T.; Feijoo, G.; Lema, J. M., Removal of estrogenic compounds from filtered secondary wastewater effluent in a continuous enzymatic membrane reactor. Identification of biotransformation products. *Environmental science & technology* **2013,** *47*, (9), 4536-4543.
23. Garcia, H. A.; Hoffman, C. M.; Kinney, K. A.; Lawler, D. F., Laccase-catalyzed oxidation of oxybenzone in municipal wastewater primary effluent. *Water Research* **2011,** *45*, (5), 1921-1932.
24. Hu, E.; Cheng, H.; Hu, Y., Microwave-induced degradation of atrazine sorbed in mineral micropores. *Environmental science & technology* **2012,** *46*, (9), 5067-5076.
25. Zhong, Y.; Liang, X.; Zhong, Y.; Zhu, J.; Zhu, S.; Yuan, P.; He, H.; Zhang, J., Heterogeneous UV/Fenton degradation of TBBPA catalyzed by titanomagnetite: catalyst characterization, performance and degradation products. *Water Res.* **2012,** *46*, (15), 4633-4644.
26. Li, F.; Li, X.; Liu, C.; Liu, T., Effect of alumina on photocatalytic activity of iron oxides for bisphenol A degradation. *J. Hazard. Mater.* **2007,** *149*, (1), 199-207.
27. Liyanapatirana, C.; Gwaltney, S. R.; Xia, K., Transformation of triclosan by Fe (III)-saturated montmorillonite. *Environmental science & technology* **2009,** *44*, (2), 668-674.
28. Qin, C.; Troya, D.; Shang, C.; Hildreth, S.; Helm, R.; Xia, K., Surface catalyzed oxidative oligomerization of 17β-estradiol by Fe3+-saturated montmorillonite. *Environmental science & technology* **2014,** *49*, (2), 956-964.
29. Seger, M. R.; Maciel, G. E., NMR investigation of the behavior of an organothiophosphate pesticide, chlorpyrifos, sorbed on montmorillonite clays. *Environmental science & technology* **2006,** *40*, (3), 797-802.

30. Wei, J.; Furrer, G.; Kaufmann, S.; Schulin, R., Influence of clay minerals on the hydrolysis of carbamate pesticides. *Environmental science & technology* **2001,** *35*, (11), 2226-2232.
31. Boyd, S. A.; Mortland, M. M., Radical formation and polymerization of chlorophenols and chloroanisole on copper (II)-smectite. *Environmental science & technology* **1986,** *20*, (10), 1056-1058.
32. Metcahf, E., Wastewater engineering: treatment and reuse. *McGrawHill, New York* **2003**.
33. Chen, S.-S.; Cheng, C.-Y.; Li, C.-W.; Chai, P.-H.; Chang, Y.-M., Reduction of chromate from electroplating wastewater from pH 1 to 2 using fluidized zero valent iron process. *J. Hazard. Mater.* **2007,** *142*, (1), 362-367.
34. Tripathi, S.; Tripathi, D. M.; Tripathi, B., Removal of Organic Content and Color from Secondary Treated Wastewater in Reference with Toxic Potential of Ozone During Ozonation. *Hydrology: Current Research* **2012,** *2011*.
35. Wang, L.; Min, M.; Li, Y.; Chen, P.; Chen, Y.; Liu, Y.; Wang, Y.; Ruan, R., Cultivation of green algae Chlorella sp. in different wastewaters from municipal wastewater treatment plant. *Appl. Biochem. Biotechnol.* **2010,** *162*, (4), 1174-1186.
36. Lew, B.; Belavski, M.; Admon, S.; Tarre, S.; Green, M., Temperature effect on UASB reactor operation for domestic wastewater treatment in temperate climate regions. *Water Sci. Technol.* **2003,** *48*, (3), 25-30.
37. Ahsan, S.; Rahman, M. A.; Kaneco, S.; Katsumata, H.; Suzuki, T.; Ohta, K., Effect of temperature on wastewater treatment with natural and waste materials. *Clean Technologies and Environmental Policy* **2005,** *7*, (3), 198-202.
38. McBride, M. B., *Environmental Chemistry of Soils.* Oxford University Press, New York.: 1994.
39. Van Emmerik, T.; Angove, M. J.; Johnson, B. B.; Wells, J. D.; Fernandes, M. B., Sorption of 17β-estradiol onto selected soil minerals. *Journal of Colloid and Interface Science* **2003,** *266*, (1), 33-39.
40. Kim, Y.-J.; Nicell, J. A., Impact of reaction conditions on the laccase-catalyzed conversion of bisphenol A. *Bioresour. Technol.* **2006,** *97*, (12), 1431-1442.
41. Xu, L.; Xu, C.; Zhao, M.; Qiu, Y.; Sheng, G. D., Oxidative removal of aqueous steroid estrogens by manganese oxides. *Water Res.* **2008,** *42*, (20), 5038-5044.
42. Murray, J. W., The surface chemistry of hydrous manganese dioxide. *J. Colloid Interface Sci.* **1974,** *46*, (3), 357-371.
43. Moreale, A.; Cloos, P.; Badot, C., Differential behaviour of Fe (III)-and Cu (II)-montmorillonite with aniline: I. suspensions with constant solid: liquid. *Clay Minerals* **1985,** *20*, 29-37.
44. Stedmon, C. A.; Markager, S.; Bro, R., Tracing dissolved organic matter in aquatic environments using a new approach to fluorescence spectroscopy. *Mar. Chem.* **2003,** *82*, (3), 239-254.
45. Aiken, G. R.; Hsu-Kim, H.; Ryan, J. N., Influence of dissolved organic matter on the environmental fate of metals, nanoparticles, and colloids. *Environmental science & technology* **2011,** *45*, (8), 3196-3201.
46. Bodhipaksha, L. C.; Sharpless, C. M.; Chin, Y.-P.; Sander, M.; Langston, W. K.; MacKay, A. A., Triplet photochemistry of effluent and natural organic matter in whole water and isolates from effluent-receiving rivers. *Environmental science & technology* **2015,** *49*, (6), 3453-3463.

47. Mao, L.; Huang, Q.; Luo, Q.; Lu, J.; Yang, X.; Gao, S., Ligninase-mediated removal of 17β-estradiol from water in the presence of natural organic matter: Efficiency and pathways. *Chemosphere* **2010,** *80*, (4), 469-473.
48. Lu, J.; Huang, Q., Removal of acetaminophen using enzyme-mediated oxidative coupling processes: II. Cross-coupling with natural organic matter. *Environmental science & technology* **2009,** *43*, (18), 7068-7073.
49. Sun, K.; Luo, Q.; Gao, Y.; Huang, Q., Laccase-catalyzed reactions of 17β-estradiol in the presence of humic acid: Resolved by high-resolution mass spectrometry in combination with 13 C labeling. *Chemosphere* **2016,** *145*, 394-401.
50. Feng, Y.; Colosi, L. M.; Gao, S.; Huang, Q.; Mao, L., Transformation and removal of tetrabromobisphenol A from water in the presence of natural organic matter via laccase-catalyzed reactions: Reaction rates, products, and pathways. *Environmental science & technology* **2013,** *47*, (2), 1001-1008.
51. Xiao, H.; Song, H.; Xie, H.; Huang, W.; Tan, J.; Wu, J., Transformation of acetaminophen using manganese dioxide− mediated oxidative processes: Reaction rates and pathways. *Journal of hazardous materials* **2013,** *250*, 138-146.
52. Auriol, M.; Filali-Meknassi, Y.; Tyagi, R. D.; Adams, C. D., Oxidation of natural and synthetic hormones by the horseradish peroxidase enzyme in wastewater. *Chemosphere* **2007,** *68*, (10), 1830-1837.
53. Auriol, M.; Filali-Meknassi, Y.; Adams, C. D.; Tyagi, R. D., Natural and synthetic hormone removal using the horseradish peroxidase enzyme: temperature and pH effects. *Water Res.* **2006,** *40*, (15), 2847-2856.

Chapter 4. Fe^{3+}-Saturated Montmorillonite Effectively Deactivates Microorganisms in Wastewater

(Submitted to Water Research)

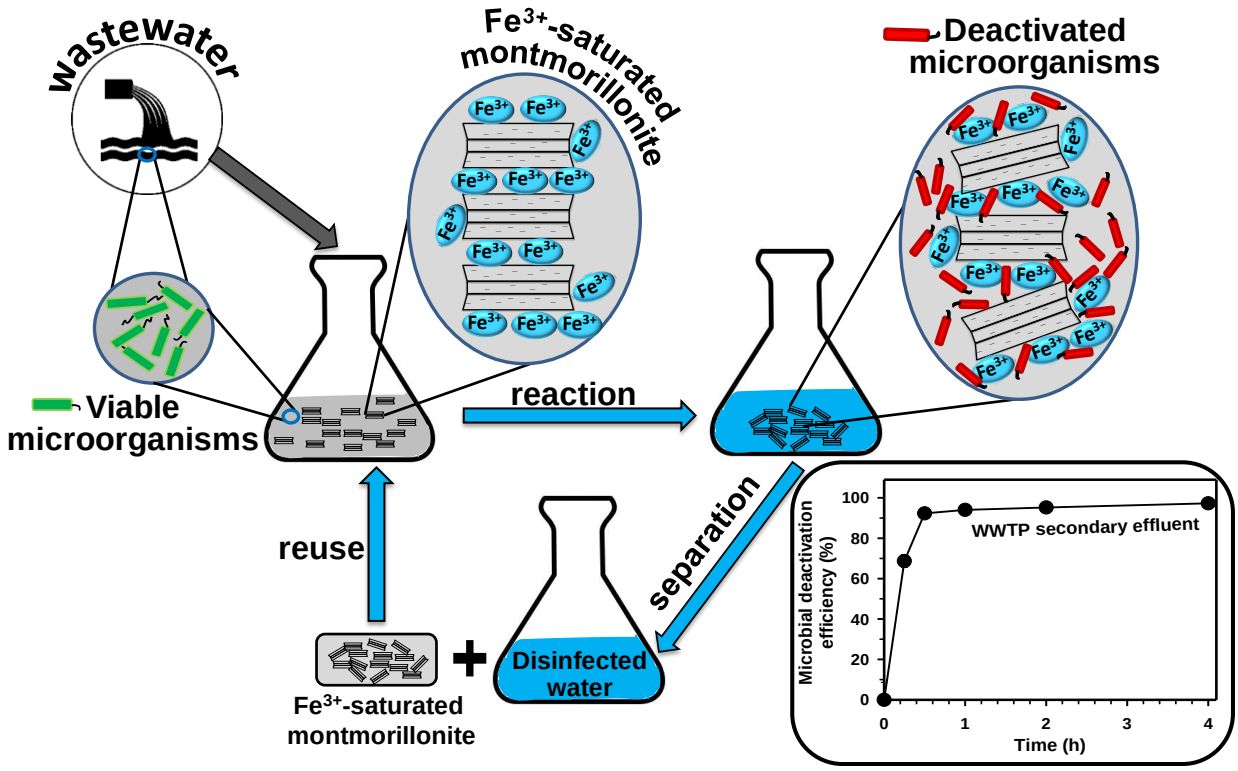

Notes: The abstract figure is only for simple demonstration of possible reaction mechanism. Sizes of different components do not reflect their actual levels for comparison.

Abstract

Existing water disinfection practices can be costly and often produce harmful disinfection byproducts. This paper reports, for the first time, that Fe^{3+}-saturated montmorillonite effectively

deactivates wastewater microorganisms. Microbial deactivation efficiency was 92±0.64% when a secondary wastewater effluent was mixed with Fe^{3+}-saturated montmorillonite at 35 mg/mL for 30 min, and further enhanced to 97±0.61% after 4-h exposure. This deactivation efficiency was similar to that when the same water was subjected to UV-disinfection. Microbial cultural results coupled with the live/dead fluorescent staining assay observation strongly suggested that Fe^{3+}-saturated montmorillonite deactivated microorganisms in wastewater through two stages: electrostatic sorption of negatively charged microbial cells to the surfaces of Fe^{3+}-saturated montmorillonite, followed by microbial deactivation due to surface-catalyzed microbial cell membrane disruption by the surface saturated Fe^{3+}. It was estimated that the ratio between wastewater microbial population and Fe^{3+}-saturated montmorillonite at less than 2×10^3 CFU/mg microbial deactivation efficiency would achieve >90%. Freeze-drying the recycled Fe^{3+}-saturated montmorillonite after each usage resulted in 82±0.51% microbial deactivation efficiency even after its fourth consecutive use. This study demonstrated the promising potential of Fe^{3+}-saturated montmorillonite as a low cost material for applications from small scale point-of-use drinking water treatment devices to large scale drinking and wastewater treatment facilities.

4.1 Introduction

Ensuring adequate access to clean water worldwide is one of the greatest global challenges in this century because 1.2 billion people throughout the world lack safe drinking water and millions of people die annually from diseases caused by harmful microorganisms in untreated or improperly treated drinking water.[1] Disinfection practices such as chlorination, ozonation, and UV treatment are commonly used for treating wastewater as well as drinking water, especially in developed countries. However, current disinfection practices could form byproducts (halogenated

disinfection byproducts, nitrosamines, bromate, etc.)[2] that pose negative impact to human health.[3] Besides, it is impractical to establish such massive treatment systems in less developed regions that lack financial resources and water sanitation services.[4] Thus, there is a need to develop alternative low cost and yet effective water disinfection materials and methods.

In the past decade, various natural or engineered nanomaterials have been developed and used as antimicrobial agents for water disinfection purpose. Those nanomaterials include silver nanoparticles,[5-7] copper and copper oxide nanoparticles,[8, 9] titanium dioxide,[10, 11] carbon nanotubes,[12, 13] zinc oxide,[14, 15] fullerenes,[16] and graphene materials.[17-20] Among them, silver-based nanomaterials have been most widely explored owing to their great antimicrobial properties to a broad spectrum of microorganisms.[6] The antimicrobial activity of silver-based nanomaterials is mainly attributed to the release of Ag^+, which further interact with the thiol functional groups in proteins, resulting in respiratory enzymes inactivation and reactive oxygen species generation.[21] Furthermore, Ag^+ can also prevent DNA replication and enhance detachment of cytoplasm membrane from cell wall.[22] However, silver-based antimicrobial materials can be expensive and show poor stability.[23] There have been concerns about their long term efficacy and economic applicability.[24] In addition, although previous research has shown that certain clay minerals such as smectites and zeolites that have high specific surface area, cation exchange capacity, and sorption capacity, can be matrix retaining metal ions including Ag^+, Zn^{2+}, and Cu^{2+}, all of which possess antimicrobial property,[25-31] their effectiveness in treating contaminated water has not been tested.

Our previous studies have demonstrated effective removal of phenolic organic compounds from wastewater due to surface catalyzed oxidative oligomerization by Fe^{3+}-saturated montmorillonite.[32, 33] It was therefore hypothesized for the current study that the surface reactivity

of Fe^{3+}-saturated montmorillonite might also capable of deactivating microorganisms in wastewater. Hence, Fe^{3+}-saturated montmorillonite could potentially be used to treat water contaminated with organic compounds as well as harmful microorganisms. The objectives of this study were: 1) to investigate the influence of exposure time and mineral concentration on the microbial deactivation efficiency of Fe^{3+}-saturated montmorillonite; 2) to evaluate the performance stability and reusability of Fe^{3+}-saturated montmorillonite for microbial deactivation. For this work, instead of targeting a specific microorganism, a wide spectrum of culturable microorganisms were tested by exposing the primary and secondary effluents from a local wastewater treatment plant to Fe^{3+}-saturated montmorillonite.

4.2 Materials and Methods

4.2.1 Chemicals and Materials.

Luria-Bertani (LB) broth powder (Lennox), agar powder, sodium chloride (≥99%) were purchased from Fisher Scientific (Fair Lawn, NJ). Na^+-montmorillonite (SWy-2, Crook County, Wyoming) was obtained from the Source Clays Repository of the Clay Minerals Society (Purdue University, West Lafayette, IN). The ultrapure water used in this study was produced by a Millipore Milli-Q water purification system (Milford, MA).

4.2.2 Fe^{3+}-Saturated Montmorillonite Preparation

Detailed description for preparation of Fe^{3+}-saturated montmorillonite can be found in previous studies.[32, 33] Briefly, Na^+-montmorillonite (Na^+ as major interlayer cation) was first purified and fractionated to <2 μm clay-sized particles and then went through six saturation-decantation cycles using 0.1 M $FeCl_3$ to saturate the montmorillonite interlayers with Fe^{3+}. The

Fe^{3+}-saturated montmorillonite was then repeatedly washed with ultrapure grade water followed by centrifugation until no Cl^- in the supernatant was detected using the $AgNO_3$ test. The washed Fe^{3+}-saturated montmorillonite was finally freeze-dried for future tests of its antimicrobial efficiency.

4.2.3 Microbial Deactivation Study Using Fe^{3+}-Saturated Montmorillonite

To prevent microbial cross contamination during each step of testing, all related glassware and materials were properly sterilized by autoclaving at 121°C for 20 min. Two mL of primary or secondary wastewater effluent from a local wastewater treatment plant was mixed with a predetermined amount of Fe^{3+}-saturated montmorillonite in a 20 mL glass vial and shaken on a horizontally moving shaker at 200 rpm for up to 4 h at 25°C. The characteristics of the primary and secondary wastewater effluents are summarized in Table 4.1. At 0.5 h, 1 h, 2 h and 4 h, triplicate vials were taken from the shaker and centrifuged at 1000 rpm for 5 min to separate the aqueous phase and mineral phase. Supernatant (aqueous phase) of each vial was withdrawn and weighed. The water trapped in the mineral sediment was calculated by the difference between the weight of the mineral and that was initially added into each vial. This was included in the later calculation of aqueous phase microbial population and excluded in the calculation of mineral phase microbial population.

Table 4.1 Characteristics of the primary and secondary wastewater effluents used for this study. (average value for samples tested in October, 2015, data from the wastewater treatment plant lab report)

Parameter	Primary	Secondary
pH	7.5	7.4
Dissolved oxygen (DO)	2.0	8.3
Biological oxygen demand (BOD)	77	2.9
Alkalinity	227	113
Total suspended solids	53	2.5

Microbial populations, expressed in colony forming unit (CFU), in the wastewater samples, the aqueous phase, and the mineral phase were quantified using the Colony Forming Count method.[34] Briefly, a wastewater or an aqueous phase sample was diluted sequentially 10-fold with saline water (0.85% NaCl) for up to 5 times. An aliquot of 100 μL was taken from each diluted solution, spread onto a pre-sterilized LB agar growth media, and incubated at 28°C for 24 h before colony counting. The collected mineral phase was re-suspended in 10 mL sterilized saline solution, hand mixed thoroughly for 1 min, sequentially diluted 10-fold using saline water (0.85% NaCl) for up to 5 times, followed by the colony forming count for each diluted mixture using the plate cultural method as described above. The sum of the microbial populations in the aqueous phase and the mineral phase was calculated as total CFU and compared with that in the wastewater before it was exposed to Fe^{3+}-saturated montmorillonite or Na^{+}-montmorillonite. The microbial deactivation efficiency was calculated using equation: Deactivation (%)=$(1-C_t/C_o)\times100$, where C_t is the total CFU at different reaction time t, C_o is the CFU of the wastewater used.

To test the reusability of Fe^{3+}-saturated montmorillonite for microbial deactivation in wastewater, the Fe^{3+}-saturated montmorillonite sediment after each deactivation cycle was collected via centrifugation and used as is for the next cycle or freeze dried before being used for the next cycle, each with a fresh batch of wastewater sample. Four consecutive cycles were tested.

4.2.4 Microbial Cell Viability Assay

Microbial cell viability during the deactivation tests was further visualized using the fluorescence-based cell live/dead Test.[19] An aliquot of 1 mL wastewater sample was incubated in 25 mL LB growth medium at 28°C until reaching mid-exponential growth phase. Microorganisms in the growth medium were then harvested by centrifugation at 7500 rpm for 10 minutes. The

microbial pellet was washed twice using saline solution to remove residual macromolecules and other growth medium constituents. The microbial pellet was first re-suspended in 2 mL wastewater, then exposed to 50 mg Fe^{3+}-saturated montmorillonite for 4 h, and finally centrifuged at 1000 rpm for 5 minutes. The mineral phase collected was re-suspended in 1 mL saline solution and stained by using the LIVE/DEAD BacLight bacterial viability kit (L7007, Invitrogen, Carlsbad, CA, USA). An aliquot of 3 μL dye mixture containing SYTO 9® and propidium iodide was added to the 1 mL mineral-saline mixture suspension and incubated in darkness for 15 min before final observation under a Zeiss fluorescence microscope (Axio Observer Z1, Carl Zeiss, Germany). With mixture of the SYTO 9® and propidium iodide (PI), bacteria with intact cell membranes stain fluorescent green (considered to be viable), and bacteria with compromised membranes stain fluorescent red (considered to be nonviable). Similar fluorescence dye methods have been applied in other studies monitoring the antimicrobial properties of nanoparticles.[15, 19, 35]

4.2.5 Statistical Analysis

Student's T-test was performed to determine whether there are significant differences in microbial cell viability between different treatments. Statistical decisions were made at a significance level of $p < 0.05$ within a 95% confidence interval.

4.3 Results and Discussion

4.3.1 Microbial Deactivation Efficiency of Fe^{3+}-Saturated Montmorillonite

Without exposure to any treatment, microbial populations in both primary and secondary wastewater effluents did not change during the 4-h testing time (data not shown). When exposed to Na^{+}-montmorillonite at 35 mg/mL for up to 1 hour, there was no statistically significant change

in the microbial populations in both primary and secondary wastewater effluents (Figure 4.1). Incubation with Na^+-montmorillonite longer than 1 hour resulted in significant microbial growth (negative values of microbial deactivation efficiency), with 42±26% and 117±38% microbial population enhancement in the primary and secondary wastewater effluents, respectively, at the end of 4-h incubation. Growth stimulation of a wide spectrum of microbial species by natural montmorillonite had been reported in the literature.[36-38] It was speculated that the relative basicity of cations such as Na^+ and Ca^{2+} sorbed on the Na^+-montmorillonite interlayer surfaces might provide optimal pH environment and nutritional support and stimulation for microbial growth.[37]

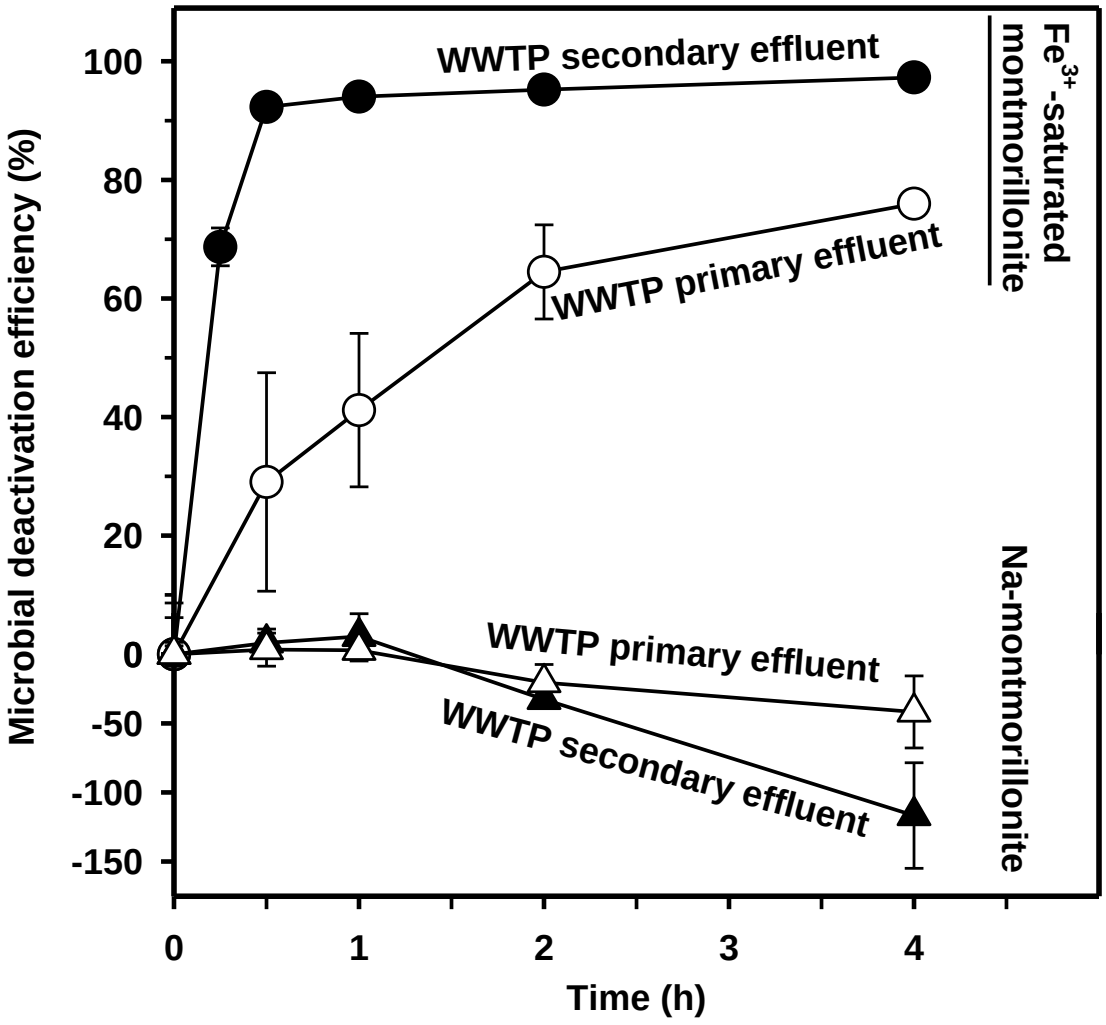

Figure 4.1 Microbial deactivation efficiencies of Fe^{3+}-saturated montmorillonite (circles) and Na^{+}-montmorillonite (upper triangles) when they were exposed to primary and secondary wastewater effluents for different length of time. The mineral concentration in the water was 35 mg/mL. The initial microbial levels in the primary and secondary effluents were $1.39x10^5$ and $2.33x10^4$ CFU/mL, respectively.

As shown in Figure 4.1, microorganisms in the secondary wastewater effluent were rapidly deactivated within 30 min of exposure to Fe^{3+}-saturated montmorillonite at 35 mg/mL, achieving deactivation efficiency of 69±3.2% and 92±0.64% after 15 and 30 min, respectively. Longer exposure of the secondary wastewater effluent to Fe^{3+}-saturated montmorillonite from 30 min to

4 h only slightly further enhanced the microbial deactivation efficiency to 97±0.61%. Comparing to the secondary wastewater effluent, the microbial deactivation efficiency was lower when the primary wastewater effluent was exposed to Fe^{3+}-saturated montmorillonite (35 mg/mL), reaching 29±18% at 30 min and 76±1.7% at 4 h.

The initial microbial population in the primary wastewater effluent (1.39×10^5 CFU/mL) was 6 times higher than that in the secondary wastewater effluent (2.33×10^4 CFU/mL). If microbial deactivation is mineral surface dependent, higher ratio of microbial population relative to the amount of Fe^{3+}-saturated montmorillonite they are exposed to would result in lower microbial deactivation efficiency. Figure 4.2a shows a significantly decreased microbial deactivation efficiency, from 93±0.71% to 23±12%, when the ratio of wastewater microbial population to Fe^{3+}-saturated montmorillonite increased from 2×10^3 to 9×10^3 CFU/mg. When this ratio further decreased from 2×10^3 to 0.7×10^3 CFU/mg, the microbial deactivation efficiency increased slightly from 93±0.71% to 98±0.83%. The results from Figure 4.2a suggests that in order to achieve >90% microbial deactivation efficiency, the microbial population to Fe^{3+}-saturated montmorillonite ratio has to be below 2×10^3 CFU/mg. As showed in Figure 4.1, the ratio of primary wastewater microbial population to Fe^{3+}-saturated montmorillonite was 4×10^3 CFU/mg, which would result in ~72% microbial deactivation efficiency. To achieve > 90% microbial deactivation efficiency in the primary wastewater effluent tested for this study, the Fe^{3+}-saturated montmorillonite concentration would have to be at least 72 mg/mL. Furthermore, in contrast to the secondary wastewater effluent (Table 4.1), the primary wastewater effluent contains more natural organic matter and other organic constituents including phenolic contaminants,[39-41] all of which may interfere with microorganism-mineral surface interactions.

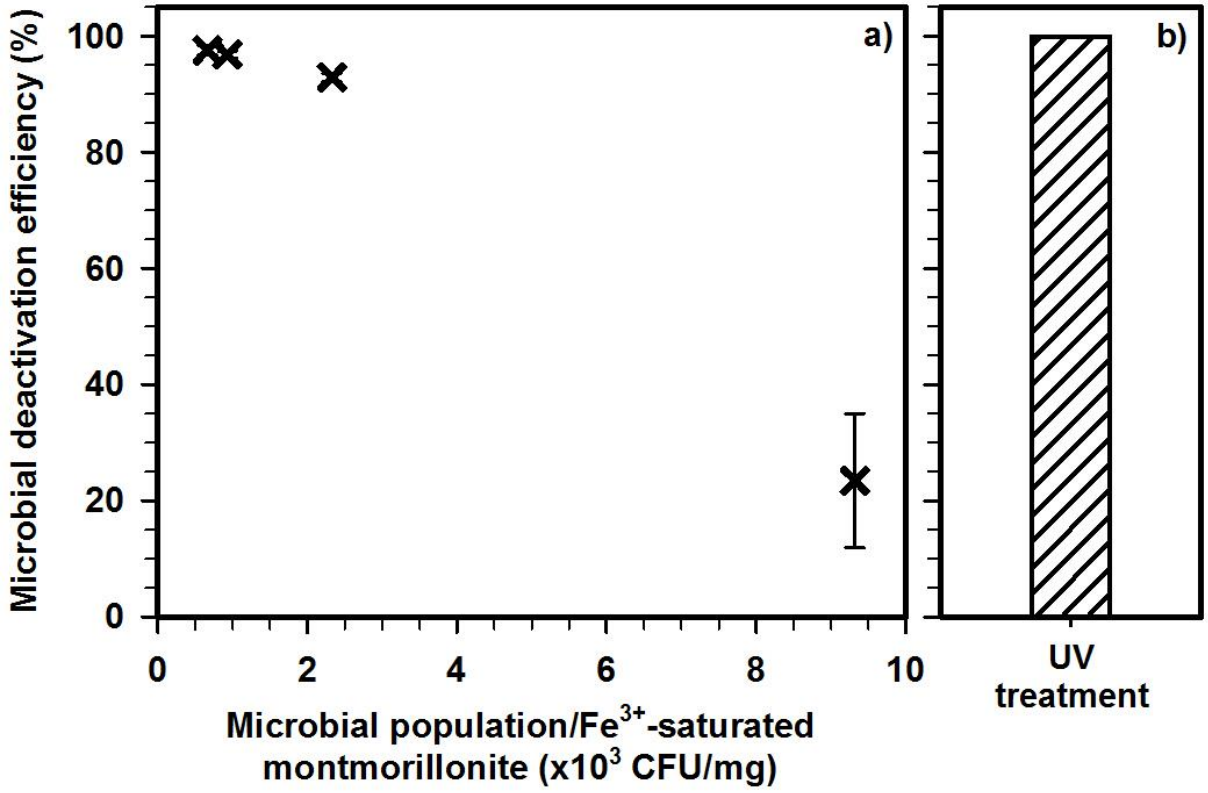

Figure 4.2 Microbial deactivation efficiencies of Fe^{3+}-saturated montmorillonite when it was exposed for 2 hours to an UV-untreated secondary wastewater effluent at different concentrations (a). The microbial deactivation efficiency of UV treatment of the secondary wastewater effluent at the WWTP where the tested wastewater samples were collected (b).

Figure 4.2b shows that the microbial deactivation efficiency of the UV treatment employed to disinfect the secondary wastewater effluent at the treatment plant was 99.9%. This outcome is comparable to that achieved by treating the secondary effluent with appropriate amount of Fe^{3+}-saturated montmorillonite treatment (Figure 4.1 and Figure 4.2a). The excellent microbial deactivation efficiency of Fe^{3+}-saturated montmorillonite reported in our study is in agreement with that of other reported nanomaterials. It was reported that single-walled carbon nanotubes and graphene oxide could deactivate *E. coli* in aqueous environment at average efficiency of 88% and 92%, respectively.[42, 43] After immersion of silver nanoparticles-coated silicon wafers into *E. coli*

and *S. aureus* inoculated growth medium for 12 hours, 99% and 98% of *E. coli* and *S. aureus* were deactivated, respectively.[44]

4.3.2 Distribution of Viable Microorganisms Between Aqueous and Mineral Phases

Figure 4.3 shows distribution patterns of viable wastewater microorganisms in the effluents exposed to Fe^{3+}-saturated montmorillonite in comparison with Na^{+}-montmorillonite. Within 30 min exposure of the primary wastewater effluent to Fe^{3+}-saturated montmorillonite at 35 mg/mL, 4.8±2.0% and 66±14% of the initial wastewater microbial population was detected as viable in the aqueous phase and mineral phase, respectively (Figure 4.3a). From 30 min to 4 h exposure, the viable microbial population associated with the Fe^{3+}-saturated montmorillonite mineral phase decreased significantly with time, while the viable microbial population in the aqueous phase remains statistically unchanged. After 4 h exposure, only 21±0.80% of the initial microbial population was viable in the mineral phase. The result shown in Figure 4.3a suggests that in the case of primary wastewater effluent, when the ratio of initial microbial population to Fe^{3+}-saturated montmorillonite was high (Figure 4.2a) and there might be high possibility of surface reaction interferences due to high organic matter content, deactivation of surface sorbed microorganisms is a slower process comparing to what were observed for the secondary wastewater effluent (Figure 4.3b).

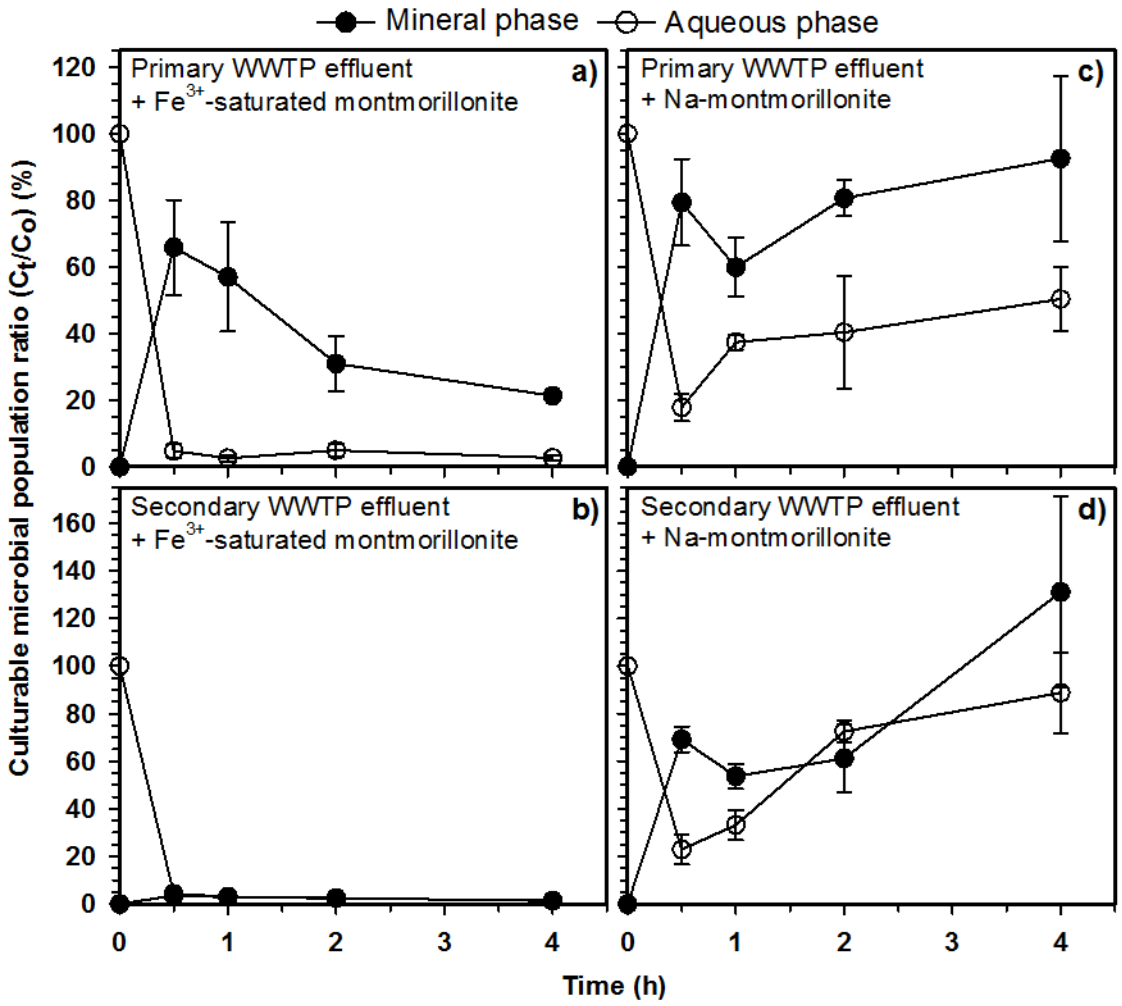

Figure 4.3 Distribution of culturable microbial population in aqueous phase and mineral phase after exposing the primary and secondary wastewater effluents to Fe^{3+}-saturated montmorillonite (left panels) and Na^{+}-montmorillonite (right panels) at 35 mg/mL for different exposure lengths. C_t is the culturable microbial population at time t and C_o is the initial clturable microbial population in a wastewater sample before exposure.

When the ratio of initial microbial population to Fe^{3+}-saturated montmorillonite was low enough to achieve >90% deactivation efficiency (Figure 4.2a), such as the case when secondary wastewater effluent was exposed to Fe^{3+}-saturated montmorillonite, microorganisms sorbed on the mineral surfaces were quickly deactivated within 30 min of exposure (Figure 4.3b). At 30 min, only 3.5±1.4% of the initial wastewater microbial population were mineral phase-associated and viable. The population of mineral surface-associated viable microorganisms remained statistically unchanged with exposure time longer than 30 min. Similar to the result of primary wastewater

effluent experiment, the fraction of initial wastewater microbial population that was viable in the aqueous phase remained low, at 4.3±0.50% and 1.3±0.30%, when the secondary wastewater effluent was exposed for 30 min and 4 h, respectively, to Fe^{3+}-saturated montmorillonite.

Contrary to the treatment with Fe^{3+}-saturated montmorillonite, significant sorption of microorganisms occurred on the Na^{+}-montmorillonite surfaces within 30 min of its exposure to the wastewater effluents (Figure 4.3c, 4.3d). After 30 min exposure of Na^{+}-montmorillonite to the primary and secondary wastewater effluents, the mineral phase-associated viable microorganisms were 79±13% and 69±5.4% of the initial microbial populations, respectively, while those remained viable in the aqueous phase were 18±4.1% and 23±6.3% of the initial microbial populations, respectively. This result indicates negligible overall microbial deactivation within 30 min exposure to Na^{+}-montmorillonite. Longer exposure time seemed to encourage microbial growth on the Na^{+}-montmorillonite mineral surfaces (Figure 4.3c, 4.3d). From 30 min to 4 h exposure of the primary and secondary wastewater effluents to Na^{+}-montmorillonite, the net growth of mineral phase-associated microorganisms increased ~17% and ~90%, respectively, while that of aqueous phase-associated microorganisms increased ~ 33% and 288%, respectively.

Because microbial cell surfaces have negatively charged sites, they can be sorbed to montmorillonite surfaces via bridging by cations or hydrated cations, both of which are electrostatically attracted to the permanent negative charges on the mineral surfaces.[45, 46] It was reported that bridging cations with higher valence could enhance microbial cell sorption on mineral surfaces than those with lower valence.[47] For example, the amount of actinomycete cells sorbed on Fe^{3+}-treated sand was observed to be close to 90 times higher than that sorbed on Na^{+}-treated sand.[47] As shown in Figure 4.3a and 4.3c, after 30 min exposure the viable populations associated with Fe^{3+}-saturated montmorillonite and Na^{+}-montmorillonite were similar in the systems with the

primary wastewater effluent. This result suggests that although Fe^{3+}-saturated montmorillonite has much higher sorption capacity for microbial cells than Na^{+}-montmorillonite, within 30 min exposure a large population of microbial cells sorbed on the Fe^{3+}-saturated montmorillonite surfaces were deactivated and become not viable for plate culture. Figure 4.3a demonstrates continuous microbial deactivation/overall growth suppression of microorganisms sorbed on the Fe^{3+}-saturated montmorillonite surfaces, while the opposite trend is shown for those sorbed on the Na^{+}-montmorillonite surfaces (Figure 4.3c, 4.3d). In the case for secondary wastewater effluent, the microbial deactivation efficiency on the Fe^{3+}-saturated montmorillonite surfaces could be greatly enhanced (Figure 4.3b) because this system had higher ratio of available mineral surface area/microbial population than that for the primary wastewater effluent system.

To further prove that the observed efficient microbial deactivation by Fe^{3+}-saturated montmorillonite is a surface process catalyzed by the Fe^{3+} sorbed on the mineral surfaces, appropriate amount of $FeCl_3$ was added to the secondary wastewater effluent to provide Fe^{3+} at a content that is equivalent to that in a wastewater system exposed to Fe^{3+}-saturated montmorillonite system at 25 mg/mL. No significant microbial deactivation was observed within 2 h incubation. Previous studies have suggested that direct contact between microbial cells and surface of antimicrobial materials is necessary for microbial deactivation.[42] It was shown that microbial cell deactivation was mainly localized on the Cu^{2+}-montmorillonite surface and was not due to the limited amount of Cu^{2+} desorbed from the mineral (1.2-2.3% of overall exchanged Cu^{2+}) into solution.[27] Similarly, in our study no significant microbial deactivation was observed in wastewater containing equivalent amount of Fe^{3+} as that desorbed from the Fe^{3+}-saturated montmorillonite when it was exposed to wastewater. The concentration of desorbed Fe^{3+} was 1.4 μg/mL when Fe^{3+}-saturated montmorillonite (10 mg/mL) was used to treat secondary wastewater,

that is, 0.14% of adsorbed Fe^{3+}. Adding Fe^{3+}-saturated montmorillonite (25 mg/mL) to wastewater lowered the pH from 7.2 to 3.3, which did not occur with Na^{+}-montmorillonite. However, this reduction of pH did not result in significant microbial deactivation in the aqueous phase (data not shown) within the experimental time. Both tests strongly support the argument that mineral surface activity of Fe^{3+}-saturated montmorillonite attributed to the observed overall microbial deactivation in the system, while change of aqueous phase chemistry due to exposure to the mineral was not a contributing factor.

4.3.3 Spectroscopy Evidence of Microbial Cell Deactivation on Fe^{3+}-Saturated Montmorillonite Surfaces

The fluorescence image of Figure 4.4a shows live and uniformly dispersed free microbial cells in the wastewater before they were exposed to Fe^{3+}-saturated montmorillonite. When they were exposed to Na^{+}-montmorillonite and Fe^{3+}-saturated montmorillonite, the microbial cells adhered onto the mineral surfaces as shown by the microorganism-mineral particle clusters in Figure. 4.4b and 4.4c, although the clusters for the former are less agglomerated. The green color microorganism-mineral clusters shown in Figure 4.4b suggests that the microbial cells sorbed on Na^{+}-montmorillonite were alive and viable. While the microbial cells sorbed on Fe^{3+}-saturated montmorillonite were clearly shown to be non-viable as indicated by the red color in the fluorescence image (Figure 4.4c). The results from Figure 4.4 strongly suggested that once microbial cells were sorbed onto Fe^{3+}-saturated montmorillonite surfaces, microbial membranes were most likely disrupted by a chemical mechanism involving the surface saturated Fe^{3+}, resulting in nonviable cells as shown in red. Further scanning electron microscopy (SEM) investigation would provide direct spectroscopic evidence on cell integrity.[48-50]

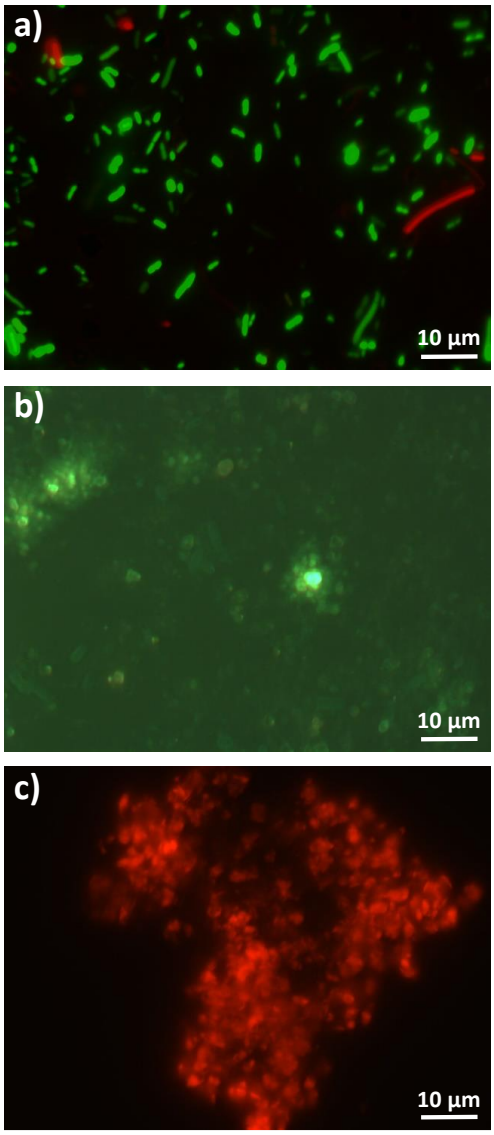

Figure 4.4 Representative fluorescence microscope images of microorganisms in a wastewater sample before exposure (a) and after exposure to Na^{+}-montmorillonite (b) and Fe^{3+}-saturated montmorillonite (c) at 25 mg/mL for 4 h.

The experimental results generated from the current investigation suggested that Fe^{3+}-saturated montmorillonite deactivated microorganisms in wastewater through the following two stages: electrostatic sorption of negatively charged microbial cells to the surfaces of Fe^{3+}-saturated montmorillonite, followed by microbial deactivation due to surface-catalyzed microbial cell membrane disruption by a possible redox process related to the surface saturated Fe^{3+}. In general, microbial deactivation can be the result of: 1) direct mechanical breakage of outer cell membranes

by sharp edged nanoparticles[35, 51, 52]; 2) chemical oxidative stress mediated cell injury that is induced by in situ production of reactive oxygen species[53, 54]; and 3) dehydration of cell membrane.[55] It is highly likely that the latter two microbial deactivation mechanisms are at play when wastewater is exposed to Fe^{3+}-saturated montmorillonite. Strong hydration force of surface sorbed Fe^{3+} could quickly induce cell membrane dehydration of microbial cells sorbed on the montmorillonite surfaces. Recent research has shown mineral surface-catalyzed Fe^{3+} reduction by organic phenolic compounds exposed to Fe^{3+}-saturated montmorillonite, forming radical cations of aromatic molecules and Fe^{2+} cations.[32, 33, 56, 57] Hence, the surface-catalyzed redox reaction and formation of radical cations could induce oxidative stress on microbial cells, resulting in disrupted microbial cell membrane and subsequent microbial deactivation. However, to pinpoint the exact microbial deactivation mechanism(s) of Fe^{3+}-saturated montmorillonite, more studies are needed to investigate the changes of cell morphology using spectroscopic methods, to monitor reactive oxygen species production, and to understand metabolic and physiological activity of microbial cells in aqueous systems with the presence of Fe^{3+}-saturated montmorillonite.

4.3.4 Reusability of Fe^{3+}-Saturated Montmorillonite for Microbial Deactivation in Wastewater

To test the reusability of Fe^{3+}-saturated montmorillonite, an experiment consisting of four consecutive 2-h long exposures of the same batches of Fe^{3+}-saturated montmorillonite at an exposure rate of 25 mg/mL to fresh secondary wastewater effluent was conducted. After each exposure, the aqueous phase and mineral phase were separated and the mineral phase was used as is or freeze dried before the next round of exposure to a new batch of wastewater. Microbial deactivation efficiencies were 97±0.58%, 86±2.3%, 69±2.6%, and 57±12% for the 1^{st}, 2^{nd}, 3^{rd}, and 4^{th} exposure, respectively, where the Fe^{3+}-saturated montmorillonite was collected and used as is

after each exposure (Figure 4.5). This decline of microbial deactivation efficiency with subsequent repeated use of the same used-as-is Fe^{3+}-saturated montmorillonite might be due to the blockage of the mineral surface reaction sites by the deactivated microbial cells remaining on the mineral surface from the previous exposure. However, when the Fe^{3+}-saturated montmorillonite was freeze-dried before each reuse, its microbial deactivation efficiency remained at 82±0.51% even when it was reused four consecutive times (Figure 4.5). Dehydration of the reused Fe^{3+}-saturated montmorillonite during freeze-drying process might help weaken the attraction between deactivated microbial cells and the mineral surfaces, resulting in their detachment from the mineral surfaces once re-exposed to the aqueous phase and, therefore, freeing up the reactive sites for further microbial deactivation. The freeze-drying followed by quick hydration might also enhance the physical removal of other coated species from wastewater.

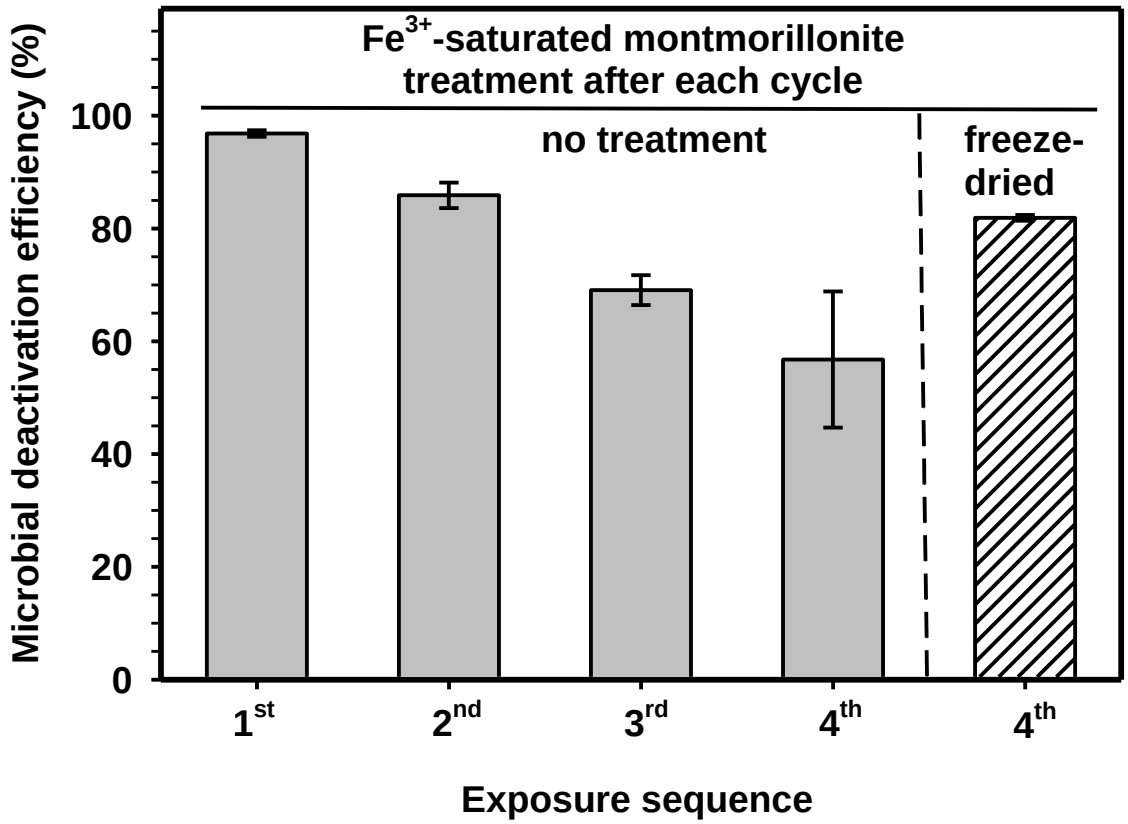

Figure 4.5 Microbial deactivation efficiency of Fe^{3+}-saturated montmorillonite used repetitively for four consecutive 2-h exposures. A fresh batch of secondary wastewater effluent was used for each exposure. The Fe^{3+}-saturated montmorillonite exposure dose was 25 mg/mL. The Fe^{3+} saturated montmorillonite was collected via centrifugation and used as is (left panel) or freeze-dried (right panel) after each exposure.

In summary, this study demonstrated, for the first time, the effectiveness of Fe^{3+}-saturated montmorillonite for microbial deactivation in wastewater. The overall results of this study suggest that Fe^{3+}-saturated montmorillonite could be used as a low cost, environmental friendly, and effective antimicrobial material for water disinfection in applications from small scale point-of-use drinking water treatment devices to large scale drinking and wastewater treatment facilities.

ACKNOWLEDEGEMENTS

We acknowledge the financial support from USDA NIFA award #2013-67019-21355. Funding for this work was provided, in part, by the Virginia Agricultural Experiment Station and the Hatch

Program of the National Institute of Food and Agriculture, U.S. Department of Agriculture. We thank Mr. Bobby Epperly from Blacksburg-VPI Sanitation Authority Treatment Plant for his assistance with wastewater sample collection. We also thank Dr. Kristi DeCourcy from the Imaging Center at Virginia Tech Fralin Life Science Institute for her assistance with the fluorescence microscope.

4.4 References

1. Shannon, M. A.; Bohn, P. W.; Elimelech, M.; Georgiadis, J. G.; Mariñas, B. J.; Mayes, A. M., Science and technology for water purification in the coming decades. *Nature* **2008,** *452*, (7185), 301-310.
2. Richardson, S. D.; Postigo, C., Drinking water disinfection by-products. In *Emerging organic contaminants and human health*, Springer: 2011; pp 93-137.
3. Krasner, S. W.; Westerhoff, P.; Chen, B.; Rittmann, B. E.; Amy, G., Occurrence of disinfection byproducts in United States wastewater treatment plant effluents. *Environmental science & technology* **2009,** *43*, (21), 8320-8325.
4. Montgomery, M. A.; Elimelech, M., Water and sanitation in developing countries: including health in the equation. *Environmental Science & Technology* **2007,** *41*, (1), 17-24.
5. Morones, J. R.; Elechiguerra, J. L.; Camacho, A.; Holt, K.; Kouri, J. B.; Ramírez, J. T.; Yacaman, M. J., The bactericidal effect of silver nanoparticles. *Nanotechnology* **2005,** *16*, (10), 2346.
6. Panáček, A.; Kvitek, L.; Prucek, R.; Kolar, M.; Vecerova, R.; Pizurova, N.; Sharma, V. K.; Nevečná, T. j.; Zboril, R., Silver colloid nanoparticles: synthesis, characterization, and their antibacterial activity. *The Journal of Physical Chemistry B* **2006,** *110*, (33), 16248-16253.
7. Dankovich, T. A.; Gray, D. G., Bactericidal paper impregnated with silver nanoparticles for point-of-use water treatment. *Environmental science & technology* **2011,** *45*, (5), 1992-1998.
8. Meghana, S.; Kabra, P.; Chakraborty, S.; Padmavathy, N., Understanding the pathway of antibacterial activity of copper oxide nanoparticles. *RSC Advances* **2015,** *5*, (16), 12293-12299.
9. Ben-Sasson, M.; Zodrow, K. R.; Genggeng, Q.; Kang, Y.; Giannelis, E. P.; Elimelech, M., Surface functionalization of thin-film composite membranes with copper nanoparticles for antimicrobial surface properties. *Environmental science & technology* **2013,** *48*, (1), 384-393.
10. Simon-Deckers, A.; Loo, S.; Mayne-L'hermite, M.; Herlin-Boime, N.; Menguy, N.; Reynaud, C.; Gouget, B.; Carrière, M., Size-, composition-and shape-dependent toxicological impact of metal oxide nanoparticles and carbon nanotubes toward bacteria. *Environmental science & technology* **2009,** *43*, (21), 8423-8429.
11. Li, Y.; Zhang, W.; Niu, J.; Chen, Y., Mechanism of photogenerated reactive oxygen species and correlation with the antibacterial properties of engineered metal-oxide nanoparticles. *Acs Nano* **2012,** *6*, (6), 5164-5173.
12. Vecitis, C. D.; Zodrow, K. R.; Kang, S.; Elimelech, M., Electronic-structure-dependent bacterial cytotoxicity of single-walled carbon nanotubes. *ACS nano* **2010,** *4*, (9), 5471-5479.

13. Tiraferri, A.; Vecitis, C. D.; Elimelech, M., Covalent binding of single-walled carbon nanotubes to polyamide membranes for antimicrobial surface properties. *ACS applied materials & interfaces* **2011,** *3*, (8), 2869-2877.
14. Applerot, G.; Lipovsky, A.; Dror, R.; Perkas, N.; Nitzan, Y.; Lubart, R.; Gedanken, A., Enhanced antibacterial activity of nanocrystalline ZnO due to increased ROS-mediated cell injury. *Adv. Funct. Mater.* **2009,** *19*, (6), 842-852.
15. Raghupathi, K. R.; Koodali, R. T.; Manna, A. C., Size-dependent bacterial growth inhibition and mechanism of antibacterial activity of zinc oxide nanoparticles. *Langmuir* **2011,** *27*, (7), 4020-4028.
16. Lyon, D. Y.; Alvarez, P. J. J., Fullerene water suspension (nC60) exerts antibacterial effects via ROS-independent protein oxidation. *Environmental science & technology* **2008,** *42*, (21), 8127-8132.
17. Wu, M.-C.; Deokar, A. R.; Liao, J.-H.; Shih, P.-Y.; Ling, Y.-C., Graphene-based photothermal agent for rapid and effective killing of bacteria. *ACS nano* **2013,** *7*, (2), 1281-1290.
18. Liu, S.; Hu, M.; Zeng, T. H.; Wu, R.; Jiang, R.; Wei, J.; Wang, L.; Kong, J.; Chen, Y., Lateral dimension-dependent antibacterial activity of graphene oxide sheets. *Langmuir* **2012,** *28*, (33), 12364-12372.
19. Perreault, F.; de Faria, A. F.; Nejati, S.; Elimelech, M., Antimicrobial properties of graphene oxide nanosheets: why size matters. *ACS nano* **2015,** *9*, (7), 7226-7236.
20. Hu, W.; Peng, C.; Luo, W.; Lv, M.; Li, X.; Li, D.; Huang, Q.; Fan, C., Graphene-based antibacterial paper. *Acs Nano* **2010,** *4*, (7), 4317-4323.
21. Matsumura, Y.; Yoshikata, K.; Kunisaki, S.-i.; Tsuchido, T., Mode of bactericidal action of silver zeolite and its comparison with that of silver nitrate. *Applied and environmental microbiology* **2003,** *69*, (7), 4278-4281.
22. Feng, Q. L.; Wu, J.; Chen, G. Q.; Cui, F. Z.; Kim, T. N.; Kim, J. O., A mechanistic study of the antibacterial effect of silver ions on Escherichia coli and Staphylococcus aureus. *Journal of biomedical materials research* **2000,** *52*, (4), 662-668.
23. Lv, M.; Su, S.; He, Y.; Huang, Q.; Hu, W.; Li, D.; Fan, C.; Lee, S. T., Long-Term Antimicrobial Effect of Silicon Nanowires Decorated with Silver Nanoparticles. *Adv. Mater.* **2010,** *22*, (48), 5463-5467.
24. Qu, X.; Brame, J.; Li, Q.; Alvarez, P. J. J., Nanotechnology for a safe and sustainable water supply: enabling integrated water treatment and reuse. *Acc. Chem. Res.* **2012,** *46*, (3), 834-843.
25. Williams, L. B.; Haydel, S. E., Evaluation of the medicinal use of clay minerals as antibacterial agents. *International geology review* **2010,** *52*, (7-8), 745-770.
26. Morrison, K. D.; Underwood, J. C.; Metge, D. W.; Eberl, D. D.; Williams, L. B., Mineralogical variables that control the antibacterial effectiveness of a natural clay deposit. *Environmental geochemistry and health* **2014,** *36*, (4), 613-631.
27. Hu, C. H.; Xu, Z. R.; Xia, M. S., Antibacterial effect of Cu 2+-exchanged montmorillonite on Aeromonas hydrophila and discussion on its mechanism. *Veterinary microbiology* **2005,** *109*, (1), 83-88.
28. Magana, S. M.; Quintana, P.; Aguilar, D. H.; Toledo, J. A.; Angeles-Chavez, C.; Cortes, M. A.; Leon, L.; Freile-Pelegrín, Y.; López, T.; Sánchez, R. M. T., Antibacterial activity of montmorillonites modified with silver. *J. Mol. Catal. A: Chem.* **2008,** *281*, (1), 192-199.

29. Tong, G.; Yulong, M.; Peng, G.; Zirong, X., Antibacterial effects of the Cu (II)-exchanged montmorillonite on Escherichia coli K88 and Salmonella choleraesuis. *Veterinary microbiology* **2005,** *105*, (2), 113-122.
30. Hrenovic, J.; Milenkovic, J.; Ivankovic, T.; Rajic, N., Antibacterial activity of heavy metal-loaded natural zeolite. *J. Hazard. Mater.* **2012,** *201*, 260-264.
31. Malachová, K.; Praus, P.; Rybková, Z.; Kozák, O., Antibacterial and antifungal activities of silver, copper and zinc montmorillonites. *Applied Clay Science* **2011,** *53*, (4), 642-645.
32. Liyanapatirana, C.; Gwaltney, S. R.; Xia, K., Transformation of triclosan by Fe (III)-saturated montmorillonite. *Environmental science & technology* **2009,** *44*, (2), 668-674.
33. Qin, C.; Troya, D.; Shang, C.; Hildreth, S.; Helm, R.; Xia, K., Surface catalyzed oxidative oligomerization of 17β-estradiol by Fe3+-saturated montmorillonite. *Environmental science & technology* **2014,** *49*, (2), 956-964.
34. Pepper, I. L.; Gerba, C. P., Chapter 10 - Cultural Methods. In *Environmental Microbiology (Third edition)*, Academic Press: San Diego, 2015; pp 195-212.
35. Liu, S.; Wei, L.; Hao, L.; Fang, N.; Chang, M. W.; Xu, R.; Yang, Y.; Chen, Y., Sharper and faster "nano darts" kill more bacteria: a study of antibacterial activity of individually dispersed pristine single-walled carbon nanotube. *Acs Nano* **2009,** *3*, (12), 3891-3902.
36. Van Loosdrecht, M. C.; Lyklema, J.; Norde, W.; Zehnder, A. J., Influence of interfaces on microbial activity. *Microbiological reviews* **1990,** *54*, (1), 75-87.
37. Stotzky, G.; Rem, L. T., Influence of clay minerals on microorganisms: I. Montmorillonite and kaolinite on bacteria. *Can. J. Microbiol.* **1966,** *12*, (3), 547-563.
38. Stotzky, G., Influence of clay minerals on microorganisms: II. Effect of various clay species, homoionic clays, and other particles on bacteria. *Can. J. Microbiol.* **1966,** *12*, (4), 831-848.
39. Katsoyiannis, A.; Samara, C., The fate of dissolved organic carbon (DOC) in the wastewater treatment process and its importance in the removal of wastewater contaminants. *Environmental Science and Pollution Research-International* **2007,** *14*, (5), 284-292.
40. Carballa, M.; Omil, F.; Lema, J. M.; Llompart, M. a.; García-Jares, C.; Rodríguez, I.; Gomez, M.; Ternes, T., Behavior of pharmaceuticals, cosmetics and hormones in a sewage treatment plant. *Water Res.* **2004,** *38*, (12), 2918-2926.
41. Nakada, N.; Tanishima, T.; Shinohara, H.; Kiri, K.; Takada, H., Pharmaceutical chemicals and endocrine disrupters in municipal wastewater in Tokyo and their removal during activated sludge treatment. *Water Res.* **2006,** *40*, (17), 3297-3303.
42. Kang, S.; Pinault, M.; Pfefferle, L. D.; Elimelech, M., Single-walled carbon nanotubes exhibit strong antimicrobial activity. *Langmuir* **2007,** *23*, (17), 8670-8673.
43. Liu, S.; Zeng, T. H.; Hofmann, M.; Burcombe, E.; Wei, J.; Jiang, R.; Kong, J.; Chen, Y., Antibacterial Activity of Graphite, Graphite Oxide, Graphene Oxide, and Reduced Graphene Oxide: Membrane and Oxidative Stress. *ACS Nano* **2011,** *5*, (9), 6971-6980-6971-6980.
44. Zhou, Y.; Jiang, X.; Tang, J.; Su, Y.; Peng, F.; Lu, Y.; Peng, R.; He, Y., A silicon-based antibacterial material featuring robust and high antibacterial activity. *Journal of Materials Chemistry B* **2014,** *2*, (6), 691-697.
45. Theng, K.; Orchard, V.; Huang, P.; Berthelin, J.; Bollag, J.; McGill, W.; Page, A., Interactions of clays with microorganisms and bacterial survival in soil: a physicochemical perspective. *Environmental impact of soil component interactions: Volume 2: metals, other inorganics, and microbial activities.* **1995**, 123-143.

46. Huang, P. M., Impacts of Physicochemical-Biological Interactions on Metal and Metalloid Transformations in Soils: An Overview (P.M. Huang). In *Biophysico-Chemical Processes of Heavy Metals and Metalloids in Soil Environments* Violante, A., P. M. Huang., and G. M.. Gadd, Ed. Wiley Interscience: 2008; pp 3-52.
47. Ruddick, S. M.; Williams, S. T., Studies on the ecology of actinomycetes in soil V. Some factors influencing the dispersal and adsorption of spores in soil. *Soil Biol. Biochem.* **1972,** *4*, (1), 93,IN7,101-100,IN10,103.
48. Hoque, J.; Akkapeddi, P.; Yadav, V.; Manjunath, G. B.; Uppu, D. S. S. M.; Konai, M. M.; Yarlagadda, V.; Sanyal, K.; Haldar, J., Broad Spectrum Antibacterial and Antifungal Polymeric Paint Materials: Synthesis, Structure–Activity Relationship, and Membrane-Active Mode of Action. *ACS applied materials & interfaces* **2015,** *7*, (3), 1804-1815.
49. Tang, J.; Chen, Q.; Xu, L.; Zhang, S.; Feng, L.; Cheng, L.; Xu, H.; Liu, Z.; Peng, R., Graphene oxide–silver nanocomposite as a highly effective antibacterial agent with species-specific mechanisms. *ACS applied materials & interfaces* **2013,** *5*, (9), 3867-3874.
50. Ma, S.; Zhan, S.; Jia, Y.; Zhou, Q., Superior antibacterial activity of Fe3O4-TiO2 nanosheets under solar light. *ACS applied materials & interfaces* **2015,** *7*, (39), 21875-21883.
51. Situ, S. F.; Samia, A. C. S., Highly efficient antibacterial iron oxide@ carbon nanochains from wustite precursor nanoparticles. *ACS applied materials & interfaces* **2014,** *6*, (22), 20154-20163.
52. Akhavan, O.; Ghaderi, E., Toxicity of graphene and graphene oxide nanowalls against bacteria. *ACS nano* **2010,** *4*, (10), 5731-5736.
53. Krishnamoorthy, K.; Veerapandian, M.; Zhang, L.-H.; Yun, K.; Kim, S. J., Antibacterial efficiency of graphene nanosheets against pathogenic bacteria via lipid peroxidation. *The Journal of Physical Chemistry C* **2012,** *116*, (32), 17280-17287.
54. Su, H.-L.; Chou, C.-C.; Hung, D.-J.; Lin, S.-H.; Pao, I.-C.; Lin, J.-H.; Huang, F.-L.; Dong, R.-X.; Lin, J.-J., The disruption of bacterial membrane integrity through ROS generation induced by nanohybrids of silver and clay. *Biomaterials* **2009,** *30*, (30), 5979-5987.
55. Beney, L.; Mille, Y.; Gervais, P., Death ofEscherichia coli during rapid and severe dehydration is related to lipid phase transition. *Appl. Microbiol. Biotechnol.* **2004,** *65*, (4), 457-464.
56. Polubesova, T.; Eldad, S.; Chefetz, B., Adsorption and oxidative transformation of phenolic acids by Fe (III)-montmorillonite. *Environmental science & technology* **2010,** *44*, (11), 4203-4209.
57. Gu, C.; Li, H.; Teppen, B. J.; Boyd, S. A., Octachlorodibenzodioxin formation on Fe (III)-montmorillonite clay. *Environmental science & technology* **2008,** *42*, (13), 4758-4763.

Chapter 5. Bacteria Deactivation Using Fe^{3+}-Saturated Montmorillonite Impregnated Paper

(To be submitted to Water Research)

Abstract

This study describes a novel method to impregnate Fe^{3+}-saturated montmorillonite in cellulose filter paper and demonstrates its effectiveness in reducing the levels of harmful microorganisms in water. Fe^{3+}-saturated montmorillonite was incorporated into paper matrix through wet-end addition during paper making process and formed uniformly impregnated paper after dried. The Scanning Electron Microscopy (SEM) imaging showed that Fe^{3+}-saturated montmorillonite was evenly dispersed and coated over the cellulose fiber surface. When it was used to filter 50 mL and 200 mL of water spiked with live *Escherichia coli* (*E. coli*) cells at 3.67×10^{8} CFU/mL, the Fe^{3+}-saturated montmorillonite impregnated filter paper with 50% of mineral/paper weight percent loading deactivated *E. coli* with 99% and 77% deactivation efficiency, respectively. When the ratio of treated volume/Fe^{3+}-saturated montmorillonite (mL/mL) decreased from 1:0.4 to 1:1.5, *E. coli* deactivation efficiency increased from 69% to 99.5% and maintained 100% at ratio of 1:3 when treating 50 mL water spiked with *E. coli* at 1.18×10^{6} CFU/mL was passed through. Dielectrophoresis (DEP) and impedance analysis of *E. coli* filtrate also confirmed that the deactivated *E. coli* passing through Fe^{3+}-saturated montmorillonite filter paper did not have trapping response (mainly dead) to DEP due to higher

membrane permeability and conductivity. For total treatment of 500 mL *E. coli*-contaminated water, 0.13 mg Fe^{3+} was released into the filtered water, accounting for 0.3% of the Fe^{3+} initially retained on the montmorillonite filter paper. The Fe^{3+} leached into the water for treating *E coli*-contaminated water could be a potential iron supplement to the human consuming the water. Assuming a 2-L water consumption/day, 0.52 mg of iron would be consumed per day. This is a level within the range of the FDA recommended daily intake of iron for an adult. The results from this study demonstrate the feasibility of using the Fe^{3+}-saturated montmorillonite impregnated paper for convenient point-of-use drinking water disinfection.

5.1 Introduction

Ensuring public access to clean and reliable water resources is one of the greatest global challenges in this century. Clean water and sanitation services are still severely lacking in developing countries. Currently, more than 1.1 billion people worldwide do not have access to clean and safe drinking water supplies.[1] The adverse health impacts due to lack access to clean water and sanitation are significant. Exposure to water contaminated by pathogenic bacteria or viruses results in problematic waterborne disease, including diarrheal diseases, intestinal helminthes, schistosomiasis, and trachoma.[2] As a result, millions suffer from preventable illness and die every year.

In developed nations, centralized wastewater treatment plants are required to apply disinfection before discharging to surface water environment in order to remove potentially harmful microorganisms in wastewater effluent. While traditional disinfection practices (chlorination, ozonation) show high effectiveness, these powerful oxidants can react with naturally occurring organic matter and form toxic disinfection byproducts (DBPs). During past few decades,

wide ranges of toxic DBPs (halogenated DBPs, carcinogenic nitrosamines, bromate) have been reported,[3] and their carcinogenic potential has raised public health concern.[4] Recent US disinfection regulations require the minimization of certain DBPs formation, which force sewage plants to discard traditional chlorine disinfection and to use UV disinfection as an alternative. However, UV disinfection is not as cost-effective as chlorination since it often requires a high dosage of radiation and thus higher energy consumption to effectively inactivate some viruses. These disadvantages urge researchers to develop new efficient, low-cost technologies to accommodate these needs.

In developing countries with limited resources, centralized wastewater and drinking water treatment facilities are still not implemented due to dispersed population, high capital cost, low efficiency service, unaffordable maintenance and lack of proper operation.[2] For these reasons, decentralized areas that rely on household water treatment and sanitation technology therefore might become viable alternative approach. Point-of-use (POU) water treatment technologies are simple, acceptable, low-cost interventions at the household and community levels that are capable of dramatically improving the microbial quality of household stored water and reducing the attendant risks of microbial disease and death.[5] With the advantage of cheap and low energy cost, point-of-use household treatment technology has therefore emerged as a primary approach.[6] Moreover, point-of-use systems can provide safe drinking water response to large-scale emergencies and disasters. Common point-of-use technologies include chlorination with safe storage, combined coagulant-chlorine disinfection systems, solar water disinfection, ceramic filters and biosand filters.[6] Although these methods have scientifically proved evidence of ability to improve water quality and reduce waterborne infectious disease, none of these have achieved

sustained and large-scale use.[6] Thereby, the demand of developing new generations of antibacterial materials for effective drinking water disinfection is becoming urgent.

Functional nanomaterials including silver nanoparticles,[7, 8] carbon nanotubes,[9] and titania nanoparticles[10] have been recently studied for possible feasibility of POU treatment application. However, there have been concerns about their long term efficacy and economic applicability.[11] For example, among all the bactericidal agents, silver nanoparticles have been widely studied due to their highly effective and broad-spectrum antimicrobial activities.[12] However, silver-based antimicrobial materials are quite expensive and show poor stability.[13] The dissolution of nano Ag into Ag^+ could lead to its eventual depletion; Therefore, concerns about their long-time efficacy and replenishment possibility have been raised for economic application.[11] For these reasons, researchers turn to develop more affordable and durable alternative materials with superior antibacterial activity for pathogenic microorganisms removal from contaminated water.

Our previous study (Chapter 4) has demonstrated that Fe^{3+}-saturated montmorillonite has great capacity to target and inactivate a broad range of bacteria in wastewater. With high specific surface area, cation exchange and sorption capacity, montmorillonite can be an ideal matrix for retaining Fe^{3+} and showing great antimicrobial property. However, how to immobilize mineral into carrier to achieve easy separation and recycling of Fe^{3+}-saturated montmorillonite has become rising problem during POU application.

With the advantages of high porosity, mechanical strength, high absorbency and natural abundance, cellulose paper material has raised attractive interest to serve as support matrix.[14] Bactericidal agents (silver, copper nanoparticle, graphene) embedded onto paper matrix have been widely reported as effective POU water treatment.[15-19] The porous structure and hydrophilic cellulose fiber allow paper fiber to absorb nanoparticles by capillary forces and produce high

nanoparticle loading onto paper upon drying.[20] Moreover, filter paper has been universally applied as inert support for unique functionalization due to simplicity.[20] Wet-end addition and surface treatment are two main approaches to attach target nanomaterials onto paper matrix. While surface treatment merely coats the nanomaterial particles over dry paper sheet surface, wet-end impregnation is made to permeate the paper fiber structure, which allows better contact and complete deposit between target particles with individual fibers in three dimensions before paper sheet formation.[21] Therefore, we proposed in this study that Fe^{3+}-saturated montmorillonite can be incorporated into pulp fiber network by stirring filter paper pulp with mineral suspension. After molding and drying, Fe^{3+}-saturated montmorillonite will be penetrated into whole cellulose fiber paper structure and such fabricated filter paper sheet will provide excellent antibacterial function.

Following the interest in paper functionalization with bacteria deactivation properties, we therefore designed paper sheet embedded with Fe^{3+}-saturated montmorillonite for the first time, which could be used for drinking water purification to eliminate the waterborne pathogenic microorganisms. To our knowledge, this is the first attempt to immobilize and prepare Fe^{3+}-saturated montmorillonite that has promising prospect as efficient POU treatment purifier.

5.2 Materials and Methods

5.2.1 Chemicals and Materials

LB broth powder (Lennox), powdered agar, sodium chloride (≥99%) were purchased from Fisher Scientific (Fair Lawn, NJ). Na^{+}-montmorillonite (SWy-2, Crook County, Wyoming) was obtained from the Source Clays Repository of the Clay Minerals Society (Purdue University, West Lafayette, IN). Whatman qualitative cellulose filter paper was used to blend with Fe^{3+}-saturated

montmorillonite in this study. The ultrapure water used in this study was produced by Millipore Milli-Q water purification system (Milford, MA). Nonpathogenic *Escherichia coli* ATCC 25922 strain was obtained from obtained from the American Type Culture Collection (ATCC, Rockville, Maryland, USA) and used as model *E. coli* microorganism for deactivation test. We choose this organism because of its role as indicator for fecal contamination in drinking water.

5.2.2 Fe^{3+}-Saturated Montmorillonite Preparation

More details for preparation of Fe^{3+}-saturated montmorillonite have been described in our previous studies.[22, 23] Briefly, Na^{+}-montmorillonite (Swy-2) was purified and fractionated to <2 μm clay-sized particles before Fe^{3+} saturation.[24] Clay-sized particles (<2 μm) Na^{+}-montmorillonite was then mixed with 0.1 M $FeCl_3$ for 6 times in order to saturate the montmorillonite interlayer with Fe^{3+}. The Fe^{3+}-saturated montmorillonite was then repeatedly washed with ultrapure grade water followed by centrifugation until free detection of Cl^{-} in supernatant with $AgNO_3$ test. The centrifuged wet Fe^{3+}-saturated montmorillonite was collected for further paper composite making.

5.2.3 Impregnation of Fe^{3+}-Saturated Montmorillonite into Paper

Pieces of filter papers were soaked in water overnight to soften the texture, and were blended into paper pulp with a kitchen blender for 5 min. The pulp was later centrifuged at 6000 *rpm* for 10 min. The mineral impregnated paper with two different minerals loadings paper (25% and 50%) were made in this study as follows: the paper pulp pellets (wet weight: 20 g, dry weight: 5.62 g.) were mixed with different amounts of wet Fe^{3+}-saturated montmorillonite (20 g wet weight equal to 5.51 g dry weight; 8 g wet weight equal to 2.21 g dry weight) and then stirred vigorously with 120 mL of water into muddy mineral-pulp slurry, during which minerals were sorbed on the surface of cellulose paper fiber. The slurry was gently poured onto deckle mould with fine screen and a thin layer of mineral blended pulp was formed on the screen, which was further pressed,

transferred and air-dried on towel surface. High and low loading Fe^{3+}-saturated montmorillonites contained 50% and 25% dry weight of Fe^{3+}-saturated montmorillonite, respectively. Similarly, paper pulp pellet (wet weight: 20 g, dry weight: 5.62 g.) were mixed with different amounts of wet Na^{+}-montmorillonite (20 g wet weight equal to 1.85 g dry weight; 50 g wet weight equal to 4.63 g dry weight) and made into Na^{+}-montmorillonite blended using the same method. High and low loading Na^{+}-montmorillonites paper contained 25% and 50% dry weight ratio of Na^{+}-montmorillonites/paper, respectively. The composite filter paper was cut to make a circle of 2.5 cm diameter to fit filter holder for syringe filtration.

5.2.4 Bacteria Deactivation Filtration Assay

To prevent microbial cross contamination during each step of testing, all related glassware and materials were properly sterilized by autoclaving at 121°C for 20 min. One mL of secondary wastewater effluent (collected from local wastewater treatment plant) was incubated in 100 mL LB medium at 37°C until mid-exponential growth phase. The cultured bacteria were then spread onto MacConkey agar plate and incubated at 37°C for 12 h. The appeared pink colonies were picked and used as *E. coli* bacteria representatives isolated from wastewater in further deactivation experiment.

E. coli suspension in saline (0.85% NaCl) was passed through mineral embedded filter paper mounted in syringe filter holder at approximate flow rate of 10 mL/min and the filtrate effluent was immediately collected. Also, *E. coli* suspension was passed through Na^{+}-montmorillonite embedded filter and the blank filter paper without any mineral incorporated as comparison. Bacteria deactivation assessment was conducted by quantification of remaining microbial population in filtrate expressed in colony forming units (CFU).[25] Briefly, the *E. coli* filtrate was diluted sequentially 10-fold with saline water (0.85% NaCl) for up to 5 times. An

aliquot of 100 μL was taken from each diluted solution, spread onto a pre-sterilized LB agar growth media, and incubated at 37°C for one day before colony counting. The microbial deactivation efficiency was calculated using equation: Deactivation (%)=1-C_{in}/C_{ef}, where C_{ef} is the CFU concentration in filtrate, C_{in} is the CFU concentration in *E. coli* suspension before filtration. All the treatments were prepared in triplicates.

5.2.5 Characterization of Fe^{3+}-Saturated Montmorillonite loaded Paper

Different mineral blended papers and blank filter paper were sputter-coated with Pt/Pd film (thickness: 8 nm) and then imaged using LEO field emission scanning electron microscope (Carl Zeiss, LEO 1550, Oberkochen, Germany). Moreover, Fe^{3+}-saturated montmorillonite filter paper after *E. coli* filtration and filtration sample was also examined under SEM. After passing 50 mL of *E. coli* suspension in saline (0.85% NaCl) through Fe^{3+}-saturated montmorillonite embedded filter papers, the filtrate was collected and further passed through Millipore membrane filter (0.45 μm) to retain remaining *E. coli* in filtrate. These samples were treated, sputter-coated in the same way and further examined by SEM.

5.2.6 Dielectrophoresis Trapping Test

E. coli filtrates after passing through Fe^{3+}-saturated montmorillonite and Na^{+}-montmorillonite paper were further stained for 20 min using a live/dead viability kit (LIVE/DEAD Backlit, Invitrogen). *E. coli* cells were later centrifuged and re-suspended in saline before injected to PDMS-based microfluidic device. Impedance measurements for each sample were conducted using an impedance analyzer (Agilent HP4192A). The frequency test was in the range 50 kHz to 950 KHz. Initial baseline impedance measurements were defined in saline solution only. 50 µL of *E. coli* suspension was introduced into each well, and impedance measurements were made for 1 h at 37 °C.

5.3 Results and Discussion

5.3.1. Effectiveness of Fe^{3+}-saturated montmorillonite impregnated filter paper for deactivation of *E. coli* in water

The bacteria deactivation effectiveness of Fe^{3+}-saturated montmorillonite integrated paper was tested using *E. coli* bacteria in comparison with Na^{+}-montmorillonite embedded paper and blank paper, and the results are presented in Figure 5.1. After effluent bacteria suspension passing through the paper, the filtrate was sampled and cultured for viable bacteria counting. Viability results showed that *E. coli* suspension filtered through blank paper did not show any CFU reduction and the viable bacteria remains ~100% in the effluent water (data not shown), indicating the original filter paper fiber structure does not filter out and eliminate bacteria from water. Similarly, a minor reduction (9-10%) of effluent bacteria after passing through Na^{+}-montmorillonite blended paper was observed, which might be due to partial adsorption onto the Na^{+}-montmorillonite embedded paper. In contrast, Fe^{3+}-saturated montmorillonite embedded paper manifested excellent deactivation capacity and showed 99% and 77% deactivation efficiency over 50 mL and 200 mL *E. coli* suspension, respectively. The mineral blended filter paper allows the direct contact of bacteria with Fe^{3+}-saturated montmorillonite during filtration process, during which the bacteria cells are quickly deactivated and the inactivated bacteria are passed through the filter papers into the effluent. After filtration, the filter paper sheets were washed again with saline and only few *E. coli* bacteria were shown retained in both Fe^{3+}-saturated montmorillonite and Na^{+}-montmorillonite paper sheets. This suggested that the primary purification mechanism is not due to the retention of bacteria by filtration but rather due to bacteria inactivation when they percolate through the Fe^{3+}-saturated montmorillonite embedded paper. Similarly, filter sheet containing silver nanoparticles was reported to deactivate bacteria in effluent during simple filtration

process.[14, 15] Fe^{3+}-saturated montmorillonite paper has shown comparable deactivation efficiency to other reported antibacterial paper.[26-28]

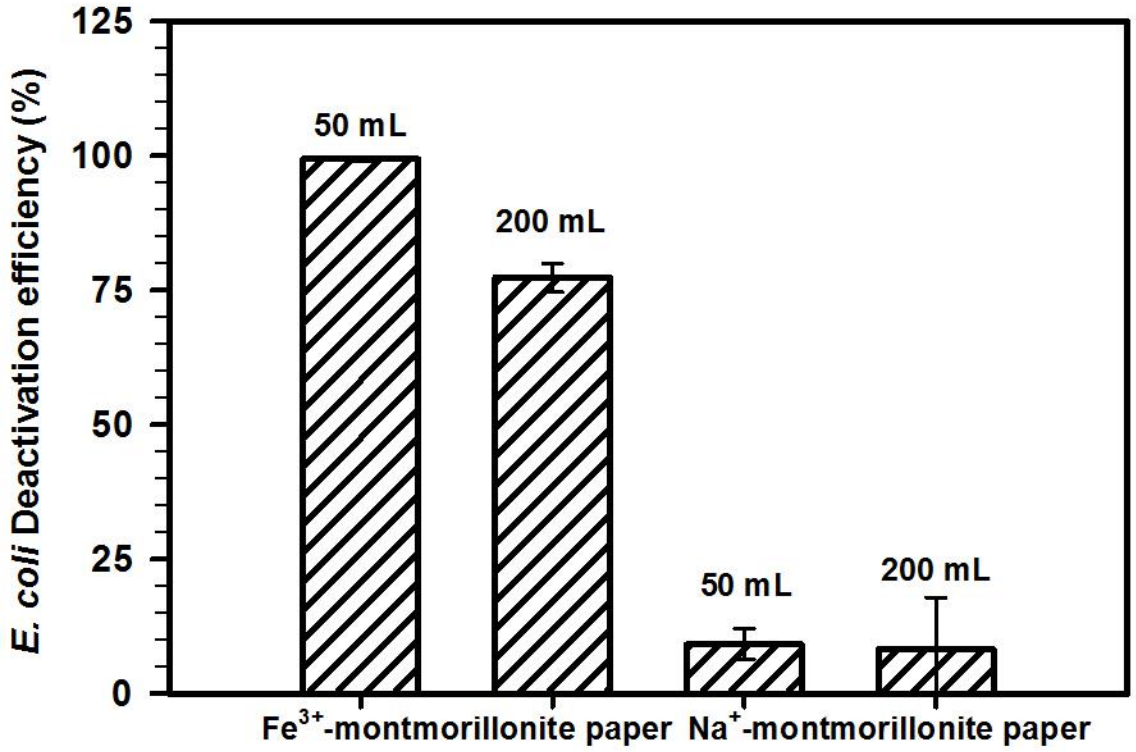

Figure 5.1 *E. coli* deactivation efficiency of Fe^{3+}-saturated montmorillonite paper (50% loading) and Na^{+}-montmorillonite paper (45% loading) for treating 50 mL and 200 mL of *E. coli* suspension. The initial *E. coli* (ATCC 25922) level was 3.67×10^{8} CFU/mL.

In laboratory antibacterial testing studies, bacteria concentrations are typically cultured to 10^{6}-10^{8} CFU per mL or higher to represent the acute case of microbial contamination in highly polluted stream water.[29] In our study, Fe^{3+}-saturated montmorillonite blended paper had still shown excellent bacteria deactivation capacity towards such high bacteria concentration. Considering that natural stream waters usually have much lower bacteria levels, we therefore expect that Fe^{3+}-saturated montmorillonite filter paper could achieve complete bacteria inactivation in natural water samples.

Figure 5.1 also showed that Fe^{3+}-saturated montmorillonite paper (50% loading) has the capacity limit of 50 mL in order to achieve almost complete *E. coli* inactivation. Therefore, effect of mineral/paper mass ratio on *E. coli* deactivation efficiency of Fe^{3+}-saturated montmorillonite paper was also studied (Figure 5.2). When the ratio of treated volume/Fe^{3+}-saturated montmorillonite (mL/mL) decreased from 1:0.4 to 1:1.5, *E. coli* deactivation efficiency increased from 69% to 99.5% and maintained 100% at ratio of 1:3. This indicated that when treating larger volume of *E. coli* contaminated water for practical use, increasing either the size of Fe^{3+}-saturated montmorillonite paper or Fe^{3+}-saturated montmorillonite loading amount in constructing the composite filter paper would help improve and maintain satisfactory microbial deactivation efficiency.

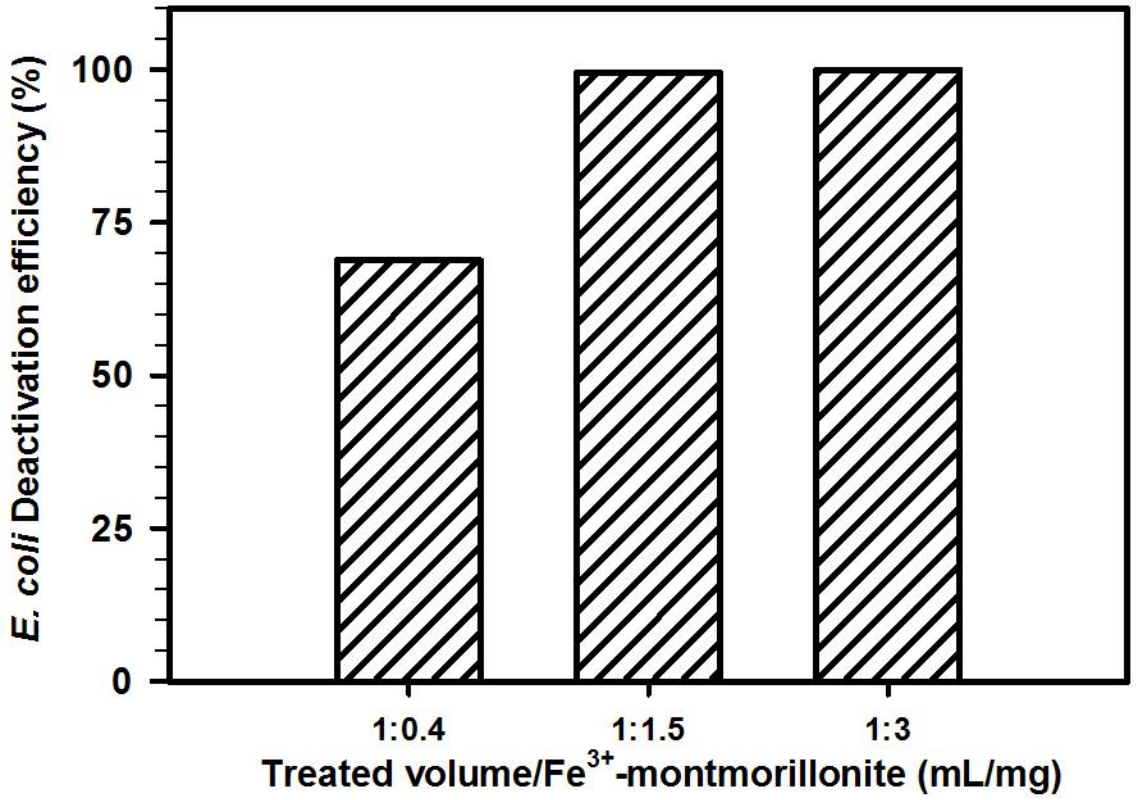

Figure 5.2 Effect of mineral/paper mass ratio on *E. coli* deactivation efficiency of Fe^{3+}-saturated montmorillonite paper. 50 mL *E. coli* suspension inoculated from a secondary wastewater effluent was used for deactivation test. The initial *E. coli* level in influent suspension was $1.18x10^6$ CFU/mL.

5.3.2. *E. coli* Deactivation Mechanisms

5.3.2.1 Scanning Electron Micrograph

Figure 5.3 shows photographs of Na^+-montmorillonite and Fe^{3+}-saturated montmorillonite impregnated paper with low (~25%) and high (~50%) loading. Compared to pure white blank filter paper, Na^+-montmorillonite embedded paper is light gray and Fe^{3+}-saturated montmorillonite has light yellow color. And the color change is more clearly visible deep with increased content of mineral loading (Figure 5.3). It should be noted that higher loading of Fe^{3+}-saturated

montmorillonite embedded paper gets brittle, indicating the incorporation of Fe^{3+}-saturated montmorillonite might have impact on the mechanical property of filter paper.

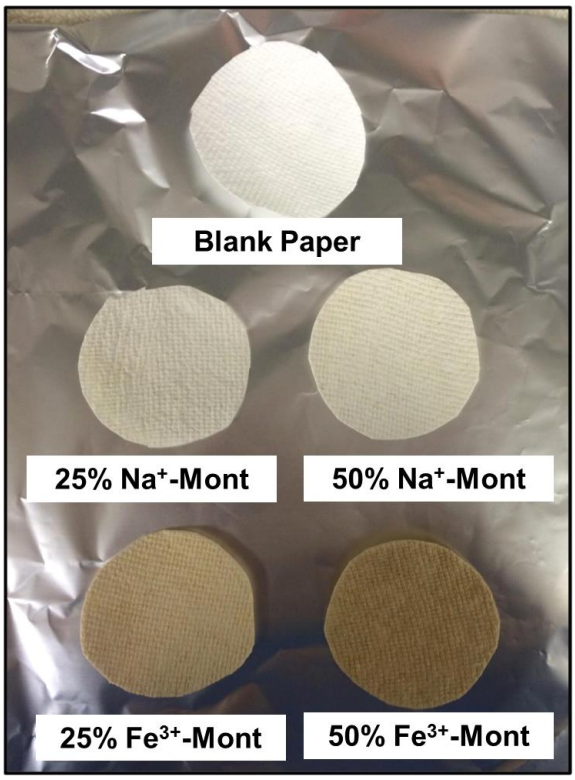

Figure 5.3 Photographs of embedded filter paper loaded with Na^{+}-montmorillonite and Fe^{3+}-saturated montmorillonite with 25% and 50% mineral mass loading amounts. Blank filter paper sheet is also displayed as comparison.

The surface morphology of embedded filter paper microstructure was characterized by SEM. SEM micrographs of filter paper before and after Fe^{3+}-saturated montmorillonite embedment are shown in Figure 5.4. SEM image of blank filter paper shows original long cellulose paper fibers are twisted together into dense network structure with smooth surface (Figure 5.4a). After Fe^{3+}-saturated montmorillonite deposition, small mineral particles were coated over cellulose fiber which made fiber surface became rough (Figure 5.4b). Backscattered electrons detector (BSED) was also applied to scan sample of Fe^{3+}-saturated montmorillonite embedded filter paper. BSE are often used to detect contrast between areas with different chemical

compositions. Under BSED mode, heavy elements (high atomic number) backscatter electrons more strongly than light elements (low atomic number), and thus appear brighter in SEM image. Therefore, the uniform distribution of brighter white areas in Figure 5.4c shows that Fe^{3+}-saturated montmorillonite (higher atomic mass with iron) was well evenly bound to paper fiber surface (darker black areas, lower atomic mass with carbon), confirming successful Fe^{3+}-saturated montmorillonite deposition into paper fiber matrix. The magnified images SEM images also show that the coated Fe^{3+}-saturated montmorillonite particles have irregular shape with approximate size of 2~3 μm in diameter. The strong attachment of Fe^{3+}-saturated montmorillonite to paper structure is very crucial during immobilization process. The major ingredient of softwood pulp cellulose is long chain polymer with hydroxyl groups that could form hydrogen bonds with the surface oxygen atoms of metal oxide nanoparticles.[19] Therefore, Fe^{3+}-saturated montmorillonite with surface oxygen atoms could be also possibly adhered to cellulose molecule without need for any further surface treatment. Similarly, the observed higher roughness of Na^{+}-montmorillonite embedded filter paper indicated the adherence of Na^{+}-montmorillonite particles over fiber surface (Figure 5.4d).

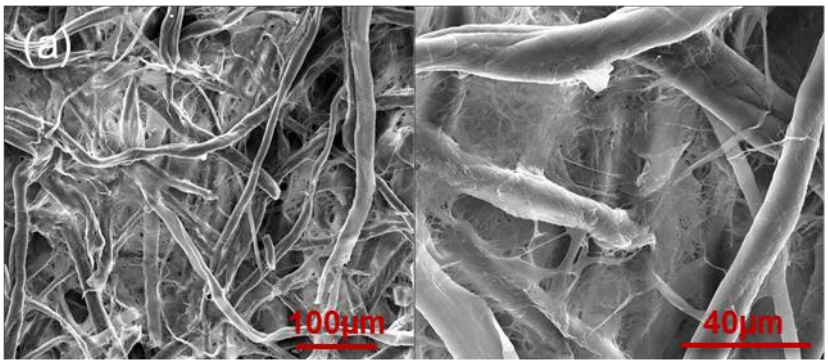

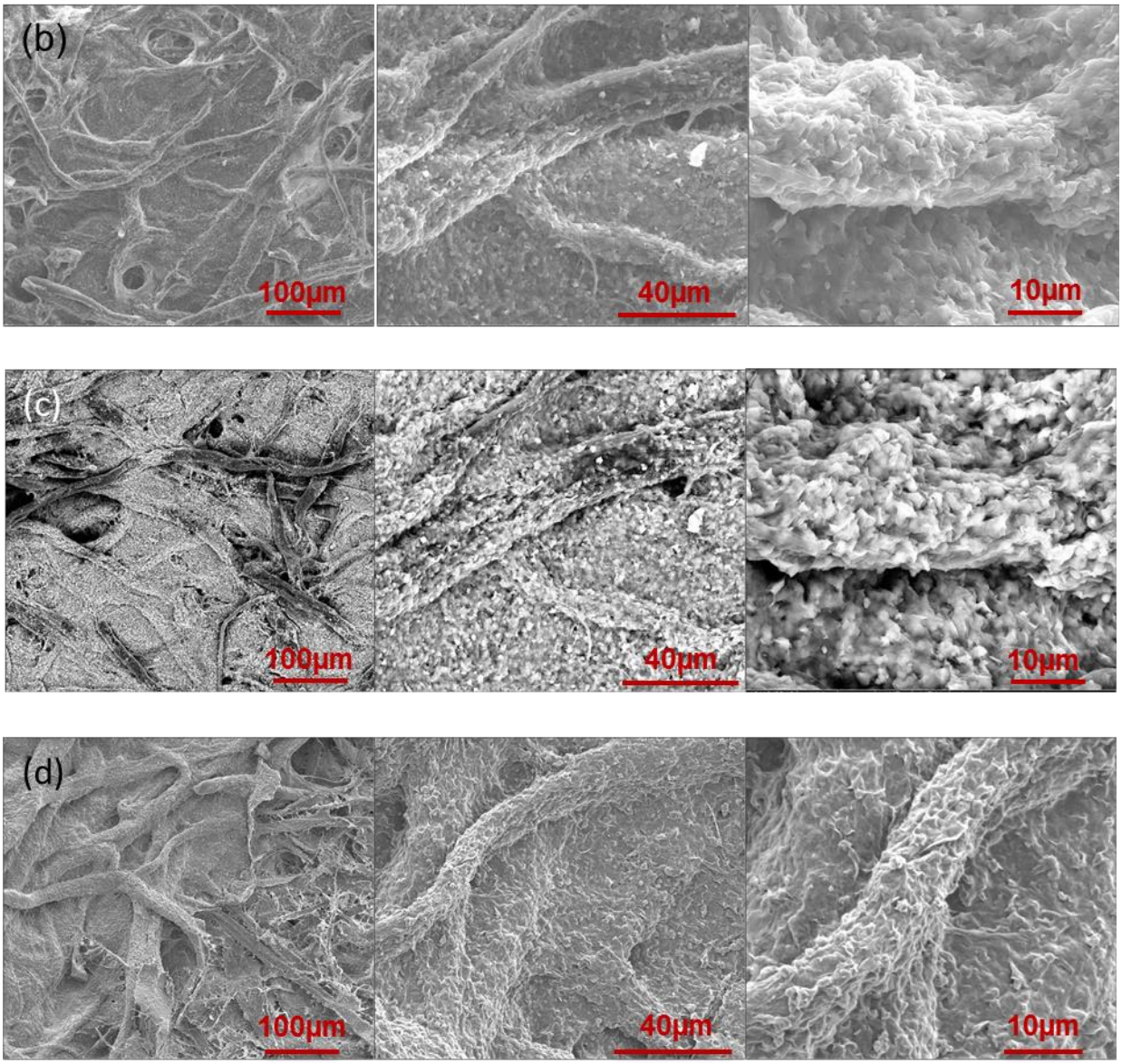

Figure 5.4 Scanning Electron Micrograph showing (a) blank filter paper sheets; (b) Fe^{3+}-saturated montmorillonite paper; (c). Backscattered electrons detector (BSED) mode of Fe^{3+}-saturated montmorillonite paper; (d). Na^{+}-montmorillonite paper.

Fe^{3+}-saturated montmorillonite embedded filter paper sample after passing through *E. coli* saline solution was also analyzed by SEM shown in Figure 5.5. The average pore size of filter paper was estimated over 20 μm, which therefore allow the quick flow filtration of *E. coli* cell (diameter: 1 μm, length: 2 μm). This observation also confirmed that the bacteria deactivation in

filtrate is not due to simple retention by paper. It is mainly due to the exposure to Fe^{3+}-saturated montmorillonite instead. The remaining *E. coli* in filter paper was shown with significant morphological changes as imaged by SEM. Their cell membranes are severely damaged and shown as wrinkled cells. The full in-depth understanding of bactericidal action mode of Fe^{3+}-saturated montmorillonite blended paper sheet is still unclear. Our previous study (Chapter 4) showed direct evidence of bacteria membrane integrity disruption upon Fe^{3+}-saturated montmorillonite exposure) and subsequent loss of viability. In general, important bacteria deactivation mechanisms mainly involve chemical oxidative stress mediated cell injury induced by in situ production of reactive oxygen species[30, 31] and direct physical disruption damage to outer cell membranes with sharpened edges.[32-34] Recent researches have shown that Fe^{3+}-saturated montmorillonite could be reduced by organic phenolic compounds, forming radical cations of aromatic molecules and reduced Fe^{2+} cations.[22, 23, 35, 36] The persistent radical presence in Fe^{3+}-saturated montmorillonite surface has been frequently reported [37-39] and these radicals can damage cell membrane, proteins and DNA, and even result in cell death. Therefore, we hypothesized that the oxidation capacity of Fe^{3+}-saturated montmorillonite might induce oxidative stress on microbial cells, further destroy membrane integrity and contribute to its highly microbial deactivation capacity. However, better sight into the primary deactivation mechanism in this study still merits more investigation.

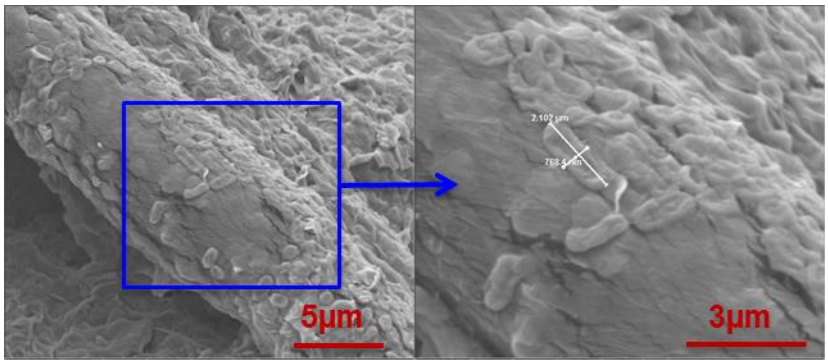

Figure 5.5 Scanning Electron Micrograph showing wrinkled damaged E. coli cell retained in Fe^{3+}-saturated montmorillonite paper.

5.3.2.2 Microbial Cell Impedance Test

The *E. coli* filtrates passing through Na^{+}-montmorillonite or Fe^{3+}-saturated montmorillonite paper were further sampled for dielectrophoresis (DEP) and impedance analysis. The experimental response of the DEP analysis as a function of the applied frequency is shown in Figure 5.6. After passing through Na^{+}-montmorillonite paper, *E. coli* in filtrate (all alive) was observed with DEP trapping of 75%-78% capture efficiency over range of frequencies from 350 kHz to 500 kHz. For untreated *E. coli* sample, DEP trapping efficiency was between 76%-88% over the same applied frequencies range. However, the trapping capacity of *E. coli* (100% deactivated by CFU counting) in filtrate after passing through Fe^{3+}-saturated montmorillonite paper was zero over all applied frequencies, indicating a complete deactivation. Such change in DEP behavior in the tested frequency range indicated that *E. coli* cell membrane structure or the dielectric properties of the cell interior was altered after contacting with Fe^{3+}-saturated montmorillonite paper. DEP and impedance analysis has been reported to selectively detect viable and non-viable *E. coli*.[40] Generally, the live cells were easily trapped in DEP while the dead cells escaped.[41] The trapping ability of live and dead microbial cells by DEP is due to differences in the properties of cell membrane. When the cell dies, the membrane became permeable and its

conductivity can be increased by four orders of magnitude.[42] The conductivity of the cell membrane was the dominant factor determining the dielectrophoretic response of the cells.[42] With such higher conductive cell membrane, dead cells exhibited less negative DEP than live cells at applied field frequencies, which contribute to much lower trapping response compared to live cells.

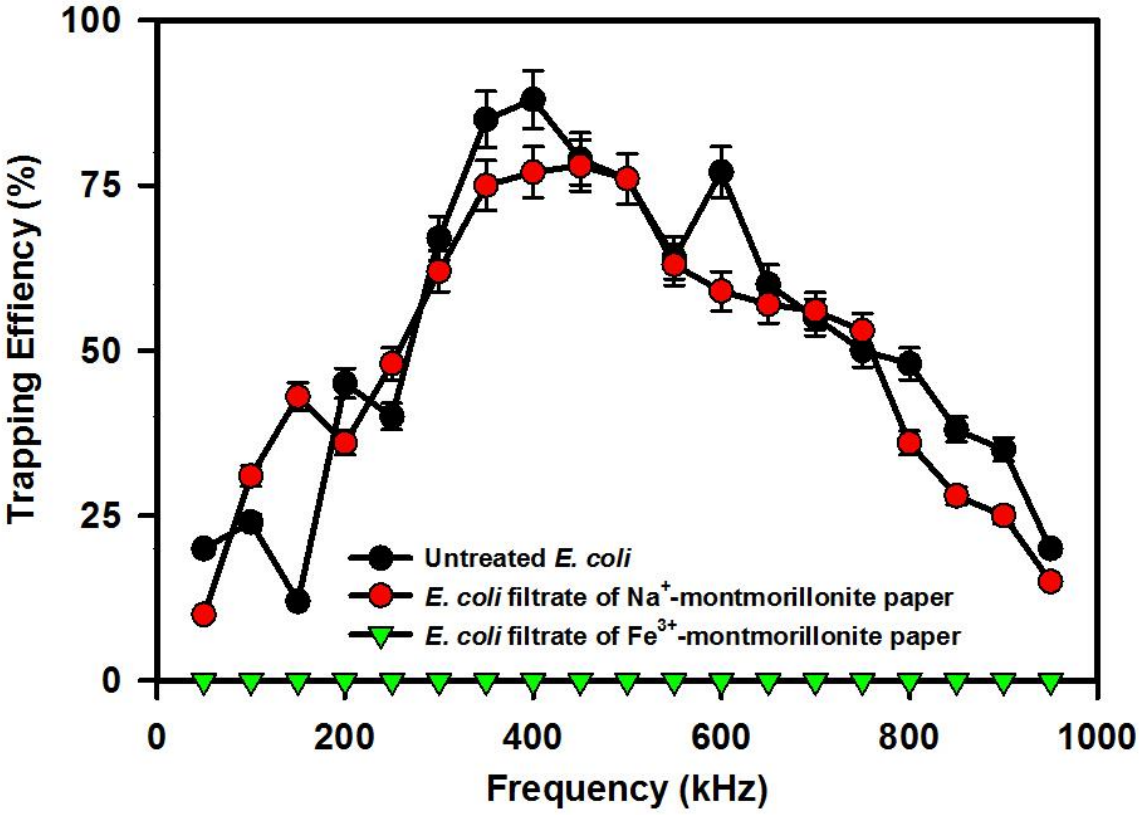

Figure 5.6 Trapping efficiency of different *E. coli* samples passing through microfluidic device in which broad frequency range of 50-950 kHz was applied using a function generator connected to a power amplifier.

5.4 Implication for Practical Applications

In this study, antibacterial filter paper has been successfully prepared by incorporation of Fe^{3+}-saturated montmorillonite into filter paper matrix in environmental friendly manner. It could serve as more affordable and effective alternative to other POU water purification methods. Our

study provided the basis for possible application of using such simple POU water treatment to disinfect microbial pathogens in poor sanitation areas. Paper-based filters are also easy to produce and distribute in rural communities, suggesting great potential of this low cost technology to provide safe drinking water at household level in resource-limiting developing countries. Moreover, the possible iron leaching from Fe^{3+}-saturated montmorillonite impregnated paper (50% mass composite) was determined by UV absorbance at 400 nm. Iron is an essential trace element for human nutrition and currently no guideline value for iron in drinking water is proposed. Estimates of the minimum daily requirement for iron depend on age, sex, physiological status and iron bioavailability and range from about 10 to 50 mg/day.[43] During each use for filtration of 500 mL *E. coli* contaminated water, 0.13 mg Fe^{3+} was released into the filtered water, accounting for 0.3% of the Fe^{3+} initially saturated in the montmorillonite that was impregnated into the filter paper. The Fe^{3+} leached into the water during filtration of the *E coli*-contaminated water could be a potential iron supplement to human nutrition. The health authorities commonly recommend drinking eight 8-ounce glasses per capita per day, which equals about 2 liters. With such water consumption/day, 0.52 mg of iron would be consumed per day. This is a level within the range of the FDA recommended daily intake of iron for an adult.

It should be also noted that small volumes of microbial contaminated water were treated with Fe^{3+}-saturated montmorillonite impregnated filter paper in this study. When this technology is applied in practical point-of-use field application, greater volume (~10 liters) should be tested with extended treatment capacity. Mineral incorporation amount on cellulose fiber surface is also required to be enough to provide adequate exposure to Fe^{3+}-saturated montmorillonite during water percolation through paper. Also, the mechanism of their deactivation against bacteria still merits more investigations in future studies. Moreover, unlike general antibacterial treatment

materials, Fe^{3+}-saturated montmorillonite also provides oxidative removal of phenolic organic compounds, which were widely studied and reported.[22, 23, 36] Therefore, Fe^{3+}-saturated montmorillonite imbedded filter paper also has potential to serve as a novel multifunctional water purifier that could achieve simultaneous and fast removal of bacteria and phenolic pollutants in future applications.

ACKNOWLEDEGEMENTS

We acknowledge the financial support from USDA-NIFA award (No.2013-67019-21355). Funding for this work was provided, in part, by the Virginia Agricultural Experiment Station and the Hatch Program of the National Institute of Food and Agriculture, U.S. Department of Agriculture. We gratefully thank Mr. Stephen McCartney in Virginia Tech Nanoscale Characterization and Fabrication Laboratory for assistance with SEM sample analysis.

5.5 References

1. Unicef, Meeting the MDG drinking water and sanitation target: a mid-term assessment of progress. **2004**.
2. Montgomery, M. A.; Elimelech, M., Water and sanitation in developing countries: including health in the equation. *Environmental Science & Technology* **2007,** *41*, (1), 17-24.
3. Krasner, S. W.; Westerhoff, P.; Chen, B.; Rittmann, B. E.; Amy, G., Occurrence of disinfection byproducts in United States wastewater treatment plant effluents. *Environmental science & technology* **2009,** *43*, (21), 8320-8325.
4. Richardson, S. D.; Plewa, M. J.; Wagner, E. D.; Schoeny, R.; DeMarini, D. M., Occurrence, genotoxicity, and carcinogenicity of regulated and emerging disinfection by-products in drinking water: a review and roadmap for research. *Mutation Research/Reviews in Mutation Research* **2007,** *636*, (1), 178-242.
5. Sobsey, M. D., *Managing water in the home: accelerated health gains from improved water supply*. World Health Organization Geneva: 2002.
6. Sobsey, M. D.; Stauber, C. E.; Casanova, L. M.; Brown, J. M.; Elliott, M. A., Point of use household drinking water filtration: a practical, effective solution for providing sustained access to safe drinking water in the developing world. *Environmental science & technology* **2008,** *42*, (12), 4261-4267.

7. Lin, S.; Huang, R.; Cheng, Y.; Liu, J.; Lau, B. L.; Wiesner, M. R., Silver nanoparticle-alginate composite beads for point-of-use drinking water disinfection. *Water Res.* **2013,** *47*, (12), 3959-3965.
8. Ren, D.; Smith, J. A., Retention and transport of silver nanoparticles in a ceramic porous medium used for point-of-use water treatment. *Environmental science & technology* **2013,** *47*, (8), 3825-3832.
9. Upadhyayula, V. K.; Deng, S.; Mitchell, M. C.; Smith, G. B., Application of carbon nanotube technology for removal of contaminants in drinking water: a review. *Sci. Total Environ.* **2009,** *408*, (1), 1-13.
10. Brame, J.; Fattori, V.; Clarke, R.; Mackeyev, Y.; Wilson, L. J.; Li, Q.; Alvarez, P., Water disinfection using nanotechnology for safer irrigation: A demonstration project in Swaziland. *Environmental Engineer and Scientist: Applied Research and Practice* **2014,** *50*, (2), 40-46.
11. Qu, X.; Brame, J.; Li, Q.; Alvarez, P. J. J., Nanotechnology for a safe and sustainable water supply: enabling integrated water treatment and reuse. *Acc. Chem. Res.* **2012,** *46*, (3), 834-843.
12. Morones, J. R.; Elechiguerra, J. L.; Camacho, A.; Holt, K.; Kouri, J. B.; Ramírez, J. T.; Yacaman, M. J., The bactericidal effect of silver nanoparticles. *Nanotechnology* **2005,** *16*, (10), 2346.
13. Lv, M.; Su, S.; He, Y.; Huang, Q.; Hu, W.; Li, D.; Fan, C.; Lee, S. T., Long-Term Antimicrobial Effect of Silicon Nanowires Decorated with Silver Nanoparticles. *Adv. Mater.* **2010,** *22*, (48), 5463-5467.
14. Dankovich, T. A., Microwave-assisted incorporation of silver nanoparticles in paper for point-of-use water purification. *Environmental Science: Nano* **2014,** *1*, (4), 367-378.
15. Dankovich, T. A.; Gray, D. G., Bactericidal paper impregnated with silver nanoparticles for point-of-use water treatment. *Environmental science & technology* **2011,** *45*, (5), 1992-1998.
16. Dankovich, T. A.; Smith, J. A., Incorporation of copper nanoparticles into paper for point-of-use water purification. *Water Res.* **2014,** *63*, 245-251.
17. Dankovich, T. A.; Levine, J. S.; Potgieter, N.; Dillingham, R.; Smith, J. A., Inactivation of bacteria from contaminated streams in Limpopo, South Africa by silver-or copper-nanoparticle paper filters. *Environmental science: water research & technology* **2016,** *2*, (1), 85-96.
18. Hu, W.; Peng, C.; Luo, W.; Lv, M.; Li, X.; Li, D.; Huang, Q.; Fan, C., Graphene-based antibacterial paper. *Acs Nano* **2010,** *4*, (7), 4317-4323.
19. Jaisai, M.; Baruah, S.; Dutta, J., Paper modified with ZnO nanorods–antimicrobial studies. *Beilstein journal of nanotechnology* **2012,** *3*, (1), 684-691.
20. Ngo, Y. H.; Li, D.; Simon, G. P.; Garnier, G., Paper surfaces functionalized by nanoparticles. *Adv. Colloid Interface Sci.* **2011,** *163*, (1), 23-38.
21. Shen, J.; Song, Z.; Qian, X.; Ni, Y., A review on use of fillers in cellulosic paper for functional applications. *Industrial & Engineering Chemistry Research* **2010,** *50*, (2), 661-666.
22. Liyanapatirana, C.; Gwaltney, S. R.; Xia, K., Transformation of triclosan by Fe (III)-saturated montmorillonite. *Environmental science & technology* **2009,** *44*, (2), 668-674.
23. Qin, C.; Troya, D.; Shang, C.; Hildreth, S.; Helm, R.; Xia, K., Surface catalyzed oxidative oligomerization of 17β-estradiol by Fe3+-saturated montmorillonite. *Environmental science & technology* **2014,** *49*, (2), 956-964.
24. Arroyo, L. J.; Li, H.; Teppen, B. J.; Boyd, S. A., A simple method for partial purification of reference clays. *Clays and Clay Minerals* **2005,** *53*, (5), 511-519.

25. Pepper, I. L.; Gerba, C. P., Chapter 10 - Cultural Methods. In *Environmental Microbiology (Third edition)*, Academic Press: San Diego, 2015; pp 195-212.
26. Özdemir, G.; Limoncu, M. H.; Yapar, S., The antibacterial effect of heavy metal and cetylpridinium-exchanged montmorillonites. *Applied Clay Science* **2010,** *48*, (3), 319-323.
27. Vyhnalkova, R.; Mansur-Azzam, N.; Eisenberg, A.; van de Ven, T. G., Ten million fold reduction of live bacteria by bactericidal filter paper. *Adv. Funct. Mater.* **2012,** *22*, (19), 4096-4100.
28. Mansur-Azzam, N.; Hosseinidoust, Z.; Woo, S. G.; Vyhnalkova, R.; Eisenberg, A.; van de Ven, T. G., Bacteria survival probability in bactericidal filter paper. *Colloids and Surfaces B: Biointerfaces* **2014,** *117*, 383-388.
29. Standard, G., Protocol for Testing Microbiological Water Purifiers. *EPA, Report of Task Force, revised April* **1987**.
30. Krishnamoorthy, K.; Veerapandian, M.; Zhang, L.-H.; Yun, K.; Kim, S. J., Antibacterial efficiency of graphene nanosheets against pathogenic bacteria via lipid peroxidation. *The Journal of Physical Chemistry C* **2012,** *116*, (32), 17280-17287.
31. Su, H.-L.; Chou, C.-C.; Hung, D.-J.; Lin, S.-H.; Pao, I.-C.; Lin, J.-H.; Huang, F.-L.; Dong, R.-X.; Lin, J.-J., The disruption of bacterial membrane integrity through ROS generation induced by nanohybrids of silver and clay. *Biomaterials* **2009,** *30*, (30), 5979-5987.
32. Situ, S. F.; Samia, A. C. S., Highly efficient antibacterial iron oxide@ carbon nanochains from wustite precursor nanoparticles. *ACS applied materials & interfaces* **2014,** *6*, (22), 20154-20163.
33. Liu, S.; Wei, L.; Hao, L.; Fang, N.; Chang, M. W.; Xu, R.; Yang, Y.; Chen, Y., Sharper and faster "nano darts" kill more bacteria: a study of antibacterial activity of individually dispersed pristine single-walled carbon nanotube. *Acs Nano* **2009,** *3*, (12), 3891-3902.
34. Akhavan, O.; Ghaderi, E., Toxicity of graphene and graphene oxide nanowalls against bacteria. *ACS nano* **2010,** *4*, (10), 5731-5736.
35. Polubesova, T.; Eldad, S.; Chefetz, B., Adsorption and oxidative transformation of phenolic acids by Fe (III)-montmorillonite. *Environmental science & technology* **2010,** *44*, (11), 4203-4209.
36. Gu, C.; Li, H.; Teppen, B. J.; Boyd, S. A., Octachlorodibenzodioxin formation on Fe (III)-montmorillonite clay. *Environmental science & technology* **2008,** *42*, (13), 4758-4763.
37. dela Cruz, A. L. N.; Gehling, W.; Lomnicki, S.; Cook, R.; Dellinger, B., Detection of environmentally persistent free radicals at a superfund wood treating site. *Environmental science & technology* **2011,** *45*, (15), 6356-6365.
38. Cruz, A. L. N. d.; Cook, R. L.; Lomnicki, S. M.; Dellinger, B., Effect of low temperature thermal treatment on soils contaminated with pentachlorophenol and environmentally persistent free radicals. *Environmental science & technology* **2012,** *46*, (11), 5971-5978.
39. Nwosu, U. G.; Roy, A.; dela Cruz, A. L. N.; Dellinger, B.; Cook, R., Formation of environmentally persistent free radical (EPFR) in iron (iii) cation-exchanged smectite clay. *Environmental Science: Processes & Impacts* **2016,** *18*, (1), 42-50.
40. Suehiro, J.; Hamada, R.; Noutomi, D.; Shutou, M.; Hara, M., Selective detection of viable bacteria using dielectrophoretic impedance measurement method. *Journal of Electrostatics* **2003,** *57*, (2), 157-168.
41. Nakidde, D.; Zellner, P.; Alemi, M. M.; Shake, T.; Hosseini, Y.; Riquelme, M. V.; Pruden, A.; Agah, M., Three dimensional passivated-electrode insulator-based dielectrophoresis. *Biomicrofluidics* **2015,** *9*, (1), 014125.

42. Lapizco-Encinas, B. H.; Simmons, B. A.; Cummings, E. B.; Fintschenko, Y., Dielectrophoretic concentration and separation of live and dead bacteria in an array of insulators. *Analytical chemistry* **2004,** *76*, (6), 1571-1579.
43. Organization, W. H., *Guidelines for drinking-water quality*. Geneva: world health organization: 2011.

Chapter 6. Conclusion

The removal and its mechanisms of estrogens and microorganisms from contaminanted water by using Fe^{3+}-saturated montmorillonite were systematically studied. Rapid βE2 transformation in the presence of Fe^{3+}-saturated montmorillonite in aqueous system was detected. The disappearance of βE2 follows first-order kinetics while the overall catalytic reaction follows the second order kinetics with an estimated reaction rate constant of 200 ± 24 (mmol βE2/g mineral)$^{-1}h^{-1}$. The halflife of βE2 in this system was estimated to be 0.50±0.06 h. βE2 oligomers were found to be the major products of βE2 transformation when exposed to Fe^{3+}-saturated montmorillonite. The βE2 oligomers, which are $>10^7$ times less water-soluble than βE2, can be settled out of the aqueous phase during wastewater treatment processes and become much less bioavailable and mobile than the parent compound. The βE2 removal efficiency remained at >84%, even after five consecutive 5-day reaction cycles using the same batch of Fe^{3+}-saturated montmorillonite and the same initial level of βE2 at each cycle. The results clearly demonstrated that Fe^{3+}-saturated montmorillonite has a great potential to be used as a cost-effective material for effective removal of phenolic organic compounds from wastewater.

Fe^{3+}-saturated montmorillonite catalysis achieved highest βE2 removal efficiency at neutral solution pH and higher temperature. Common cations did not have impact on the reaction efficiency. The presence of dissolved organic matter in model water system slightly reduced βE2 removal efficiency. Although the βE2 removal efficiencies were significantly lower when wastewater secondary effluents were treated with the same dosage of Fe^{3+}-saturated montmorillonite, the results from this investigation suggested that increasing dosage of Fe^{3+}-saturated montmorillonite for more available reaction sites for βE2 would further increase the

removal efficiency. The laboratory batch experimental results in this study provide the evidence that Fe^{3+}-saturated montmorillonite can be utilized with high stability in practical applications for elimination of estrogen and other phenolic pollutants in wastewater.

This thesis also demonstrated, for the first time, the effectiveness of Fe^{3+}-saturated montmorillonite for microbial deactivation in wastewater. Microbial cultural results coupled with the live/dead fluorescent staining assay observation strongly points to the conclusion that Fe^{3+}-saturated montmorillonite deactivated microorganisms in wastewater through the following two steps: electrostatic sorption of negatively charged microbial cells to the surfaces of Fe^{3+}-saturated montmorillonite, followed by microbial deactivation due to surface-catalyzed microbial cell membrane disruption by the surface saturated Fe^{3+}. Microbial deactivation efficiency was 92±0.64% when a secondary wastewater effluent was mixed with Fe^{3+}-saturated montmorillonite at 35 mg/mL for 30 min, and further reached to 97±0.61% after 4-h exposure. This deactivation efficiency was similar to that obtained when the same water was subjected to UV-disinfection. It was estimated that the ratio between wastewater microbial population and Fe^{3+}-saturated montmorillonite at less than 2×10^3 CFU/mg would achieve >90% microbial deactivation efficiency. The overall results suggest that Fe^{3+}-saturated montmorillonite could be used as a low cost, environmental friendly, and effective antimicrobial material for water disinfection in applications from small scale point-of-use drinking water treatment devices to large scale drinking and wastewater treatment facilities.

Antibacterial filter paper has been successfully prepared by incorporating Fe^{3+}-saturated montmorillonite into filter paper matrix in environmental friendly manner. It could serve as more affordable and effective alternative to other point-of-use water purification methods. Paper-based filters are also easy to produce and distribute in rural communities, carrying a great potential of

this low cost technology to provide safe drinking water at household level in resource-limiting developing countries. During each use for treating 500 mL *Escherichia coli* contaminated water, 0.13 mg Fe^{3+} was released into the treated water, accounting for 0.3% of the Fe^{3+} initially saturated in the montmorillonite that was impregnated into the filter paper. This leached Fe^{3+} during filtration of the *E coli*-contaminated water could be a potential iron supplement to the person consuming the water. When it was used to treat 50 mL and 200 mL water spiked with live *E. coli* cells at 3.67×10^8 CFU/mL, the Fe^{3+}-saturated montmorillonite impregnated filter paper with 50% of mineral/paper weight percent loading deactivated 99% and 77% of spiked *E. coli* living cells, respectively. When the ratio of treated volume/Fe^{3+}-saturated montmorillonite (mL/mL) decreased from 1:0.4 to 1:1.5, *E. coli* deactivation efficiency increased from 69% to 99.5% and maintained 100% at ratio of 1:3 when treating 50 mL water spiked with *E. coli* at 1.18×10^6 CFU/mL was passed through. Dielectrophoresis (DEP) and impedance analysis of *E. coli* filtrate also confirmed that the deactivated *E. coli* passing through Fe^{3+}-saturated montmorillonite filter paper did not have trapping response (mainly dead) to DEP due to higher membrane permeability and conductivity. Overall, Fe^{3+}-saturated montmorillonite embedded filter paper also has potential to serve as a novel multifunctional water purifier that could achieve simultaneous and fast removal of bacteria and phenolic pollutants in future applications.

Appendix

Appendix Table S1. Coordinates of βE2, eight dimer isomers, and five trimer isomers

βE2

C	4.65714	-0.27300	0.16019
C	4.04124	-1.48961	-0.14263
C	2.66830	-1.52026	-0.35786
C	1.86433	-0.37034	-0.27802
C	2.49972	0.85132	0.02060
C	3.88383	0.88383	0.23602
H	4.64400	-2.39005	-0.20720
H	2.21400	-2.47606	-0.59840
C	0.36130	-0.43221	-0.56780
C	1.72472	2.15263	0.14339
H	4.36233	1.83634	0.46625
C	0.31414	2.07922	-0.44781
C	-0.38659	0.79693	0.01534
C	-0.31049	-1.76079	-0.14497
C	-1.86099	0.71057	-0.38446
C	-1.82445	-1.79401	-0.44593
C	-2.55378	-0.57455	0.14020
C	-3.98016	-0.33133	-0.39646
C	-2.83851	1.84668	-0.01459
C	-4.24278	1.17820	-0.12097
H	-3.96655	-0.50554	-1.48552
O	-4.92030	-1.21163	0.20983
C	-2.59808	-0.66743	1.68152
H	-3.05161	0.21695	2.14004
H	-3.20120	-1.53067	1.97679
H	-1.60141	-0.78610	2.11552
H	-4.80449	1.27151	0.81467
H	-4.85513	1.62893	-0.91048
H	-2.65472	2.20852	1.00416
H	-2.73759	2.71073	-0.67914
H	-1.87889	0.63419	-1.48585
H	-0.31416	0.76006	1.11339
H	-2.25845	-2.72720	-0.06519
H	-1.96956	-1.80368	-1.53664
H	0.15766	-2.60091	-0.66993

H	-0.12848	-1.93373	0.92353
H	0.23937	-0.36046	-1.66363
H	0.36268	2.09064	-1.54654
H	-0.25567	2.96709	-0.14798
H	1.64861	2.41792	1.20918
H	2.29482	2.96557	-0.32502
O	6.01164	-0.27634	0.36541
H	6.29799	0.62817	0.56627
H	-5.78759	-1.03345	-0.18457

Dimer 7-3'

C	4.65714	-0.27300	0.16019
C	4.04124	-1.48961	-0.14263
C	2.66830	-1.52026	-0.35786
C	1.86433	-0.37034	-0.27802
C	2.49972	0.85132	0.02060
C	3.88383	0.88383	0.23602
H	4.64400	-2.39005	-0.20720
H	2.21400	-2.47606	-0.59840
C	0.36130	-0.43221	-0.56780
C	1.72472	2.15263	0.14339
H	4.36233	1.83634	0.46625
C	0.31414	2.07922	-0.44781
C	-0.38659	0.79693	0.01534
C	-0.31049	-1.76079	-0.14497
C	-1.86099	0.71057	-0.38446
C	-1.82445	-1.79401	-0.44593
C	-2.55378	-0.57455	0.14020
C	-3.98016	-0.33133	-0.39646
C	-2.83851	1.84668	-0.01459
C	-4.24278	1.17820	-0.12097
H	-3.96655	-0.50554	-1.48552
O	-4.92030	-1.21163	0.20983
C	-2.59808	-0.66743	1.68152
H	-3.05161	0.21695	2.14004
H	-3.20120	-1.53067	1.97679
H	-1.60141	-0.78610	2.11552
H	-4.80449	1.27151	0.81467
H	-4.85513	1.62893	-0.91048
H	-2.65472	2.20852	1.00416
H	-2.73759	2.71073	-0.67914
H	-1.87889	0.63419	-1.48585
H	-0.31416	0.76006	1.11339
H	-2.25845	-2.72720	-0.06519
H	-1.96956	-1.80368	-1.53664
H	0.15766	-2.60091	-0.66993

H	-0.12848	-1.93373	0.92353
H	0.23937	-0.36046	-1.66363
H	0.36268	2.09064	-1.54654
H	-0.25567	2.96709	-0.14798
H	1.64861	2.41792	1.20918
H	2.29482	2.96557	-0.32502
O	6.01164	-0.27634	0.36541
H	6.29799	0.62817	0.56627
H	-5.78759	-1.03345	-0.18457

Dimer 3-7'

C	7.24948	-2.43861	-1.91044
C	7.80535	-1.83593	-0.58759
C	6.54536	-1.42282	0.20153
C	5.71700	-0.79639	-0.94972
C	5.83250	-1.81741	-2.10226
C	6.76356	-0.34915	1.27824
C	5.43067	0.25743	1.76644
C	4.53386	0.76933	0.61319
C	4.34280	-0.30050	-0.49411
C	3.49760	0.30753	-1.61628
C	2.08656	0.64108	-1.12152
C	2.04351	1.29626	0.25180
C	3.18852	1.33817	1.07975
C	0.80964	1.82553	0.70057
C	0.73592	2.41893	1.97417
C	1.86727	2.47901	2.78777
C	3.06810	1.94234	2.33799
O	-0.47010	2.92841	2.37083
C	5.89485	-2.68017	0.81924
O	8.62191	-2.72461	0.16721
H	1.80822	2.94092	3.77207
H	3.92885	2.00101	2.99536
C	-0.43129	1.75760	-0.13653
H	8.37639	-0.92034	-0.81656
H	5.66651	-3.44305	0.06827
H	6.58457	-3.13056	1.53870
H	4.96271	-2.44789	1.34162
H	7.19962	-3.52778	-1.80556
H	7.91177	-2.22648	-2.75762
H	5.05455	-2.58609	-2.02575
H	5.71475	-1.34629	-3.08319
H	6.27765	0.09896	-1.27075
H	3.77878	-1.14626	-0.07115
H	7.31839	-0.75898	2.13159
H	7.38675	0.45372	0.85649

H	5.66759	1.08045	2.45025
H	4.87266	-0.47788	2.36007
H	5.09006	1.59418	0.13291
H	3.99342	1.21724	-1.98638
H	3.42536	-0.37726	-2.46981
H	1.48782	-0.28047	-1.08063
H	1.58117	1.28153	-1.85188
H	-0.36759	3.30630	3.25828
H	9.40633	-2.92829	-0.36454
C	-1.42838	0.80941	0.10870
C	-2.61051	0.73025	-0.64016
C	-2.78528	1.65564	-1.69071
C	-1.79729	2.61053	-1.94684
C	-0.63558	2.67266	-1.18241
H	-1.25950	0.11337	0.92370
C	-3.65347	-0.35671	-0.36157
C	-4.04257	1.67849	-2.54268
H	-1.92559	3.33112	-2.75071
O	0.29046	3.63062	-1.49906
H	0.99778	3.58611	-0.83191
C	-4.90230	0.41826	-2.40235
C	-5.04753	0.03426	-0.92506
C	-3.73356	-0.79039	1.12197
C	-6.02067	-1.12067	-0.67524
C	-4.80329	-1.87263	1.37983
C	-6.17832	-1.46363	0.82888
C	-7.21330	-2.60301	0.72370
C	-7.47041	-1.04848	-1.20161
C	-8.23182	-2.10289	-0.34216
C	-6.77054	-0.31048	1.66864
H	-7.72225	0.05294	1.26796
H	-6.96149	-0.66269	2.68637
H	-6.09244	0.54508	1.72799
O	-7.78821	-2.90189	1.99156
H	-6.69422	-3.49706	0.33876
H	-8.40487	-3.63950	1.86849
H	-8.61516	-2.93091	-0.94964
H	-9.08988	-1.65809	0.17339
H	-5.56648	-2.01276	-1.14129
H	-5.40478	0.92478	-0.38502
H	-3.34920	-1.25487	-0.92881
H	-7.89230	-0.04706	-1.05510
H	-7.53196	-1.26279	-2.27338
H	-4.44304	-0.41798	-2.95009
H	-5.88444	0.59157	-2.85878
H	-3.77177	1.84336	-3.59357

H	-4.64536	2.55232	-2.25137
H	-4.86313	-2.08861	2.45406
H	-4.48993	-2.80672	0.88977
H	-3.92211	0.09171	1.74704
H	-2.76523	-1.18719	1.44696

Dimer 3-3’

C	7.24948	-2.43861	-1.91044
C	7.80535	-1.83593	-0.58759
C	6.54536	-1.42282	0.20153
C	5.71700	-0.79639	-0.94972
C	5.83250	-1.81741	-2.10226
C	6.76356	-0.34915	1.27824
C	5.43067	0.25743	1.76644
C	4.53386	0.76933	0.61319
C	4.34280	-0.30050	-0.49411
C	3.49760	0.30753	-1.61628
C	2.08656	0.64108	-1.12152
C	2.04351	1.29626	0.25180
C	3.18852	1.33817	1.07975
C	0.80964	1.82553	0.70057
C	0.73592	2.41893	1.97417
C	1.86727	2.47901	2.78777
C	3.06810	1.94234	2.33799
O	-0.47010	2.92841	2.37083
C	5.89485	-2.68017	0.81924
O	8.62191	-2.72461	0.16721
H	1.80822	2.94092	3.77207
H	3.92885	2.00101	2.99536
C	-0.43129	1.75760	-0.13653
H	8.37639	-0.92034	-0.81656
H	5.66651	-3.44305	0.06827
H	6.58457	-3.13056	1.53870
H	4.96271	-2.44789	1.34162
H	7.19962	-3.52778	-1.80556
H	7.91177	-2.22648	-2.75762
H	5.05455	-2.58609	-2.02575
H	5.71475	-1.34629	-3.08319
H	6.27765	0.09896	-1.27075
H	3.77878	-1.14626	-0.07115
H	7.31839	-0.75898	2.13159
H	7.38675	0.45372	0.85649
H	5.66759	1.08045	2.45025
H	4.87266	-0.47788	2.36007
H	5.09006	1.59418	0.13291
H	3.99342	1.21724	-1.98638

H	3.42536	-0.37726	-2.46981
H	1.48782	-0.28047	-1.08063
H	1.58117	1.28153	-1.85188
H	-0.36759	3.30630	3.25828
H	9.40633	-2.92829	-0.36454
C	-1.42838	0.80941	0.10870
C	-2.61051	0.73025	-0.64016
C	-2.78528	1.65564	-1.69071
C	-1.79729	2.61053	-1.94684
C	-0.63558	2.67266	-1.18241
H	-1.25950	0.11337	0.92370
C	-3.65347	-0.35671	-0.36157
C	-4.04257	1.67849	-2.54268
H	-1.92559	3.33112	-2.75071
O	0.29046	3.63062	-1.49906
H	0.99778	3.58611	-0.83191
C	-4.90230	0.41826	-2.40235
C	-5.04753	0.03426	-0.92506
C	-3.73356	-0.79039	1.12197
C	-6.02067	-1.12067	-0.67524
C	-4.80329	-1.87263	1.37983
C	-6.17832	-1.46363	0.82888
C	-7.21330	-2.60301	0.72370
C	-7.47041	-1.04848	-1.20161
C	-8.23182	-2.10289	-0.34216
C	-6.77054	-0.31048	1.66864
H	-7.72225	0.05294	1.26796
H	-6.96149	-0.66269	2.68637
H	-6.09244	0.54508	1.72799
O	-7.78821	-2.90189	1.99156
H	-6.69422	-3.49706	0.33876
H	-8.40487	-3.63950	1.86849
H	-8.61516	-2.93091	-0.94964
H	-9.08988	-1.65809	0.17339
H	-5.56648	-2.01276	-1.14129
H	-5.40478	0.92478	-0.38502
H	-3.34920	-1.25487	-0.92881
H	-7.89230	-0.04706	-1.05510
H	-7.53196	-1.26279	-2.27338
H	-4.44304	-0.41798	-2.95009
H	-5.88444	0.59157	-2.85878
H	-3.77177	1.84336	-3.59357
H	-4.64536	2.55232	-2.25137
H	-4.86313	-2.08861	2.45406
H	-4.48993	-2.80672	0.88977
H	-3.92211	0.09171	1.74704

H	-2.76523	-1.18719	1.44696

Dimer 1-3’

C	7.24948	-2.43861	-1.91044
C	7.80535	-1.83593	-0.58759
C	6.54536	-1.42282	0.20153
C	5.71700	-0.79639	-0.94972
C	5.83250	-1.81741	-2.10226
C	6.76356	-0.34915	1.27824
C	5.43067	0.25743	1.76644
C	4.53386	0.76933	0.61319
C	4.34280	-0.30050	-0.49411
C	3.49760	0.30753	-1.61628
C	2.08656	0.64108	-1.12152
C	2.04351	1.29626	0.25180
C	3.18852	1.33817	1.07975
C	0.80964	1.82553	0.70057
C	0.73592	2.41893	1.97417
C	1.86727	2.47901	2.78777
C	3.06810	1.94234	2.33799
O	-0.47010	2.92841	2.37083
C	5.89485	-2.68017	0.81924
O	8.62191	-2.72461	0.16721
H	1.80822	2.94092	3.77207
H	3.92885	2.00101	2.99536
C	-0.43129	1.75760	-0.13653
H	8.37639	-0.92034	-0.81656
H	5.66651	-3.44305	0.06827
H	6.58457	-3.13056	1.53870
H	4.96271	-2.44789	1.34162
H	7.19962	-3.52778	-1.80556
H	7.91177	-2.22648	-2.75762
H	5.05455	-2.58609	-2.02575
H	5.71475	-1.34629	-3.08319
H	6.27765	0.09896	-1.27075
H	3.77878	-1.14626	-0.07115
H	7.31839	-0.75898	2.13159
H	7.38675	0.45372	0.85649
H	5.66759	1.08045	2.45025
H	4.87266	-0.47788	2.36007
H	5.09006	1.59418	0.13291
H	3.99342	1.21724	-1.98638
H	3.42536	-0.37726	-2.46981
H	1.48782	-0.28047	-1.08063
H	1.58117	1.28153	-1.85188
H	-0.36759	3.30630	3.25828

H	9.40633	-2.92829	-0.36454
C	-1.42838	0.80941	0.10870
C	-2.61051	0.73025	-0.64016
C	-2.78528	1.65564	-1.69071
C	-1.79729	2.61053	-1.94684
C	-0.63558	2.67266	-1.18241
H	-1.25950	0.11337	0.92370
C	-3.65347	-0.35671	-0.36157
C	-4.04257	1.67849	-2.54268
H	-1.92559	3.33112	-2.75071
O	0.29046	3.63062	-1.49906
H	0.99778	3.58611	-0.83191
C	-4.90230	0.41826	-2.40235
C	-5.04753	0.03426	-0.92506
C	-3.73356	-0.79039	1.12197
C	-6.02067	-1.12067	-0.67524
C	-4.80329	-1.87263	1.37983
C	-6.17832	-1.46363	0.82888
C	-7.21330	-2.60301	0.72370
C	-7.47041	-1.04848	-1.20161
C	-8.23182	-2.10289	-0.34216
C	-6.77054	-0.31048	1.66864
H	-7.72225	0.05294	1.26796
H	-6.96149	-0.66269	2.68637
H	-6.09244	0.54508	1.72799
O	-7.78821	-2.90189	1.99156
H	-6.69422	-3.49706	0.33876
H	-8.40487	-3.63950	1.86849
H	-8.61516	-2.93091	-0.94964
H	-9.08988	-1.65809	0.17339
H	-5.56648	-2.01276	-1.14129
H	-5.40478	0.92478	-0.38502
H	-3.34920	-1.25487	-0.92881
H	-7.89230	-0.04706	-1.05510
H	-7.53196	-1.26279	-2.27338
H	-4.44304	-0.41798	-2.95009
H	-5.88444	0.59157	-2.85878
H	-3.77177	1.84336	-3.59357
H	-4.64536	2.55232	-2.25137
H	-4.86313	-2.08861	2.45406
H	-4.48993	-2.80672	0.88977
H	-3.92211	0.09171	1.74704
H	-2.76523	-1.18719	1.44696

Dimer 7-7’

C	7.24948	-2.43861	-1.91044

C	7.80535	-1.83593	-0.58759
C	6.54536	-1.42282	0.20153
C	5.71700	-0.79639	-0.94972
C	5.83250	-1.81741	-2.10226
C	6.76356	-0.34915	1.27824
C	5.43067	0.25743	1.76644
C	4.53386	0.76933	0.61319
C	4.34280	-0.30050	-0.49411
C	3.49760	0.30753	-1.61628
C	2.08656	0.64108	-1.12152
C	2.04351	1.29626	0.25180
C	3.18852	1.33817	1.07975
C	0.80964	1.82553	0.70057
C	0.73592	2.41893	1.97417
C	1.86727	2.47901	2.78777
C	3.06810	1.94234	2.33799
O	-0.47010	2.92841	2.37083
C	5.89485	-2.68017	0.81924
O	8.62191	-2.72461	0.16721
H	1.80822	2.94092	3.77207
H	3.92885	2.00101	2.99536
C	-0.43129	1.75760	-0.13653
H	8.37639	-0.92034	-0.81656
H	5.66651	-3.44305	0.06827
H	6.58457	-3.13056	1.53870
H	4.96271	-2.44789	1.34162
H	7.19962	-3.52778	-1.80556
H	7.91177	-2.22648	-2.75762
H	5.05455	-2.58609	-2.02575
H	5.71475	-1.34629	-3.08319
H	6.27765	0.09896	-1.27075
H	3.77878	-1.14626	-0.07115
H	7.31839	-0.75898	2.13159
H	7.38675	0.45372	0.85649
H	5.66759	1.08045	2.45025
H	4.87266	-0.47788	2.36007
H	5.09006	1.59418	0.13291
H	3.99342	1.21724	-1.98638
H	3.42536	-0.37726	-2.46981
H	1.48782	-0.28047	-1.08063
H	1.58117	1.28153	-1.85188
H	-0.36759	3.30630	3.25828
H	9.40633	-2.92829	-0.36454
C	-1.42838	0.80941	0.10870
C	-2.61051	0.73025	-0.64016
C	-2.78528	1.65564	-1.69071

C	-1.79729	2.61053	-1.94684
C	-0.63558	2.67266	-1.18241
H	-1.25950	0.11337	0.92370
C	-3.65347	-0.35671	-0.36157
C	-4.04257	1.67849	-2.54268
H	-1.92559	3.33112	-2.75071
O	0.29046	3.63062	-1.49906
H	0.99778	3.58611	-0.83191
C	-4.90230	0.41826	-2.40235
C	-5.04753	0.03426	-0.92506
C	-3.73356	-0.79039	1.12197
C	-6.02067	-1.12067	-0.67524
C	-4.80329	-1.87263	1.37983
C	-6.17832	-1.46363	0.82888
C	-7.21330	-2.60301	0.72370
C	-7.47041	-1.04848	-1.20161
C	-8.23182	-2.10289	-0.34216
C	-6.77054	-0.31048	1.66864
H	-7.72225	0.05294	1.26796
H	-6.96149	-0.66269	2.68637
H	-6.09244	0.54508	1.72799
O	-7.78821	-2.90189	1.99156
H	-6.69422	-3.49706	0.33876
H	-8.40487	-3.63950	1.86849
H	-8.61516	-2.93091	-0.94964
H	-9.08988	-1.65809	0.17339
H	-5.56648	-2.01276	-1.14129
H	-5.40478	0.92478	-0.38502
H	-3.34920	-1.25487	-0.92881
H	-7.89230	-0.04706	-1.05510
H	-7.53196	-1.26279	-2.27338
H	-4.44304	-0.41798	-2.95009
H	-5.88444	0.59157	-2.85878
H	-3.77177	1.84336	-3.59357
H	-4.64536	2.55232	-2.25137
H	-4.86313	-2.08861	2.45406
H	-4.48993	-2.80672	0.88977
H	-3.92211	0.09171	1.74704
H	-2.76523	-1.18719	1.44696

Dimer 1-7’

C	7.24948	-2.43861	-1.91044
C	7.80535	-1.83593	-0.58759
C	6.54536	-1.42282	0.20153
C	5.71700	-0.79639	-0.94972
C	5.83250	-1.81741	-2.10226

C	6.76356	-0.34915	1.27824
C	5.43067	0.25743	1.76644
C	4.53386	0.76933	0.61319
C	4.34280	-0.30050	-0.49411
C	3.49760	0.30753	-1.61628
C	2.08656	0.64108	-1.12152
C	2.04351	1.29626	0.25180
C	3.18852	1.33817	1.07975
C	0.80964	1.82553	0.70057
C	0.73592	2.41893	1.97417
C	1.86727	2.47901	2.78777
C	3.06810	1.94234	2.33799
O	-0.47010	2.92841	2.37083
C	5.89485	-2.68017	0.81924
O	8.62191	-2.72461	0.16721
H	1.80822	2.94092	3.77207
H	3.92885	2.00101	2.99536
C	-0.43129	1.75760	-0.13653
H	8.37639	-0.92034	-0.81656
H	5.66651	-3.44305	0.06827
H	6.58457	-3.13056	1.53870
H	4.96271	-2.44789	1.34162
H	7.19962	-3.52778	-1.80556
H	7.91177	-2.22648	-2.75762
H	5.05455	-2.58609	-2.02575
H	5.71475	-1.34629	-3.08319
H	6.27765	0.09896	-1.27075
H	3.77878	-1.14626	-0.07115
H	7.31839	-0.75898	2.13159
H	7.38675	0.45372	0.85649
H	5.66759	1.08045	2.45025
H	4.87266	-0.47788	2.36007
H	5.09006	1.59418	0.13291
H	3.99342	1.21724	-1.98638
H	3.42536	-0.37726	-2.46981
H	1.48782	-0.28047	-1.08063
H	1.58117	1.28153	-1.85188
H	-0.36759	3.30630	3.25828
H	9.40633	-2.92829	-0.36454
C	-1.42838	0.80941	0.10870
C	-2.61051	0.73025	-0.64016
C	-2.78528	1.65564	-1.69071
C	-1.79729	2.61053	-1.94684
C	-0.63558	2.67266	-1.18241
H	-1.25950	0.11337	0.92370
C	-3.65347	-0.35671	-0.36157

C	-4.04257	1.67849	-2.54268
H	-1.92559	3.33112	-2.75071
O	0.29046	3.63062	-1.49906
H	0.99778	3.58611	-0.83191
C	-4.90230	0.41826	-2.40235
C	-5.04753	0.03426	-0.92506
C	-3.73356	-0.79039	1.12197
C	-6.02067	-1.12067	-0.67524
C	-4.80329	-1.87263	1.37983
C	-6.17832	-1.46363	0.82888
C	-7.21330	-2.60301	0.72370
C	-7.47041	-1.04848	-1.20161
C	-8.23182	-2.10289	-0.34216
C	-6.77054	-0.31048	1.66864
H	-7.72225	0.05294	1.26796
H	-6.96149	-0.66269	2.68637
H	-6.09244	0.54508	1.72799
O	-7.78821	-2.90189	1.99156
H	-6.69422	-3.49706	0.33876
H	-8.40487	-3.63950	1.86849
H	-8.61516	-2.93091	-0.94964
H	-9.08988	-1.65809	0.17339
H	-5.56648	-2.01276	-1.14129
H	-5.40478	0.92478	-0.38502
H	-3.34920	-1.25487	-0.92881
H	-7.89230	-0.04706	-1.05510
H	-7.53196	-1.26279	-2.27338
H	-4.44304	-0.41798	-2.95009
H	-5.88444	0.59157	-2.85878
H	-3.77177	1.84336	-3.59357
H	-4.64536	2.55232	-2.25137
H	-4.86313	-2.08861	2.45406
H	-4.48993	-2.80672	0.88977
H	-3.92211	0.09171	1.74704
H	-2.76523	-1.18719	1.44696

Dimer 3-1’

C	7.24948	-2.43861	-1.91044
C	7.80535	-1.83593	-0.58759
C	6.54536	-1.42282	0.20153
C	5.71700	-0.79639	-0.94972
C	5.83250	-1.81741	-2.10226
C	6.76356	-0.34915	1.27824
C	5.43067	0.25743	1.76644
C	4.53386	0.76933	0.61319
C	4.34280	-0.30050	-0.49411

C	3.49760	0.30753	-1.61628
C	2.08656	0.64108	-1.12152
C	2.04351	1.29626	0.25180
C	3.18852	1.33817	1.07975
C	0.80964	1.82553	0.70057
C	0.73592	2.41893	1.97417
C	1.86727	2.47901	2.78777
C	3.06810	1.94234	2.33799
O	-0.47010	2.92841	2.37083
C	5.89485	-2.68017	0.81924
O	8.62191	-2.72461	0.16721
H	1.80822	2.94092	3.77207
H	3.92885	2.00101	2.99536
C	-0.43129	1.75760	-0.13653
H	8.37639	-0.92034	-0.81656
H	5.66651	-3.44305	0.06827
H	6.58457	-3.13056	1.53870
H	4.96271	-2.44789	1.34162
H	7.19962	-3.52778	-1.80556
H	7.91177	-2.22648	-2.75762
H	5.05455	-2.58609	-2.02575
H	5.71475	-1.34629	-3.08319
H	6.27765	0.09896	-1.27075
H	3.77878	-1.14626	-0.07115
H	7.31839	-0.75898	2.13159
H	7.38675	0.45372	0.85649
H	5.66759	1.08045	2.45025
H	4.87266	-0.47788	2.36007
H	5.09006	1.59418	0.13291
H	3.99342	1.21724	-1.98638
H	3.42536	-0.37726	-2.46981
H	1.48782	-0.28047	-1.08063
H	1.58117	1.28153	-1.85188
H	-0.36759	3.30630	3.25828
H	9.40633	-2.92829	-0.36454
C	-1.42838	0.80941	0.10870
C	-2.61051	0.73025	-0.64016
C	-2.78528	1.65564	-1.69071
C	-1.79729	2.61053	-1.94684
C	-0.63558	2.67266	-1.18241
H	-1.25950	0.11337	0.92370
C	-3.65347	-0.35671	-0.36157
C	-4.04257	1.67849	-2.54268
H	-1.92559	3.33112	-2.75071
O	0.29046	3.63062	-1.49906
H	0.99778	3.58611	-0.83191

C	-4.90230	0.41826	-2.40235
C	-5.04753	0.03426	-0.92506
C	-3.73356	-0.79039	1.12197
C	-6.02067	-1.12067	-0.67524
C	-4.80329	-1.87263	1.37983
C	-6.17832	-1.46363	0.82888
C	-7.21330	-2.60301	0.72370
C	-7.47041	-1.04848	-1.20161
C	-8.23182	-2.10289	-0.34216
C	-6.77054	-0.31048	1.66864
H	-7.72225	0.05294	1.26796
H	-6.96149	-0.66269	2.68637
H	-6.09244	0.54508	1.72799
O	-7.78821	-2.90189	1.99156
H	-6.69422	-3.49706	0.33876
H	-8.40487	-3.63950	1.86849
H	-8.61516	-2.93091	-0.94964
H	-9.08988	-1.65809	0.17339
H	-5.56648	-2.01276	-1.14129
H	-5.40478	0.92478	-0.38502
H	-3.34920	-1.25487	-0.92881
H	-7.89230	-0.04706	-1.05510
H	-7.53196	-1.26279	-2.27338
H	-4.44304	-0.41798	-2.95009
H	-5.88444	0.59157	-2.85878
H	-3.77177	1.84336	-3.59357
H	-4.64536	2.55232	-2.25137
H	-4.86313	-2.08861	2.45406
H	-4.48993	-2.80672	0.88977
H	-3.92211	0.09171	1.74704
H	-2.76523	-1.18719	1.44696

Dimer 7-1’

C	7.24948	-2.43861	-1.91044
C	7.80535	-1.83593	-0.58759
C	6.54536	-1.42282	0.20153
C	5.71700	-0.79639	-0.94972
C	5.83250	-1.81741	-2.10226
C	6.76356	-0.34915	1.27824
C	5.43067	0.25743	1.76644
C	4.53386	0.76933	0.61319
C	4.34280	-0.30050	-0.49411
C	3.49760	0.30753	-1.61628
C	2.08656	0.64108	-1.12152
C	2.04351	1.29626	0.25180
C	3.18852	1.33817	1.07975

C	0.80964	1.82553	0.70057
C	0.73592	2.41893	1.97417
C	1.86727	2.47901	2.78777
C	3.06810	1.94234	2.33799
O	-0.47010	2.92841	2.37083
C	5.89485	-2.68017	0.81924
O	8.62191	-2.72461	0.16721
H	1.80822	2.94092	3.77207
H	3.92885	2.00101	2.99536
C	-0.43129	1.75760	-0.13653
H	8.37639	-0.92034	-0.81656
H	5.66651	-3.44305	0.06827
H	6.58457	-3.13056	1.53870
H	4.96271	-2.44789	1.34162
H	7.19962	-3.52778	-1.80556
H	7.91177	-2.22648	-2.75762
H	5.05455	-2.58609	-2.02575
H	5.71475	-1.34629	-3.08319
H	6.27765	0.09896	-1.27075
H	3.77878	-1.14626	-0.07115
H	7.31839	-0.75898	2.13159
H	7.38675	0.45372	0.85649
H	5.66759	1.08045	2.45025
H	4.87266	-0.47788	2.36007
H	5.09006	1.59418	0.13291
H	3.99342	1.21724	-1.98638
H	3.42536	-0.37726	-2.46981
H	1.48782	-0.28047	-1.08063
H	1.58117	1.28153	-1.85188
H	-0.36759	3.30630	3.25828
H	9.40633	-2.92829	-0.36454
C	-1.42838	0.80941	0.10870
C	-2.61051	0.73025	-0.64016
C	-2.78528	1.65564	-1.69071
C	-1.79729	2.61053	-1.94684
C	-0.63558	2.67266	-1.18241
H	-1.25950	0.11337	0.92370
C	-3.65347	-0.35671	-0.36157
C	-4.04257	1.67849	-2.54268
H	-1.92559	3.33112	-2.75071
O	0.29046	3.63062	-1.49906
H	0.99778	3.58611	-0.83191
C	-4.90230	0.41826	-2.40235
C	-5.04753	0.03426	-0.92506
C	-3.73356	-0.79039	1.12197
C	-6.02067	-1.12067	-0.67524

C	-4.80329	-1.87263	1.37983
C	-6.17832	-1.46363	0.82888
C	-7.21330	-2.60301	0.72370
C	-7.47041	-1.04848	-1.20161
C	-8.23182	-2.10289	-0.34216
C	-6.77054	-0.31048	1.66864
H	-7.72225	0.05294	1.26796
H	-6.96149	-0.66269	2.68637
H	-6.09244	0.54508	1.72799
O	-7.78821	-2.90189	1.99156
H	-6.69422	-3.49706	0.33876
H	-8.40487	-3.63950	1.86849
H	-8.61516	-2.93091	-0.94964
H	-9.08988	-1.65809	0.17339
H	-5.56648	-2.01276	-1.14129
H	-5.40478	0.92478	-0.38502
H	-3.34920	-1.25487	-0.92881
H	-7.89230	-0.04706	-1.05510
H	-7.53196	-1.26279	-2.27338
H	-4.44304	-0.41798	-2.95009
H	-5.88444	0.59157	-2.85878
H	-3.77177	1.84336	-3.59357
H	-4.64536	2.55232	-2.25137
H	-4.86313	-2.08861	2.45406
H	-4.48993	-2.80672	0.88977
H	-3.92211	0.09171	1.74704
H	-2.76523	-1.18719	1.44696

Trimer 7-3', 3-3''

C	7.24948	-2.43861	-1.91044
C	7.80535	-1.83593	-0.58759
C	6.54536	-1.42282	0.20153
C	5.71700	-0.79639	-0.94972
C	5.83250	-1.81741	-2.10226
C	6.76356	-0.34915	1.27824
C	5.43067	0.25743	1.76644
C	4.53386	0.76933	0.61319
C	4.34280	-0.30050	-0.49411
C	3.49760	0.30753	-1.61628
C	2.08656	0.64108	-1.12152
C	2.04351	1.29626	0.25180
C	3.18852	1.33817	1.07975
C	0.80964	1.82553	0.70057
C	0.73592	2.41893	1.97417
C	1.86727	2.47901	2.78777

C	3.06810	1.94234	2.33799
O	-0.47010	2.92841	2.37083
C	5.89485	-2.68017	0.81924
O	8.62191	-2.72461	0.16721
H	1.80822	2.94092	3.77207
H	3.92885	2.00101	2.99536
C	-0.43129	1.75760	-0.13653
H	8.37639	-0.92034	-0.81656
H	5.66651	-3.44305	0.06827
H	6.58457	-3.13056	1.53870
H	4.96271	-2.44789	1.34162
H	7.19962	-3.52778	-1.80556
H	7.91177	-2.22648	-2.75762
H	5.05455	-2.58609	-2.02575
H	5.71475	-1.34629	-3.08319
H	6.27765	0.09896	-1.27075
H	3.77878	-1.14626	-0.07115
H	7.31839	-0.75898	2.13159
H	7.38675	0.45372	0.85649
H	5.66759	1.08045	2.45025
H	4.87266	-0.47788	2.36007
H	5.09006	1.59418	0.13291
H	3.99342	1.21724	-1.98638
H	3.42536	-0.37726	-2.46981
H	1.48782	-0.28047	-1.08063
H	1.58117	1.28153	-1.85188
H	-0.36759	3.30630	3.25828
H	9.40633	-2.92829	-0.36454
C	-1.42838	0.80941	0.10870
C	-2.61051	0.73025	-0.64016
C	-2.78528	1.65564	-1.69071
C	-1.79729	2.61053	-1.94684
C	-0.63558	2.67266	-1.18241
H	-1.25950	0.11337	0.92370
C	-3.65347	-0.35671	-0.36157
C	-4.04257	1.67849	-2.54268
H	-1.92559	3.33112	-2.75071
O	0.29046	3.63062	-1.49906
H	0.99778	3.58611	-0.83191
C	-4.90230	0.41826	-2.40235
C	-5.04753	0.03426	-0.92506
C	-3.73356	-0.79039	1.12197
C	-6.02067	-1.12067	-0.67524
C	-4.80329	-1.87263	1.37983
C	-6.17832	-1.46363	0.82888
C	-7.21330	-2.60301	0.72370

C	-7.47041	-1.04848	-1.20161
C	-8.23182	-2.10289	-0.34216
C	-6.77054	-0.31048	1.66864
H	-7.72225	0.05294	1.26796
H	-6.96149	-0.66269	2.68637
H	-6.09244	0.54508	1.72799
O	-7.78821	-2.90189	1.99156
H	-6.69422	-3.49706	0.33876
H	-8.40487	-3.63950	1.86849
H	-8.61516	-2.93091	-0.94964
H	-9.08988	-1.65809	0.17339
H	-5.56648	-2.01276	-1.14129
H	-5.40478	0.92478	-0.38502
H	-3.34920	-1.25487	-0.92881
H	-7.89230	-0.04706	-1.05510
H	-7.53196	-1.26279	-2.27338
H	-4.44304	-0.41798	-2.95009
H	-5.88444	0.59157	-2.85878
H	-3.77177	1.84336	-3.59357
H	-4.64536	2.55232	-2.25137
H	-4.86313	-2.08861	2.45406
H	-4.48993	-2.80672	0.88977
H	-3.92211	0.09171	1.74704
H	-2.76523	-1.18719	1.44696

Trimer 3-3', 7-7''

C	7.24948	-2.43861	-1.91044
C	7.80535	-1.83593	-0.58759
C	6.54536	-1.42282	0.20153
C	5.71700	-0.79639	-0.94972
C	5.83250	-1.81741	-2.10226
C	6.76356	-0.34915	1.27824
C	5.43067	0.25743	1.76644
C	4.53386	0.76933	0.61319
C	4.34280	-0.30050	-0.49411
C	3.49760	0.30753	-1.61628
C	2.08656	0.64108	-1.12152
C	2.04351	1.29626	0.25180
C	3.18852	1.33817	1.07975
C	0.80964	1.82553	0.70057
C	0.73592	2.41893	1.97417
C	1.86727	2.47901	2.78777
C	3.06810	1.94234	2.33799
O	-0.47010	2.92841	2.37083
C	5.89485	-2.68017	0.81924
O	8.62191	-2.72461	0.16721

H	1.80822	2.94092	3.77207
H	3.92885	2.00101	2.99536
C	-0.43129	1.75760	-0.13653
H	8.37639	-0.92034	-0.81656
H	5.66651	-3.44305	0.06827
H	6.58457	-3.13056	1.53870
H	4.96271	-2.44789	1.34162
H	7.19962	-3.52778	-1.80556
H	7.91177	-2.22648	-2.75762
H	5.05455	-2.58609	-2.02575
H	5.71475	-1.34629	-3.08319
H	6.27765	0.09896	-1.27075
H	3.77878	-1.14626	-0.07115
H	7.31839	-0.75898	2.13159
H	7.38675	0.45372	0.85649
H	5.66759	1.08045	2.45025
H	4.87266	-0.47788	2.36007
H	5.09006	1.59418	0.13291
H	3.99342	1.21724	-1.98638
H	3.42536	-0.37726	-2.46981
H	1.48782	-0.28047	-1.08063
H	1.58117	1.28153	-1.85188
H	-0.36759	3.30630	3.25828
H	9.40633	-2.92829	-0.36454
C	-1.42838	0.80941	0.10870
C	-2.61051	0.73025	-0.64016
C	-2.78528	1.65564	-1.69071
C	-1.79729	2.61053	-1.94684
C	-0.63558	2.67266	-1.18241
H	-1.25950	0.11337	0.92370
C	-3.65347	-0.35671	-0.36157
C	-4.04257	1.67849	-2.54268
H	-1.92559	3.33112	-2.75071
O	0.29046	3.63062	-1.49906
H	0.99778	3.58611	-0.83191
C	-4.90230	0.41826	-2.40235
C	-5.04753	0.03426	-0.92506
C	-3.73356	-0.79039	1.12197
C	-6.02067	-1.12067	-0.67524
C	-4.80329	-1.87263	1.37983
C	-6.17832	-1.46363	0.82888
C	-7.21330	-2.60301	0.72370
C	-7.47041	-1.04848	-1.20161
C	-8.23182	-2.10289	-0.34216
C	-6.77054	-0.31048	1.66864
H	-7.72225	0.05294	1.26796

H	-6.96149	-0.66269	2.68637
H	-6.09244	0.54508	1.72799
O	-7.78821	-2.90189	1.99156
H	-6.69422	-3.49706	0.33876
H	-8.40487	-3.63950	1.86849
H	-8.61516	-2.93091	-0.94964
H	-9.08988	-1.65809	0.17339
H	-5.56648	-2.01276	-1.14129
H	-5.40478	0.92478	-0.38502
H	-3.34920	-1.25487	-0.92881
H	-7.89230	-0.04706	-1.05510
H	-7.53196	-1.26279	-2.27338
H	-4.44304	-0.41798	-2.95009
H	-5.88444	0.59157	-2.85878
H	-3.77177	1.84336	-3.59357
H	-4.64536	2.55232	-2.25137
H	-4.86313	-2.08861	2.45406
H	-4.48993	-2.80672	0.88977
H	-3.92211	0.09171	1.74704
H	-2.76523	-1.18719	1.44696

Trimer 7-3', 3-7''

C	7.24948	-2.43861	-1.91044
C	7.80535	-1.83593	-0.58759
C	6.54536	-1.42282	0.20153
C	5.71700	-0.79639	-0.94972
C	5.83250	-1.81741	-2.10226
C	6.76356	-0.34915	1.27824
C	5.43067	0.25743	1.76644
C	4.53386	0.76933	0.61319
C	4.34280	-0.30050	-0.49411
C	3.49760	0.30753	-1.61628
C	2.08656	0.64108	-1.12152
C	2.04351	1.29626	0.25180
C	3.18852	1.33817	1.07975
C	0.80964	1.82553	0.70057
C	0.73592	2.41893	1.97417
C	1.86727	2.47901	2.78777
C	3.06810	1.94234	2.33799
O	-0.47010	2.92841	2.37083
C	5.89485	-2.68017	0.81924
O	8.62191	-2.72461	0.16721
H	1.80822	2.94092	3.77207
H	3.92885	2.00101	2.99536
C	-0.43129	1.75760	-0.13653
H	8.37639	-0.92034	-0.81656

H	5.66651	-3.44305	0.06827
H	6.58457	-3.13056	1.53870
H	4.96271	-2.44789	1.34162
H	7.19962	-3.52778	-1.80556
H	7.91177	-2.22648	-2.75762
H	5.05455	-2.58609	-2.02575
H	5.71475	-1.34629	-3.08319
H	6.27765	0.09896	-1.27075
H	3.77878	-1.14626	-0.07115
H	7.31839	-0.75898	2.13159
H	7.38675	0.45372	0.85649
H	5.66759	1.08045	2.45025
H	4.87266	-0.47788	2.36007
H	5.09006	1.59418	0.13291
H	3.99342	1.21724	-1.98638
H	3.42536	-0.37726	-2.46981
H	1.48782	-0.28047	-1.08063
H	1.58117	1.28153	-1.85188
H	-0.36759	3.30630	3.25828
H	9.40633	-2.92829	-0.36454
C	-1.42838	0.80941	0.10870
C	-2.61051	0.73025	-0.64016
C	-2.78528	1.65564	-1.69071
C	-1.79729	2.61053	-1.94684
C	-0.63558	2.67266	-1.18241
H	-1.25950	0.11337	0.92370
C	-3.65347	-0.35671	-0.36157
C	-4.04257	1.67849	-2.54268
H	-1.92559	3.33112	-2.75071
O	0.29046	3.63062	-1.49906
H	0.99778	3.58611	-0.83191
C	-4.90230	0.41826	-2.40235
C	-5.04753	0.03426	-0.92506
C	-3.73356	-0.79039	1.12197
C	-6.02067	-1.12067	-0.67524
C	-4.80329	-1.87263	1.37983
C	-6.17832	-1.46363	0.82888
C	-7.21330	-2.60301	0.72370
C	-7.47041	-1.04848	-1.20161
C	-8.23182	-2.10289	-0.34216
C	-6.77054	-0.31048	1.66864
H	-7.72225	0.05294	1.26796
H	-6.96149	-0.66269	2.68637
H	-6.09244	0.54508	1.72799
O	-7.78821	-2.90189	1.99156
H	-6.69422	-3.49706	0.33876

H	-8.40487	-3.63950	1.86849
H	-8.61516	-2.93091	-0.94964
H	-9.08988	-1.65809	0.17339
H	-5.56648	-2.01276	-1.14129
H	-5.40478	0.92478	-0.38502
H	-3.34920	-1.25487	-0.92881
H	-7.89230	-0.04706	-1.05510
H	-7.53196	-1.26279	-2.27338
H	-4.44304	-0.41798	-2.95009
H	-5.88444	0.59157	-2.85878
H	-3.77177	1.84336	-3.59357
H	-4.64536	2.55232	-2.25137
H	-4.86313	-2.08861	2.45406
H	-4.48993	-2.80672	0.88977
H	-3.92211	0.09171	1.74704
H	-2.76523	-1.18719	1.44696

Trimer 7-7', 3-3''

C	7.24948	-2.43861	-1.91044
C	7.80535	-1.83593	-0.58759
C	6.54536	-1.42282	0.20153
C	5.71700	-0.79639	-0.94972
C	5.83250	-1.81741	-2.10226
C	6.76356	-0.34915	1.27824
C	5.43067	0.25743	1.76644
C	4.53386	0.76933	0.61319
C	4.34280	-0.30050	-0.49411
C	3.49760	0.30753	-1.61628
C	2.08656	0.64108	-1.12152
C	2.04351	1.29626	0.25180
C	3.18852	1.33817	1.07975
C	0.80964	1.82553	0.70057
C	0.73592	2.41893	1.97417
C	1.86727	2.47901	2.78777
C	3.06810	1.94234	2.33799
O	-0.47010	2.92841	2.37083
C	5.89485	-2.68017	0.81924
O	8.62191	-2.72461	0.16721
H	1.80822	2.94092	3.77207
H	3.92885	2.00101	2.99536
C	-0.43129	1.75760	-0.13653
H	8.37639	-0.92034	-0.81656
H	5.66651	-3.44305	0.06827
H	6.58457	-3.13056	1.53870
H	4.96271	-2.44789	1.34162
H	7.19962	-3.52778	-1.80556

H	7.91177	-2.22648	-2.75762
H	5.05455	-2.58609	-2.02575
H	5.71475	-1.34629	-3.08319
H	6.27765	0.09896	-1.27075
H	3.77878	-1.14626	-0.07115
H	7.31839	-0.75898	2.13159
H	7.38675	0.45372	0.85649
H	5.66759	1.08045	2.45025
H	4.87266	-0.47788	2.36007
H	5.09006	1.59418	0.13291
H	3.99342	1.21724	-1.98638
H	3.42536	-0.37726	-2.46981
H	1.48782	-0.28047	-1.08063
H	1.58117	1.28153	-1.85188
H	-0.36759	3.30630	3.25828
H	9.40633	-2.92829	-0.36454
C	-1.42838	0.80941	0.10870
C	-2.61051	0.73025	-0.64016
C	-2.78528	1.65564	-1.69071
C	-1.79729	2.61053	-1.94684
C	-0.63558	2.67266	-1.18241
H	-1.25950	0.11337	0.92370
C	-3.65347	-0.35671	-0.36157
C	-4.04257	1.67849	-2.54268
H	-1.92559	3.33112	-2.75071
O	0.29046	3.63062	-1.49906
H	0.99778	3.58611	-0.83191
C	-4.90230	0.41826	-2.40235
C	-5.04753	0.03426	-0.92506
C	-3.73356	-0.79039	1.12197
C	-6.02067	-1.12067	-0.67524
C	-4.80329	-1.87263	1.37983
C	-6.17832	-1.46363	0.82888
C	-7.21330	-2.60301	0.72370
C	-7.47041	-1.04848	-1.20161
C	-8.23182	-2.10289	-0.34216
C	-6.77054	-0.31048	1.66864
H	-7.72225	0.05294	1.26796
H	-6.96149	-0.66269	2.68637
H	-6.09244	0.54508	1.72799
O	-7.78821	-2.90189	1.99156
H	-6.69422	-3.49706	0.33876
H	-8.40487	-3.63950	1.86849
H	-8.61516	-2.93091	-0.94964
H	-9.08988	-1.65809	0.17339
H	-5.56648	-2.01276	-1.14129

H	-5.40478	0.92478	-0.38502
H	-3.34920	-1.25487	-0.92881
H	-7.89230	-0.04706	-1.05510
H	-7.53196	-1.26279	-2.27338
H	-4.44304	-0.41798	-2.95009
H	-5.88444	0.59157	-2.85878
H	-3.77177	1.84336	-3.59357
H	-4.64536	2.55232	-2.25137
H	-4.86313	-2.08861	2.45406
H	-4.48993	-2.80672	0.88977
H	-3.92211	0.09171	1.74704
H	-2.76523	-1.18719	1.44696

Trimer 3-3', 7-3''

C	7.24948	-2.43861	-1.91044
C	7.80535	-1.83593	-0.58759
C	6.54536	-1.42282	0.20153
C	5.71700	-0.79639	-0.94972
C	5.83250	-1.81741	-2.10226
C	6.76356	-0.34915	1.27824
C	5.43067	0.25743	1.76644
C	4.53386	0.76933	0.61319
C	4.34280	-0.30050	-0.49411
C	3.49760	0.30753	-1.61628
C	2.08656	0.64108	-1.12152
C	2.04351	1.29626	0.25180
C	3.18852	1.33817	1.07975
C	0.80964	1.82553	0.70057
C	0.73592	2.41893	1.97417
C	1.86727	2.47901	2.78777
C	3.06810	1.94234	2.33799
O	-0.47010	2.92841	2.37083
C	5.89485	-2.68017	0.81924
O	8.62191	-2.72461	0.16721
H	1.80822	2.94092	3.77207
H	3.92885	2.00101	2.99536
C	-0.43129	1.75760	-0.13653
H	8.37639	-0.92034	-0.81656
H	5.66651	-3.44305	0.06827
H	6.58457	-3.13056	1.53870
H	4.96271	-2.44789	1.34162
H	7.19962	-3.52778	-1.80556
H	7.91177	-2.22648	-2.75762
H	5.05455	-2.58609	-2.02575
H	5.71475	-1.34629	-3.08319
H	6.27765	0.09896	-1.27075

H	3.77878	-1.14626	-0.07115
H	7.31839	-0.75898	2.13159
H	7.38675	0.45372	0.85649
H	5.66759	1.08045	2.45025
H	4.87266	-0.47788	2.36007
H	5.09006	1.59418	0.13291
H	3.99342	1.21724	-1.98638
H	3.42536	-0.37726	-2.46981
H	1.48782	-0.28047	-1.08063
H	1.58117	1.28153	-1.85188
H	-0.36759	3.30630	3.25828
H	9.40633	-2.92829	-0.36454
C	-1.42838	0.80941	0.10870
C	-2.61051	0.73025	-0.64016
C	-2.78528	1.65564	-1.69071
C	-1.79729	2.61053	-1.94684
C	-0.63558	2.67266	-1.18241
H	-1.25950	0.11337	0.92370
C	-3.65347	-0.35671	-0.36157
C	-4.04257	1.67849	-2.54268
H	-1.92559	3.33112	-2.75071
O	0.29046	3.63062	-1.49906
H	0.99778	3.58611	-0.83191
C	-4.90230	0.41826	-2.40235
C	-5.04753	0.03426	-0.92506
C	-3.73356	-0.79039	1.12197
C	-6.02067	-1.12067	-0.67524
C	-4.80329	-1.87263	1.37983
C	-6.17832	-1.46363	0.82888
C	-7.21330	-2.60301	0.72370
C	-7.47041	-1.04848	-1.20161
C	-8.23182	-2.10289	-0.34216
C	-6.77054	-0.31048	1.66864
H	-7.72225	0.05294	1.26796
H	-6.96149	-0.66269	2.68637
H	-6.09244	0.54508	1.72799
O	-7.78821	-2.90189	1.99156
H	-6.69422	-3.49706	0.33876
H	-8.40487	-3.63950	1.86849
H	-8.61516	-2.93091	-0.94964
H	-9.08988	-1.65809	0.17339
H	-5.56648	-2.01276	-1.14129
H	-5.40478	0.92478	-0.38502
H	-3.34920	-1.25487	-0.92881
H	-7.89230	-0.04706	-1.05510
H	-7.53196	-1.26279	-2.27338

H	-4.44304	-0.41798	-2.95009
H	-5.88444	0.59157	-2.85878
H	-3.77177	1.84336	-3.59357
H	-4.64536	2.55232	-2.25137
H	-4.86313	-2.08861	2.45406
H	-4.48993	-2.80672	0.88977
H	-3.92211	0.09171	1.74704
H	-2.76523	-1.18719	1.44696